

Epithelial-mesenchymal feedback signalling during
vertebrate organogenesis:
Genetic analysis of BMP-Gremlin1 antagonistic interactions

Inauguraldissertation

zur

Erlangung der Würde eines Doktors der Philosophie
vorgelegt der
Philosophisch-Naturwissenschaftlichen Fakultät
der Universität Basel

von

Alexandre Gonçalves

aus Lissabon, Portugal

Basel, 2010

Genehmigt von der Philosophisch-Naturwissenschaftlichen Fakultät auf Antrag
von

Prof. Dr. Rolf Zeller und Prof. Dr. Markus Affolter

Basel, den 2. März 2010

Prof. Dr. Eberhard Parlow

Dekan

I. TABLE OF CONTENTS

I. TABLE OF CONTENTS	p4
II. LIST OF ABBREVIATIONS	p9
III. ABSTRACT	p13
IV. INTRODUCTION	p14
OVERVIEW OF KIDNEY DEVELOPMENT	p14
INITIATION OF URETERIC BUD FORMATION AND BRANCHING	
MORPHOGENESIS: A MOLECULAR PERSPECTIVE	p20
<i>The GDNF/RET signalling module – the UB outgrowth and</i>	
<i>branching morphogenesis engine</i>	p21
<i>Early regulation of GDNF/RET feedback signalling loop</i>	p22
THE ROLE OF BMP SIGNALLING IN METANEPHRIC KIDNEY	
DEVELOPMENT	p25
<i>The BMP signalling pathway</i>	p25
<i>BMP signalling ligands during kidney development</i>	p27
<i>BMP receptors</i>	p30
<i>BMP signal transduction</i>	p33
<i>SMAD mediated BMP signal transduction</i>	p34
<i>Non-SMAD mediated BMP signal transduction</i>	p35
<i>Extracellular regulation of BMP ligand activity and availability</i>	p37
<i>BMP extracellular antagonists</i>	p37
<i>BMP extracellular agonists</i>	p39

V. AIM OF THE THESIS	p41
The current state of research	p41
Objectives	p42
Detailed description	p42
VI. MATERIAL AND METHODS	p45
Genetic analysis of the GREM1–BMP4 interactions	p45
<i>Grem1 and Bmp4 mouse strains and research approach</i>	p45
<i>Bmp4 spatiotemporal conditional inactivation</i>	p46
Genetic analysis of GREM1–BMP7 interactions	p47
Molecular and morphological analysis of embryos and organs	p49
<i>Paraffin embedding</i>	p49
<i>Coating slides with 3-triethoxysilylpropylamine (TESPA)</i>	p50
<i>Histological sectioning of paraffin-embedded samples</i>	p51
<i>Whole-mount in situ hybridization - modified from David Wilkson's protocol</i>	p51
<i>β-Galactosidase staining of embryos and kidney rudiments</i>	p54
<i>Immunohistochemistry (IHC) assays</i>	p57
<i>PODOCALYXIN and CYTOKERATIN Double Immunostaining</i>	p57
Kidney rudiment cultures	p59
<i>Kidney primordia culture</i>	p59
<i>Semi-quantitative RT-PCR analysis</i>	p60

Affymetrix gene chip microarray analysis	p61
<i>Kidney rudiments collection, gender determination and RNA isolation</i>	p61
<i>RNA isolation and analysis</i>	p62
<i>Affymetrix Genechip® hybridization and scanning</i>	p62
<i>Genedata Expressionist Microarray data mining and Ingenuity® (Ingenuity Systems Inc.) pathway analysis</i>	p63

VII. REDUCTION OF BMP4 ACTIVITY BY GREMLIN1 ENABLES

URETERIC BUD OUTGROWTH AND GDNF/WNT11 FEEDBACK

SIGNALING DURING KIDNEY BRANCHING MORPHOGENESIS p64

Summary p64

Introduction p65

Results p70

The BMP antagonist gremlin 1 induces supernumerary epithelial buds and restores invasion and branching in

Grem1-deficient kidney primordia p70

The Grem1 deficiency causes aberrant nuclear accumulation of pSMAD proteins in the metanephric mesenchyme around the ureteric bud

p77

Genetic reduction of BMP4 activity in Grem1-deficient mouse embryos rescues metanephric kidney organogenesis and postnatal kidney functions

p83

Discussion p91

VIII. GENETIC ANALYSIS OF THE BMP7-GREMLIN1

INTERACTIONS DURING KIDNEY EPITHELIAL BRANCHING p96

Summary p96

Introduction p97

Results p99

Complete genetic inactivation of Bmp7 restores the failure to initiate branching morphogenesis in Grem1 deficient kidneys p99

Inactivation of Grem1 improves glomeruli and collecting duct formation in Bmp7 deficient kidneys p103

Inactivation of Bmp7 in Grem1^{ΔΔ} kidney rudiments restores the GDNF/Ret/Wnt11 feedback signalling loop and onset of nephrogenesis p106

Six2 positive nephrogenic progenitors are partially restored in Grem1^{ΔΔ}; Bmp7^{ΔΔ} embryos p108

Comparative analysis of the Grem1, Bmp4 and Bmp7 expression patterns during early kidney development p111

Discussion p113

IX. CONCLUSION AND OUTLOOK p116

APPENDIX 1. TM-CRE MEDIATED INACTIVATION OF BMP4

DURING KIDNEY DEVELOPMENT p118

Introduction	p118
Methods and Aims	p118
Results	p119
Conclusion	p124
APPENDIX 2. MICROARRAY ANALYSIS OF THE GREM1-BMP4 ANTAGONISTIC INTERACTIONS	p126
Introduction	p126
Methods and Aims	p126
Results	p127
Conclusion	p132
X. ACKNOWLEDGMENTS	p134
XI. REFERENCES	p139
XII. <i>CURRICULUM VITAE</i> AND PUBLICATION LIST	p159

II. LIST OF ABBREVIATIONS

β -Gal	β -galactosidase
Δ	null allele
A-P	anterior-posterior
Δc	conditionally induced null allele
A.G.	Alexandre Gonçalves
B4	<i>Bmp4</i>
B7	<i>Bmp7</i>
BMP	bone morphogenetic protein
bp	base pair
BSA	bovine serum albumin
CAGG	cytomegalovirus immediate-early enhancer and chicken β -actin promoter/enhancer
CAKUT	congenital anomalies of the kidney and urinary tract
cDNA	complementary DNA
Co-Smad	common-mediator Smad
cRNA	complementary RNA
DEPC	diethyl pyrocarbonate

dH ₂ O	deionized water
DMEM	dulbecco's Modified Eagle Medium
DNA	Deoxyribonucleic
E	embryonic day
e-m	epithelial-mesenchymal
EDTA	ethylenediaminetetraacetic acid
EMT	epithelial-to-mesenchymal transition
ER	estrogen receptor
f	floxed allele
FGF	fibroblast growth factor
GFP	Green Fluorescent Protein
<i>Grem1</i> , G1	<i>Gremlin1</i>
H	<i>Hoxb7</i>
Hox	homeobox gene
H/E	haematoxylin and eosin staining
I-Smads	inhibitory smads
IHC	immunohistochemistry
IM	intermediate mesoderm
IP	intraperitoneal
J.D. Bénazet	Jean-Denis Bénazet

K3	$K_3Fe(CN_6)$
K4	$K_4Fe(CN_6)$
LacZ	lactose operon gene Z
miRNAs	microRNAs
Msx	muscle segment homeobox homolog
ND	nephric ducts
O.M	Odyssé Michos
O/N	overnight
p.c.	<i>post coitum</i>
PAS	periodic acid schiff
PBS	phosphate buffer saline
PBT	PBS with 0.1% Tween 20
PCP	planar cell polarity
PCR	polymerase chain reaction
pK	proteinase K
R-Smads	receptor-regulated smads
R.Z.	Rolf Zeller
RNA	ribonucleic acid
rpm	rotations per minute
rRNA	ribosomal RNA

RT	room temperature
SGBS	Simpson-Golabi-Behmel syndrome
Smad	mothers against decapentaplegic homolog
Spry	Sprouty
tg	transgene
TM	tamoxifen
Wt	wild-type
X-gal	5-bromo-4-chloro-3-hydroxyindole

III. ABSTRACT

Branching morphogenesis of the metanephric kidney relies on an intricate molecular system that controls a highly regulated developmental program. Metanephric kidney organogenesis involves a complex system of epithelial mesenchymal interactions that orchestrate an elaborate epithelial branching process. Although it has already been shown that BMP signalling is involved in this process the present study reveals the functional importance and relevant interactions of BMPs with the antagonist GREMLIN1 (GREM1). Our genetic and molecular analysis identifies GREM1 as an essential negative modulator of BMP4 signaling during initiation of kidney branching morphogenesis. GREM1 is essential for positioning the ureteric bud, initiating its outgrowth and proper epithelial branching. GREM1 is not only required to antagonize BMP4 but genetic analysis of its interactions with BMP7 reveals a more general role in modulating BMP signaling. In light of these GREM1 interactions with BMP4 and BMP7, my Ph.D. research indicates that GREM1 orchestrates initiation and progression of epithelial branching by establishing spatiotemporal control of BMP activity in the mesenchyme surrounding the Wolffian duct, ureteric bud and likely also branching epithelium.

IV. INTRODUCTION

One important aim of developmental biology is to gain insight into the intricate mechanisms that control organogenesis. The main topic of my thesis focuses on epithelial-mesenchymal (e-m) feedback signalling during mouse kidney development. In this section I will describe the molecular pathways that control cell proliferation, patterning and differentiation during mammalian metanephric kidney development. Although the central research aim was to analyse the BMP (bone morphogenetic proteins) – Gremlin1 antagonistic interactions, modulation of the BMP pathway and its interactions with other key molecular pathways was genetically and molecularly addressed. The aim of my thesis research was to provide insight into the early events leading to the ureteric bud formation and initiation of epithelial branching morphogenesis.

Overview of kidney development

Mammalian vertebrate kidney development reflects evolution of kidneys in vertebrates. It recapitulates the transition from the ancestral aquatic environment to a terrestrial “dry” niche by formation of a pronephros, mesonephros and metanephros. One can say that mammalian kidney developmental programmes are in agreement with Ernst Haeckel’s dictum “ontogeny recapitulates phylogeny”. This is also illustrated by kidney development in mouse, *Xenopus* and zebrafish embryos (see figure 1; Ohno, 1995).

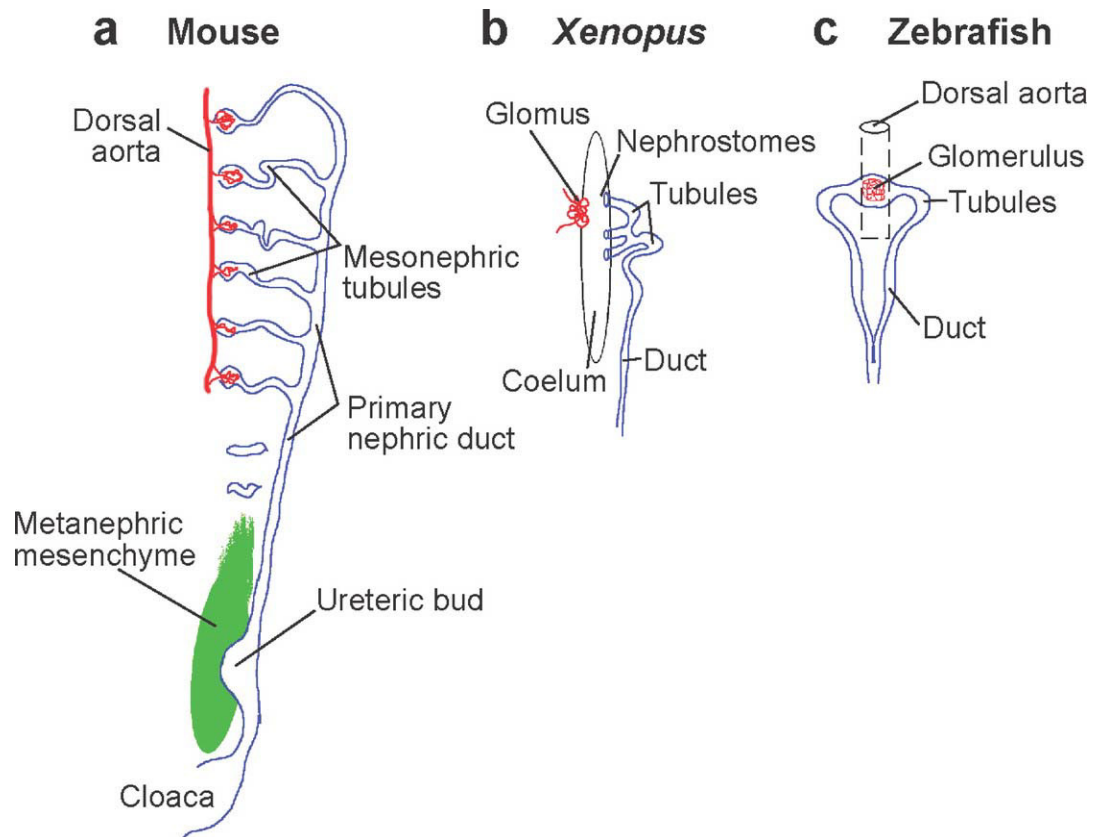


Fig. 1. Early patterning of the mouse, *Xenopus*, and zebrafish kidneys. (a) One side of the developing mouse intermediate mesoderm is shown at approximately E10.5. More anterior, the primary nephric duct connects to a series of well-developed mesonephric tubules, and more posterior it exhibits a single ureteric bud. The metanephric mesenchyme will generate most of the adult metanephric kidney. (b) In the *Xenopus* embryo, by stage 38, the pronephros is fully functional and consists of a glomus that filters into the coelum. Filtrate is reabsorbed by the ciliated nephrostomes and passed down the duct. (c) The zebrafish larva has a single midline glomerulus filtering from the dorsal aorta. Two bilateral pronephric tubules direct the filtrate lateral and caudally down the ducts (from Dressler, 2006).

The murine kidney development is initiated around embryonic day 8.0 as the intermediate mesoderm (IM) receives signals from the surface ectoderm and gives rise to two lateral paired epithelial ducts, the nephric ducts (ND) (Obara-

Ishihara et al., 1999). The Wolffian duct (WD) differentiates from mesoderm within the ND (reason why ND and WD are often considered synonyms of the same structure) and will induce formation of the pronephric and mesonephric kidneys/tubules as it extends caudally. Although pronephric tubules are functional in fish and amphibian larvae, there is no known function for them in mammals. Both the pronephric tubules and the rostral most region of the pronephric duct degenerate rapidly. The mesonephric kidney is the second kidney type to be formed, but it is also a transient structure that arises caudally to the pronephros by E9.0 (Saxen, 1987). As more mesonephric tubules are formed caudally, the rostral-most mesonephric tubules start to degenerate. Although in humans no evidence for a functional role of the mesonephros has been found, the murine mesonephric kidney appears to play an important role in the development of epididymal ducts of the male embryo (Sainio and Raatikainen-Ahokas, 1999; Saxen, 1987). The development of the definitive kidney, the metanephric kidney, is induced at around E10.5. The caudal region of the WD starts to swell and the resulting epithelial thickening will form the ureteric bud (UB) at the level of the hindlimb (Fig. 1).

Reciprocal signalling between the metanephric mesenchyme (MM) and the UB initiates and maintains metanephric kidney branching morphogenesis (Fig. 2). The UB elongates towards the adjacent (MM) and, as this invasion occurs, a complex sequence of e-m signalling events induce formation of the collecting duct (CD) system, as a consequence of repetitive branching of the UB (Fig.2A; Dressler, 2002; Saxen, 1987).

After initiation of branching morphogenesis, another important process commences. The tips of the branched UB will induce the surrounding mesenchyme to condense and form the nephrogenic mesenchyme. The nephrogenic mesenchymal cells will proliferate, epithelise and form the renal vesicle (Fig.2B). The renal vesicle assumes a primary comma-shape, due to the radial plane of cell division to the vesicle lumen, polarization of the renal vesicle and cell elongation. Consequently, cells furthest from the collecting duct will elongate and additional cell movements will result in formation of a second slit, giving rise to an S-shaped structure, whose distal tubule will be inserted into the collecting system. At the S-shape stage, cells will differentiate and form the Bowman's capsule, followed by appearance of the first presumptive podocytes. When the proximal cleft is invaded by endothelial cells, glomerulogenesis is initiated (Fig. 2B and 3A). Nephrogenesis results in formation of the renal vesicles, which are the basic units of the metanephric kidney that filter hazardous metabolites from the circulating blood and are required to regulate the blood water content (Dressler, 2002; Saxen, 1987).

The nephrogenesis process is reiterated many times and, depending on the organism, it will be continued after birth (Hartman et al., 2007). The metanephric kidney is composed of hundreds of thousands of nephrons (roughly 1 million nephrons per human kidney) giving rise to the glomeruli as already mentioned (Dressler, 2002; Saxen, 1987). As the podocytes develop, the blood filtrating surface area increases and the metanephric kidney achieves its final and complex functional character (Fig.3).

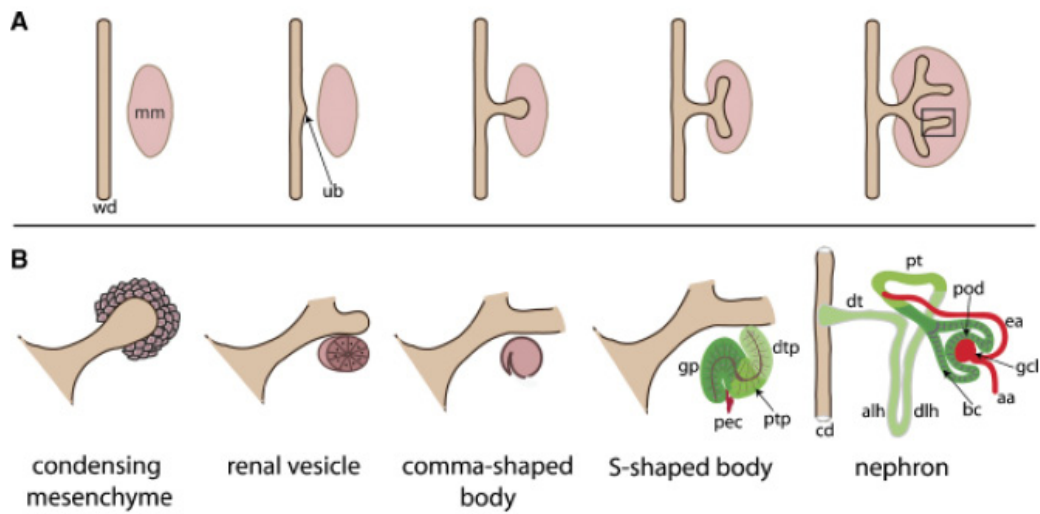


Fig. 2. Morphogenesis of the metanephric kidney. (A) Metanephric kidney development commences with metanephric mesenchyme (mm) induced out of pocketing of the ureteric bud (ub) from the caudal aspect of the Wolffian duct (wd). The ureteric bud then grows towards and invades the mesenchyme and begins to undergo dichotomous branching morphogenesis. (B) Branching epithelial tips (boxed in A) signal adjacent mesenchymal cells to condense around the tip and undergo a mesenchyme–epithelial transformation forming the renal vesicle, comma-shaped body, and S-shaped body. The S-shaped body is comprised of three segments that undergo growth and differentiation to form the fully differentiated nephron. The segment of the S-shaped body nearest the ureteric duct (light green colour in S-shaped body and nephron) is comprised of distal tubule progenitors (dtp) that ultimately fuse with the collecting duct (cd) and become the distal tubule (dt), ascending loop of Henle (alh), and descending loop of Henle (dlh). The middle segment of the S-shaped body (medium green colour in S-shaped body and nephron) is comprised of proximal tubule progenitors (ptp) and ultimately becomes the proximal tubule (pt). The most distal segment in the S-shaped body (dark green colour in S-shaped body and nephron) is comprised of glomerular progenitors (gp) that form the glomerular podocytes (gp) and Bowman's capsule (bc). Presumptive endothelial cells (pec) invade the developing glomerulus, giving rise to glomerular capillary loops (gcl) and the afferent (aa) and efferent (ea) arterioles (from Cain et al., 2008).

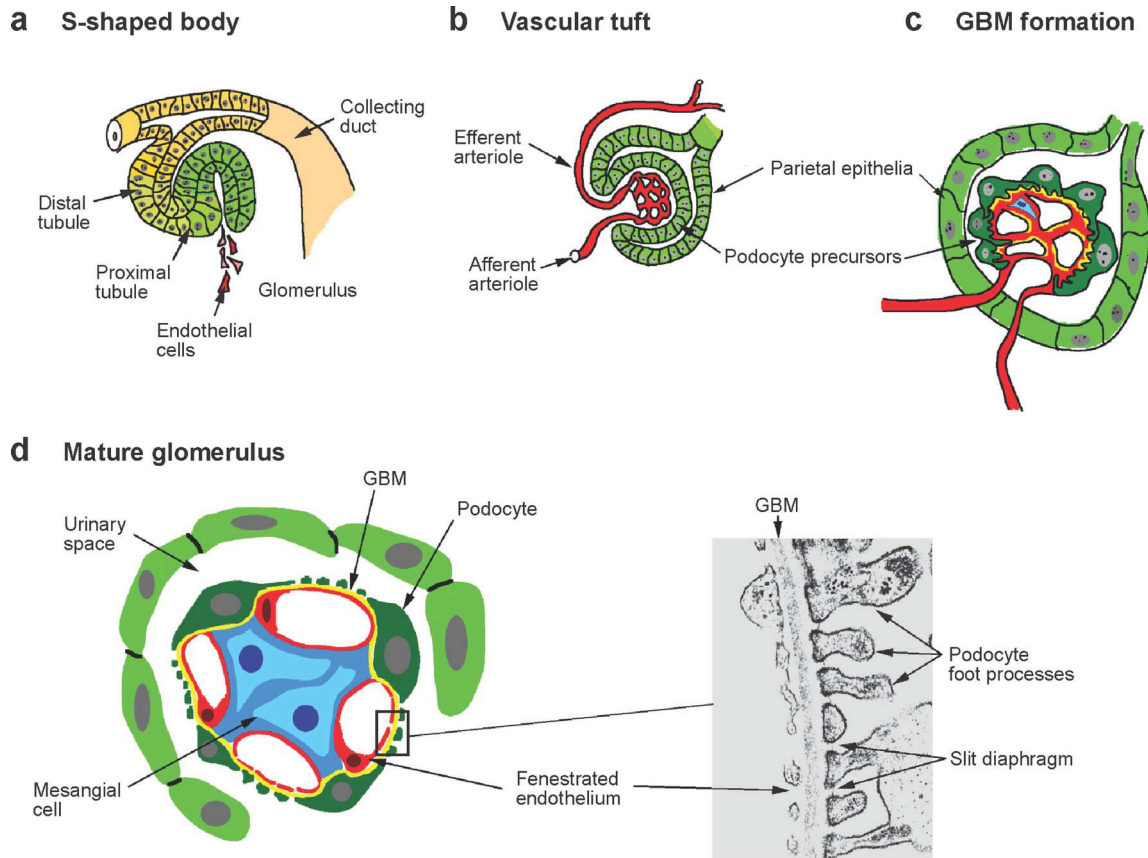


Fig. 3. Development of the glomerulus. The sequential stages of glomerular development are outlined schematically. (a) The S-shaped body is infiltrated by endothelial cells to generate a primitive vascular tuft within the cup-shaped glomerular precursor region. (b) The visceral epithelial cells, or podocyte precursors, contact the endothelial cells and begin to differentiate. (c) The glomerular basement membrane (GBM) is formed at the boundary between podocyte and endothelial cells. Podocytes begin to extend primary and secondary foot processes. (d) A schematic cross section through a mature glomerulus shows the relationships among the capillary endothelial cells, mesangial cells, GBM, and podocytes that are evident at later stages and in mature glomeruli. A high-magnification electron micrograph (*d, inset*) shows a typical cross section through the GBM. Note the fenestrated endothelium on the capillary side and the interdigitated podocyte foot processes on the urinary space side. Note also the precise distance between interdigitations at the slit diaphragm (from Dressler, 2006).

Alterations of ureteric epithelial branching morphogenesis will lead to renal malformations. Kidney agenesis, dysplasia, cysts formation and reduction of nephron number are just some of the many abnormalities observed in several human diseases and syndromes (Costantini, 2006). Considering that congenital abnormalities of the kidney and urinary tract (CAKUT) occur in about 1 out of 500 newborns and constitute 20-30% of all anomalies identified during the prenatal period (Schedl, 2007), the study of the altered molecular mechanisms underlying these anomalies is very relevant to understanding the aetiology of these congenital malformation.

Initiation of ureteric bud formation and branching morphogenesis: A molecular perspective

The early events leading to the formation of the metanephric kidney are responsible for the future of this crucial organ that contributes to making the *Mammalia* the most developed and advanced class among vertebrates. As discussed, metanephric kidney development is initiated as the epithelial UB is formed.

The GDNF/RET signalling module – the UB outgrowth and branching morphogenesis engine

Our current understanding shows that the glial cell line-derived neurotrophic factor (GDNF), its receptor encoded by the proto-oncogene tyrosine kinase RET and the co-receptor GDNF-family alpha ($GFR\alpha$), constitute the main components of an engine that drives initiation of the UB, its outgrowth and branching morphogenesis (Shakya et al., 2005). The textbook model indicated that mesenchymal cells located in metanephric mesenchyme (MM) secrete GDNF, a protein ligand that signals through the receptor RET and its co-receptor $GFR\alpha$ expressed by the epithelium (Costantini and Shakya, 2006). Recently, it has been shown that *Ret* expressing epithelial cells are a heterogeneous population that will compete and move towards the caudal WD, where the ones expressing highest *Ret* levels will initiate UB formation (Chi et al., 2009). However, non-RET expressing cells also contribute to the rearrangement of the WD from a simple to a pseudostratified epithelium. In addition, paired box gene 2 (*PAX2*), expressed by the mesenchyme surrounding the Wolffian duct (Dressler et al., 1990), is required for GDNF activation (Brophy et al., 2001) by enhancing RET activation (Brophy et al., 2003). *Ret* and *Gfr α* are initially expressed along the entire Wolffian duct epithelium, but as mesenchymal *Gdnf* activates this receptor complex, and the ureteric bud elongates towards the MM, their expression is up-regulated in the UB tip (Shakya et al., 2005; Towers et al., 1998). Branching morphogenesis is initiated when the epithelial UB assumes a T shape (Saxen, 1987). The ureteric bud branch tips express high levels of *Ret*, strengthening the GDNF mediated

activation (Costantini and Shakya, 2006). Interestingly, inactivation of *Wnt11* by gene targeting has shown that the embryonic and post-natal kidneys remain smaller (Majumdar et al., 2003). That observation together with down-regulation of *Ret* and *Gdnf* expression showed that WNT11 is required for the propagation of the GDNF/RET feedback signalling loop.

Early regulation of GDNF/RET feedback signalling loop

UB formation and reiterated epithelial branching morphogenesis are tightly regulated to prevent misexpression leading to malformations. As mentioned earlier, deregulation of GDNF/RET signalling interactions are quite striking (Jain et al., 2006). *Gdnf*, *Ret* or *Gfra1* inactivation most frequently leads to a failure to form a metanephric UB, resulting in complete renal agenesis, although rudimentary kidneys may form 30–50% of the time depending on genetic background (Costantini and Shakya, 2006; Moore et al., 1996; Schuchardt et al., 1996). Genetic inactivation of *Ret* in mouse results in incomplete kidney agenesis, due to a failure of the UB to elongate (Schuchardt et al., 1996). Considering the recent findings (Chi et al., 2009), it is possible that the previously described variable *Ret* loss of function phenotype (Schuchardt et al., 1996) is a consequence of the *Ret* independent ability of WD epithelial cells to rearrange and contribute to the epithelial conversion. Several targets of GDNF/RET signalling have been identified: the ERK MAPK, PI3Kinase/Akt and PLC γ pathways (Costantini, 2006), the canonical WNT pathway β -catenin (Clevers, 2006) and, more recently, a set of ETS transcription factors (*Etv4* and

Etv5) (Lu et al., 2009), which are themselves required for correct kidney epithelial branching morphogenesis.

Not only is it of importance to enhance GDNF/RET signalling, but restricting the location of these interactions is equally important. One gene involved in this restriction is Sprouty1 (*Spry1*), which belongs to the SPRY family of proteins that inhibit the Ras-ERK pathway downstream of various receptor tyrosine kinases (Fig. 4A; Chandramouli et al., 2008). Inactivation of *Spry1* in mouse embryos results in formation of supernumerary ureteric buds along the WD (Fig. 4D-F), which display abnormal/ectopic *Gdnf/Ret* expression, suggesting that the *Spry1* mutant phenotype is caused by increased sensitivity of the WD to GDNF/RET signalling. This results in formation of multiple ureters and multiplex kidneys (Basson et al., 2005). Most importantly, ectopic expression of the human *Spry2* in the mouse ureteric bud results in down-regulation of *Wnt11*, *Gdnf* and *Fgf7* expression, preventing normal kidney morphogenesis. Furthermore, it has been shown that over-expression of *Spry2* interferes with FGF signal transduction (Chi et al., 2004). Taken together, these results indicate that intra-cellular SPRYs are necessary to reduce the sensitivity of the WD to GDNF to restrict UB formation to one site (Basson et al., 2005; Chi et al., 2004). In addition, *Slit2* (ligand) and *Robo2* (receptor) are also required to restrict GDNF/RET feedback signalling to the caudal WD. *Slit2* and *Robo2* deficient mutant mouse embryos display abnormal *Gdnf* expression in the anterior nephrogenic mesenchyme that results in the formation of supernumerary UBs (Grieshammer et al., 2004). Furthermore, it has been shown that forkhead/winged helix gene *Foxc1* homozygous mutant mouse

embryos present several metanephric kidney abnormalities such as duplex kidneys, double ureters and hydroureters, as a consequence of ectopic mesonephric tubules and anterior ureteric buds (Kume et al., 2000).

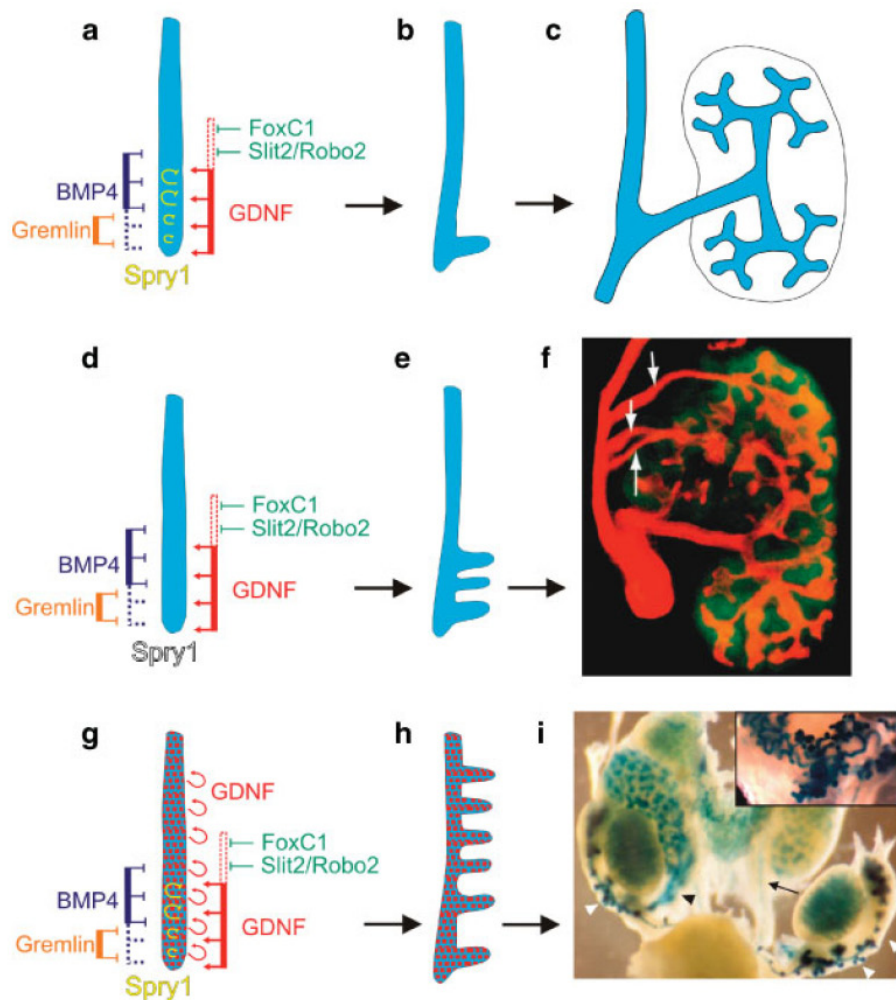


Fig. 4. The role of GDNF in ureteric bud formation is modulated by multiple mechanisms.

Ureteric bud outgrowth from the Wolffian duct is stimulated by GDNF, which is expressed in a broad domain of the adjacent intermediate mesoderm (a, red bar and arrows). The *Gdnf* expression domain is restricted by the transcription factor *Foxc1* and by *Slit2/Robo2* signalling; in their absence, it is expanded anteriorly (dashed red box), resulting in ectopic ureteric buds (not shown). *SPRY1* in the Wolffian duct negatively regulates the response to GDNF (yellow symbols). *BMP4* suppresses the response of GDNF, and is itself suppressed by *GREM1*.

Together, these mechanisms result in outgrowth of a single, correctly positioned ureteric bud (b), and formation of a single kidney (c). Knockout of *Spry1* (d) results in the formation of multiple ureteric buds (e) leading to multiple ureters and multiplex kidneys (f). Transgenic misexpression of GDNF throughout the Wolffian duct (g) overcomes these mechanisms of negative regulation and leads to multiple ureteric buds along the entire Wolffian duct (h). Some of these ectopic buds connect to the kidney (i, black arrowhead; black arrow points to the normal ureter), while others branch outside the kidney (white arrowheads). Inset: continued extra-renal branching of ectopic ureteric buds expressing GDNF (from Costantini and Shakya, 2006).

The role of BMP signalling in metanephric kidney development

In addition to the GDNF/RET interactions described, genetic and molecular analysis in mouse embryos has also provided evidence of the requirement of BMP signalling during early kidney development and for kidney homeostasis (Bush et al., 2004; Dudley and Robertson, 1997; Martinez et al., 2002; Michos et al., 2004; Miyazaki et al., 2000; Oxburgh et al., 2005; Zhu et al., 2006).

The BMP signalling pathway

Bone morphogenetic proteins (BMPs) comprise the largest subfamily of the transforming growth factor- β (TGF- β) superfamily of secreted proteins (Massagué, 1998). Several members of the BMP family are required for mesoderm formation, development and patterning of many different organ systems (Hogan, 1996). The involvement of this TGF β subfamily in biological processes such as cell proliferation, apoptosis, differentiation and

morphogenesis has triggered a lot of interest in the functions of BMPs during development and disease processes (Hogan, 1996; Pregizer and Mortlock, 2009).

BMPs are extracellular proteins that have been originally identified as secreted factors able to induce ectopic bone tissue formation *in vivo* (Urist, 1965). The BMP family members, like all TGF- β family members, are synthesized as large inactive precursor proteins that become active by cleavage of the amino acid motif -Arg-Ser-Lys-Arg- yielding a C-terminal mature protein, which forms dimers (Aono et al., 1995; Cui et al., 2001). All BMPs, with the exception of BMP1, share the highly conserved 7 cysteine knot characteristic of members of this transforming growth factor- β family (Fukagawa et al., 1994; Takahara et al., 1996). Heterodimerization of different BMPs, such as BMP2/5, BMP2/6, BMP2/7 and BMP4/7 occurs *in vivo* and *in vitro*, and heterodimers are functionally more potent than the corresponding homodimers of each of the BMP proteins (Fig. 5; Little and Mullins, 2009; Nishimatsu and Thomsen, 1998; Sieber et al., 2009).

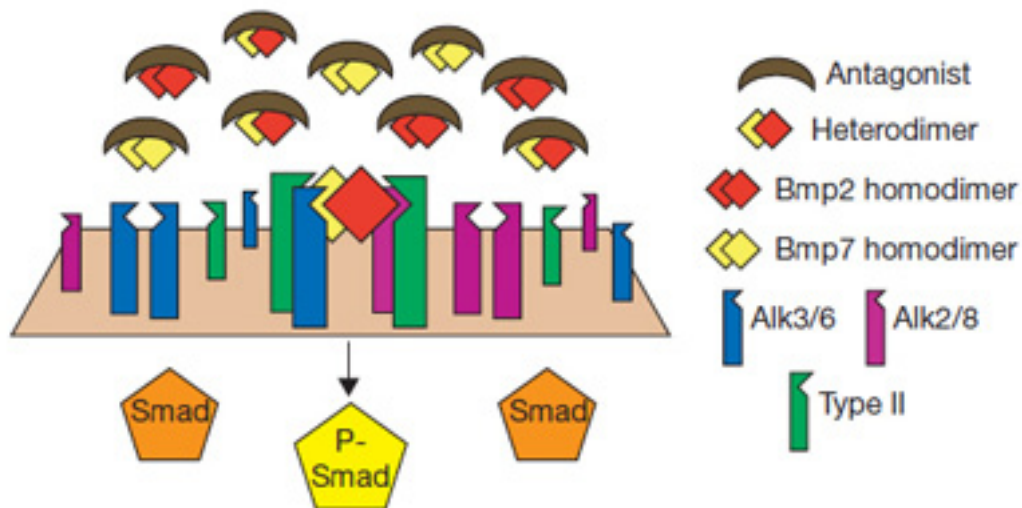


Fig. 5. Model of heterodimer-mediated dorsoventral patterning. Schematic representation of the putative interaction mechanism between the postulated BMP-2/7 heterodimers and the BMP receptors. Extracellular BMP antagonists bind to the dimerized BMP ligands, preventing them to activate the receptor. Following activation of the BMP receptors by a BMP-2/7 heterodimer, the receptor will phosphorylate the intracellular SMAD proteins. This in turn triggers a signalling cascade that initiates BMP signalling transduction (from Little and Mullins, 2009).

BMP signalling ligands during kidney development

As previously described, BMP proteins are required during early embryonic development for germ layer formation, their inactivation often results in early lethality (Hogan, 1996). The initial BMP transgenic and knockout studies unveiled the various role of the different BMP ligands in developmental processes (Table 1; Cao and Chen, 2005; Hogan, 1996).

Table 1 – BMP Ligands Mutant Renal Phenotypes.

BMP ligands	Phenotypes
BMP2	Homozygous lethal between E7 and E10.5 due to amnion/chorion and cardiac development defects. Heterozygous embryos display an increase of the ureteric bud cells proliferation.
BMP3	No renal phenotype reported.
BMP4	Homozygous lethal between E6.5 and E9.5 due to early mesodermal differentiation defects or late mesodermal derived abnormal deficiencies. Heterozygous display kidney dysplasia phenotypes, including hypo/dysplastic kidneys, hydroureters, ectopic ureterovesical junction, and double collecting duct system.
BMP5	Hydronephrosis.
BMP6	No renal phenotype reported.
BMP7	Homozygous –null mice display renal dysgenesis, hydroureter formation and overall arrested development at E14.5.

The initial expression analysis revealed that several *Bmp* genes are expressed early during metanephric kidney development in specific patterns. (Dudley and Robertson, 1997). Briefly, *Bmp* transcripts were detected throughout metanephric kidney development in structures such as the metanephric mesenchyme, ureter, developing tubules and glomeruli (Dudley and Robertson, 1997). A schematic representation of the expression patterns of the different BMP ligands is shown in Fig. 6.

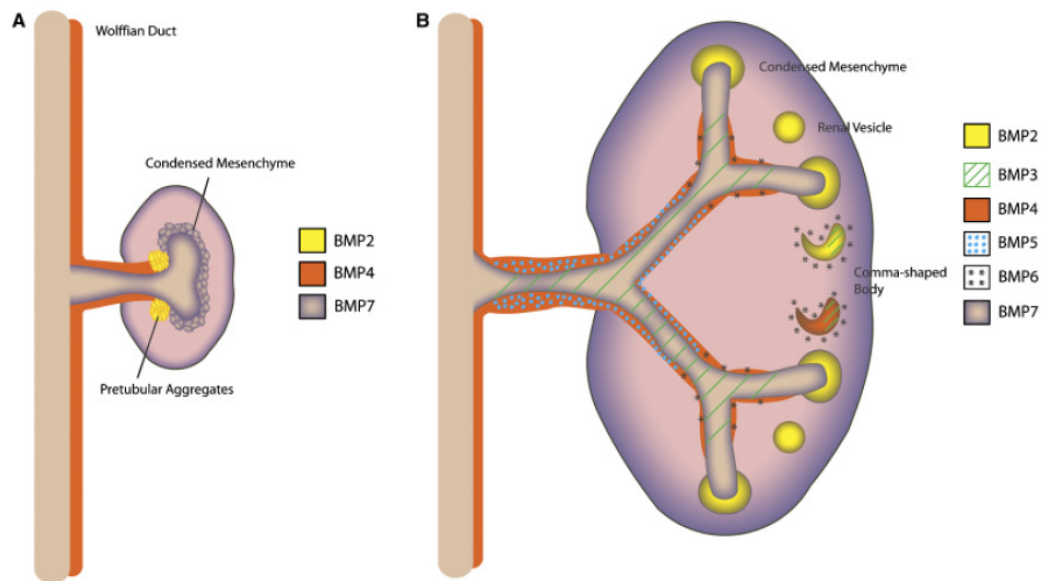


Fig. 6. Metanephric expression of bone morphogenetic protein (BMP) ligands. Transcripts for BMP2-7 have been detected during different stages of metanephric development in distinct and overlapping domains. This schematic depicts the expression patterns following invasion of the metanephric mesenchyme by the ureteric bud at \approx E11.5 (A) and at a later developmental stage, \approx E13.5 (B; from Cain et al., 2008).

Both *Bmp2* and *Bmp4* deficient mouse embryos are lethal at a very early developmental stage (Table 1). *Bmp2* deficient embryos die between E7 and E10.5 due to amnion/chorion and cardiac defects (Zhang and Bradley, 1996), while *Bmp4* deficient embryos display variable phenotypes. Some *Bmp4* deficient embryos die due to disruption of mesoderm formation at E6.5 and others perish around E9.5 due to developmental retardation with disorganized posterior structures and malformed extraembryonic mesoderm (Winnier et al., 1995). With respect to kidney development, interesting results were obtained by analysis of *Bmp2* and *Bmp4* single heterozygous mice. The *Bmp2* heterozygous mouse embryos displayed an increase in proliferation of ureteric

bud cells, although branching morphogenesis was not significantly affected (Hartwig et al., 2005). *Bmp4* heterozygous mice exhibited several phenotypes such as cysts formation, hydronephrosis and glomerulocystic abnormalities (Dunn et al., 1997). In addition, *Bmp3* and *Bmp6* are both expressed during kidney development (Dudley and Robertson, 1997) but mutant mice displayed no renal phenotypes, pointing to functional redundancy or compensation (Daluisi et al., 2001; Solloway et al., 1998). In *Bmp5* deficient mice the most obvious phenotype affects bones and hydronephrosis is also observed (Kingsley et al., 1992). Finally, *Bmp7* deficient mouse embryos display dysplastic kidneys and hydroureters with an arrest of nephrogenesis at E14.5 due to lack of sufficient progenitors (Dudley et al., 1995). In summary, inactivation of different BMP ligands results in a variety of metanephric malformations. Therefore a more detailed analysis of their functions and interactions with other morphoregulatory pathways such as the GDNF/RET signalling system is required.

BMP receptors

Not only BMP ligands, but also the BMP receptors, are expressed in partially overlapping patterns (Challen et al., 2005). As previously mentioned, BMP dimers bind to type I and type II heterodimeric transmembrane serine/threonine kinase receptor complexes (Fig. 7; Aono et al., 1995). Thus far, six different BMP receptors have been identified that interact with different types of different BMP (Nohno et al., 1995; ten Dijke et al., 1994). Type I receptors include Activin

receptor type 1A (ActR1a or Alk2), BMP receptor type IA (BR1A or Alk3) and BMP receptor type IB (BR1B or Alk6).

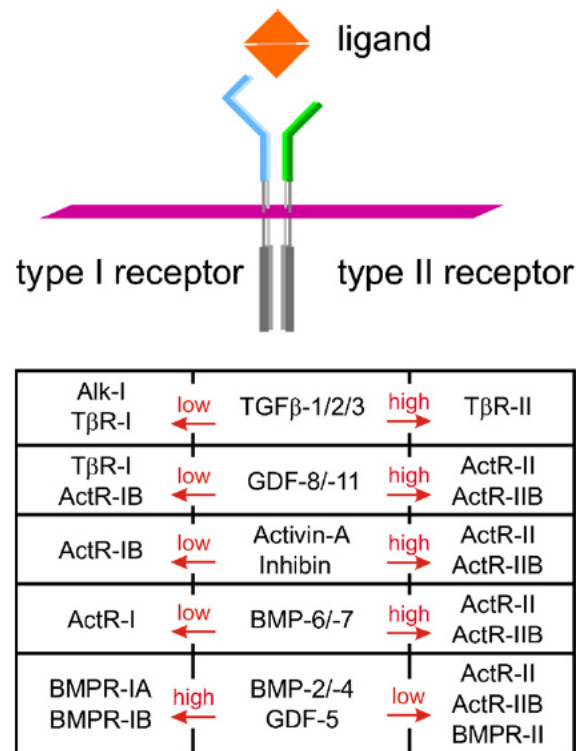


Fig. 7. Promiscuity of ligand–receptor interaction. Presentation of the preferential receptor usage of particular ligands. Graded differences in the binding affinities of individual ligand–receptor interactions are indicated (from Nickel et al., 2009).

Type II BMP receptors include BMP receptor II (BR1I), Activin receptors type IIA and IIB (ActR1IA and ActR1IB; Miyazono et al., 2005). Considering that different BMPs have different affinities for the receptors and, in addition, BMPs can either homodimerize or heterodimerize with other BMPs, this allows for a possible molecular explanation for the variance of phenotypes observed in BMP mutant mice (Hogan, 1996). BMP2 and BMP4 bind BR1A and BR1B type I receptors with a high affinity while their affinity to type II receptor BR1I is rather low (Koenig et al., 1994). Conversely, BMP7 interacts with high affinity with the type II receptors ActR1IB and ActR1IB, while its affinity for type

I receptors is rather low. Structural analysis of BMP7 reveals the much better affinity of the extracellular domain of the type II receptor in contrast to the 5-fold lower affinity for type I receptors (Greenwald et al., 2003). The BRII is active as part of a BMP heterodimeric receptors complex and upon binding of a BMP ligand, the BRI intracellular domain is phosphorylated which results in initiation of BMP signal transduction (Fig.8; Derynck and Zhang, 2003; Wrana et al., 1994).

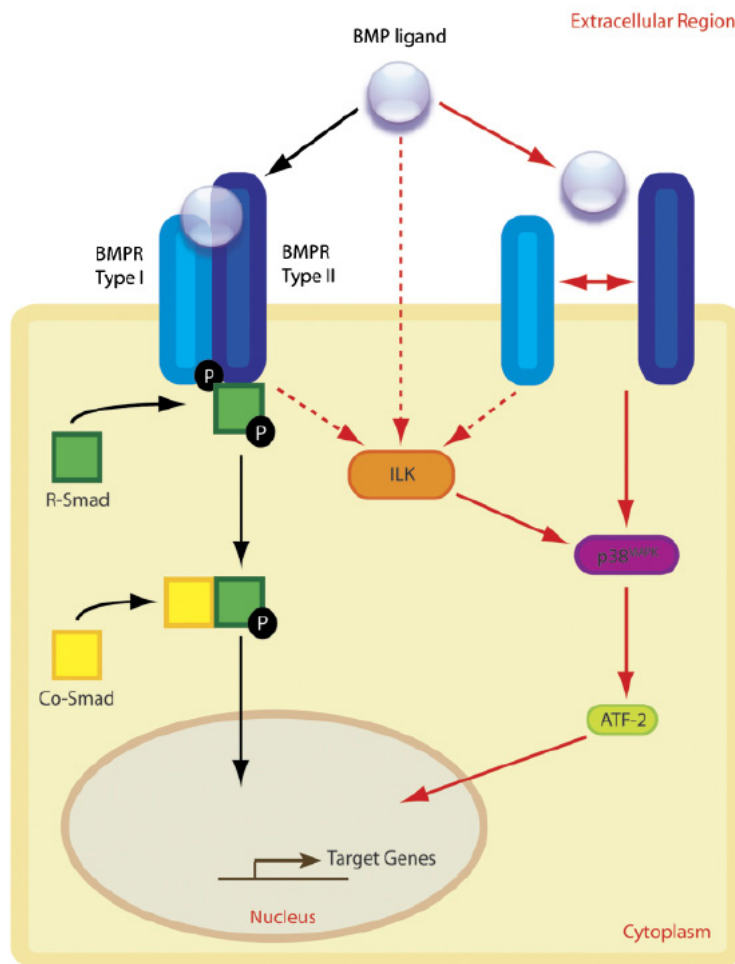


Fig. 8. Bone morphogenetic protein (BMP)-mediated signalling pathway. Canonical BMP-SMAD signalling (black arrows) is initiated by ligand binding to preformed heteromeric receptor complexes: a type I receptor (ALK2, ALK3, or ALK6) and a type II receptor (BMPRII). The phosphorylated type I receptor in turn phosphorylates a pathway-specific cytoplasmic signal-

transducing acceptor protein known as a receptor-activated SMAD (R-SMAD) (SMAD1, 5, or 8). R-SMADs then form heteromeric complexes with the common-mediator SMAD (Co-SMAD) SMAD4 in the cytoplasm and translocate into the nucleus where they interact with other transcription factors or regulate transcription of various target genes themselves. Non-canonical BMP signalling (red arrows) results in activation of the mitogen-activated protein kinase (MAPK) family of signalling molecules and is initiated by ligand-induced formation of heteromeric receptor complexes. Recent evidence suggests non-canonical BMP signalling may also occur via the activation of an integrin-linked kinase (ILK)/p38^{MAPK}/activating transcription factor-2 (ATF-2) signalling pathway. The initiator of ILK remains unknown but could involve ligand-induced or preformed heteromeric receptor complexes and/or ALK-independent receptor activation (dashed arrows). ALK, activin-like kinase (from Nickel et al., 2009).

BMP signal transduction

To summarize the so called “default” *modus operandi* of the BMP family - BMP ligands signalling is mediated via activation of intramembrane serine/threonine receptors kinase that either activate or repress intra-cellular SMAD proteins - homologues of both the *Drosophila* protein, mothers against decapentaplegic (MAD) and the *Caenorhabditis elegans* protein SMA - that upon BMP mediated signal transduction translocate to the nucleus and either activate or repress BMP target genes (Attisano and Wrana, 1998; Derynck et al., 1996). Many studies, involving the use of diverse animal models and research strategies, have contributed to the state-of-the-art knowledge concerning the key players involved in TGF- β /BMP signal transduction (Moustakas and Heldin, 2009). In addition, both the BMP and TGF- β signalling pathways can also trigger SMAD independent signal transduction pathways that involve MAP kinase pathways (von Bubnoff and Cho, 2001).

SMAD mediated BMP signal transduction

Canonical BMP signal transduction requires SMAD proteins (Attisano and Wrana, 1998; Derynck et al., 1996), which are highly conserved at their amino- and carboxyl-terminal regions (MH1 and MH2 to their homology to MAD proteins). These conserved domains are separated by a less conserved proline-rich linker region (Hoodless et al., 1996; Kim et al., 1997). The *Smad* gene family can be subdivided into three sub-families: receptor-regulated, common-mediator and inhibitory SMADs (Massagué et al., 2005). The receptor-regulated SMADs (R-SMADs) are composed of the cytoplasmic SMAD1, SMAD2, SMAD3, SMAD5, and SMAD8. SMAD 1, 5, and 8 are mostly substrates for the BMP receptors, while SMAD 2 and 3 are substrates for the TGF- β , activin, and Nodal receptors. The common-mediator (Co-Smad) SMAD4 heterodimerizes with the R-Smads and encodes a nuclear translocation signal. Once in the nucleus, the R-SMAD:SMAD4 complex associates with a variety of cofactors that regulate the transcriptional response. In contrast, SMAD6 and SMAD7 are inhibitory SMAD (I-SMAD or anti-SMAD) that interfere with SMAD-receptor or SMAD-SMAD interactions (Attisano and Wrana, 1998; Imamura et al., 1997; Massagué, 1998; Massagué et al., 2005; Moustakas and Heldin, 2009; Nakao et al., 1997). SMAD6 preferentially inhibits SMAD-dependent BMP signalling (Imamura et al., 1997) while TGF- β signalling can be inhibited by both SMAD6 and SMAD7 (Imamura et al., 1997; Nakao et al., 1997). Particular TGF- β and BMP –specific SMAD complexes can induce the expression of the I-SMAD that will negatively regulate signalling strength and duration (Fig.8; Attisano and Wrana, 1998).

Non-Smad mediated BMP signal transduction

Both BMP and TGF- β ligand mediated signal transduction can be SMAD independent, whereby some of those downstream pathways regulate SMAD activation while others induce unrelated responses (Derynck and Zhang, 2003). BMP/TGF β can activate several mitogen-activated protein kinases (MAPKs), including extracellular signal-regulated kinases (ERKs), c-Jun, N-terminal kinases (JNKs) and p38 kinases (Attisano and Wrana, 1998; Derynck and Zhang, 2003; Yu et al., 2002). Several different kinases involved in these non-SMAD signal pathways have been identified and the alternative signal transduction map is becoming more complex (Miyazono et al., 2010; Moustakas and Heldin, 2009). A schematic representation of that alternative BMP/TGF β signal transduction pathways is shown in Figure 9. Alternative activation of the TAK1/MEKK1 and Ras signal transduction pathway has been shown to play an important role during kidney development. In particular BMP7 induces collecting duct cells in a SMAD independent manner via activation of the p38 MAPK integrin-linked kinase (ILK)/p38 MAPK/activatin transcription factor- 2 (ATF-2) pathway (Hu et al., 2004; Leung-Hagesteijn et al., 2005). Moreover, it has been demonstrated Ras/MEK activation is necessary and sufficient for TGF β mediated Erk1 activation (Yue et al., 1999). Concomitantly, it was further demonstrated that ERK phosphorylates ADAM-17 which responds to kidney mesangial cells in a mouse model for renal fibrosis (Bell and Gooz, 2010).

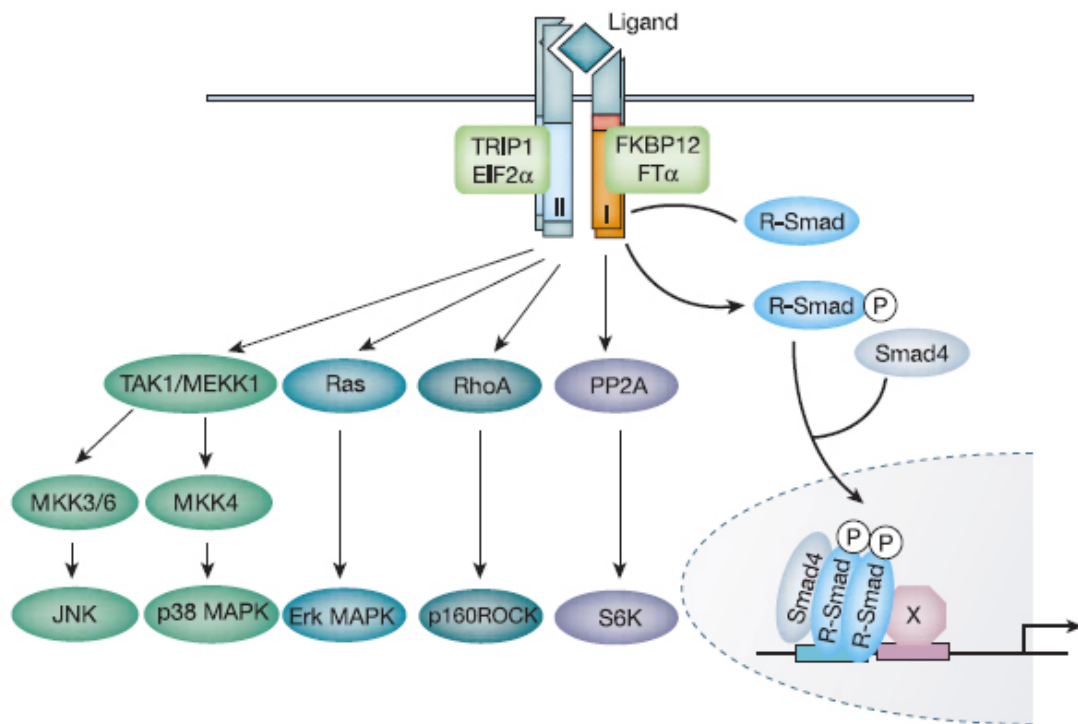


Fig. 9. TGF-β receptor signalling through SMAD independent pathways. Apart from proteins that interact with receptors and SMADs, other proteins (green) can associate with the type II or type I receptors and regulate TGF-β ligand signalling without an apparent direct effect on SMAD activation. In addition, the activated receptor complex activates non-SMAD signalling pathways, such as MAPK, PP2A/p70^{S6K}, RhoA and TAK1/MEKK1. Only the best-characterized pathways are shown (from Derynck and Zhang, 2003).

Extracellular regulation of BMP ligand activity and availability

In addition to regulation of BMP signal transduction, extracellular antagonists and agonists fine tune the interactions of ligands with their cognate receptors. The following sections will focus on extracellular modulators that are involved in metanephric kidney development.

BMP extracellular antagonists

BMP antagonists function by direct binding to BMP ligands, thus inhibiting their binding to their cognate receptors, which modulates BMP activity or defies boundaries of signalling (Hsu et al., 1998). Although several antagonists are expressed in the metanephric kidney from an early stage, only a few seem to play a role in nephrogenesis (Cain et al., 2008).

Gremlin1 (*Grem1*) is a member of the DAN/Cerberus gene family (Hsu et al., 1998). *Gremlin1* was identified in *Xenopus laevis* embryos, due to its ability to induce a secondary axis, as a consequence of antagonising BMP signalling. That study also showed that *Grem1* is expressed in the *Xenopus* pronephric kidneys, which provided the first hints of *Grem1* potential roles in kidney development (Hsu et al., 1998). *Grem1* expression is first detected in the mouse embryo around E8.5, in the intermediate mesoderm, somites, roof plate of the posterior neural tube fore- and hindlimb buds (Pearce et al., 1999). GREM1 was identified as a BMP antagonist required for its role in maintaining the SHH/FGF loop that controls limb distal outgrowth (Capdevila et al., 1999 ; Zuniga et al., 1999). Genetic analysis of the GREM1-BMP antagonistic interactions revealed

that its morphoregulatory function in the epithelial-mesenchymal feedback signalling loops is required for the mouse limb bud development, renal branching morphogenesis and lung development (Michos et al., 2004). In particular, complete agenesis was observed in *Grem1* deficient embryos. At an early stage, normal Wolffian ducts and ureteric buds form in *Grem1* deficient mouse embryos. That *Grem1* may also function postnatally was evidenced by a study in which rats were treated with streptozotocin to induce diabetic nephropathy *in vivo* (Wardle, 1975; Rossini et al., 1977). Such rats displayed high *Grem1* levels in the renal cortex and abnormal *Bmp2* induction (McMahon et al., 2000). This study also associated the GREM1 up-regulation with high glucose levels resulting from the diabetic nephropathy. Taken together these studies suggested that GREM1 is a potential endogenous antagonist of BMPs in diabetic glomerular context. Furthermore, clinical studies indicated that *Grem1* might be a downstream mediator of TGF- β , suggesting a role for *Grem1* in epithelial-to-mesenchymal transition (EMT) as is observed in chronic allograft nephropathies. Such nephropathies are the most common cause of end-stage renal disease in kidney transplant patients (Carvajal et al., 2008).

The BMP antagonist **Noggin** was first identified as a secreted protein that was able to dorsalize the *Xenopus laevis* ventral mesoderm, like Spemann's organizer (Smith and Harland, 1992; Smith et al., 1993). NOGGIN binds several BMP ligands with different affinities, such as BMP2 and BMP4 with high and BMP7 with low affinity (Brunet et al., 1998; McMahon et al., 1998). Despite the fact that *Noggin* knock-out mice do not display any renal phenotypes, NOGGIN may play a role in nephrogenesis (McMahon et al., 1998). Indeed, ectopic

expression of *Noggin* in podocytes using the *Nephrin* promoter revealed a defect in mesangial cells (Miyazaki et al., 2006). This ectopic expression was sufficient to inhibit BMP signalling, which resulted in cyst formation and decreased mesangial cells population. Another important clue of a possible NOGGIN involvement in tissue homeostasis was obtained by analysing the regeneration process following ischemic acute renal failure (Villanueva et al., 2006). *Noggin* expression was detected in the impaired kidney, in correlation to the local up-regulation of BMP7, which indicates that NOGGIN might be involved in tissue regeneration after acute renal failure.

BMP extracellular agonists

While BMP antagonists negatively modulate the BMP activity, other extracellular signals positively modulate BMP signalling (agonists) (Balemans and Van Hul, 2002). Several BMP agonists have been identified and some of them are likely required during metanephric kidney development.

KCP, the mouse Kielin/chordin-like protein, was identified from an embryonic kidney cDNA library (Lin et al., 2005). In cultured cells it was shown that KCP enhances BMP7 expression and increases SMAD1 mediated BMP signal transduction. While KCP deficient mice do not display overt kidney phenotypes, their recovery from acute renal injury is impaired as a likely consequence of KCPs normal branching in enhancing BMP7 signal transduction (Lin et al., 2005). Recent additional insights into the KCP functions have been obtained. While KCP enhances BMP activity, it inhibits TGF- β through SMAD2/3 signal

transduction. Therefore KCP may modulate TGF- β superfamily signalling during kidney homeostasis by inhibiting TGF- β and enhancing BMP signalling during acute renal injury (Lin et al., 2006).

CV2 (CROSSVEINLESS2 – also known as BMPER) was identified in *Drosophila* because of its properties to enhance BMP signalling during the formation of the wing cross veins (Conley et al., 2000). The protein encoded by the *Cv2* gene, not only co-localizes with but also, potentiates Gbb (Glass bottom boat), a *Drosophila* BMP orthologue (Ballard et al.; Conley et al., 2000).

Several studies with *Cv2* orthologue genes in vertebrate embryos established that CV2 enhances in particular BMP7 signalling (Ikeya et al., 2006). *Cv2* deficient mice show skeletal and eye phenotypes, along with kidney malformations. *Cv2* expression in the metanephric mesenchyme and developing nephrons correlates with the hypoplastic kidney phenotypes and reduced nephron numbers. The generation of compound mutant mice and embryos revealed that inactivation of *Kcp* in a *Cv2* mouse aggravates the acute kidney deficiencies (Ikeya et al., 2006).

Considering the current state of knowledge in BMP signalling during metanephric kidney development several questions remain open. BMP signalling can be regulated by antagonists, agonists and receptor availability but only a thorough investigation into how BMP ligands interact with one another and how BMP signals are transduced will provide a better understanding of their role during kidney organogenesis.

V. AIM OF THE THESIS

The current state of research

Genetic analysis has established a critical role for the extra-cellular BMP antagonist GREMLIN1 in establishment of epithelial-mesenchymal (E-M) feedback signalling during limb and kidney organogenesis (Michos et al., 2004; Zuniga et al., 1999; Zuniga et al., 2004). Inactivation of *Grem1* in mouse embryos by homologous recombination causes severe defects of distal limb bud development and complete renal agenesis (Michos et al., 2004). Molecular and embryological studies revealed an absolute requirement for *Grem1*-mediated antagonism (i.e. inhibition) of BMP activity to enable progression of limb bud and metanephric kidney organogenesis. In particular, *Grem1*-mediated E-M feedback signalling is required to initiate the transition from static to dynamically propagated signalling centres as organogenesis progresses (Michos et al., 2004) and for temporal coordination of the cellular response to morphogenetic signals (Panman et al., 2006). *Grem1* acts upstream of GDNF-RET-mediated branching morphogenesis in the developing metanephric kidney and upstream of SHH-controlled patterning in the limb bud. Therefore, further analysis of the BMP-Grem1 antagonistic interactions will provide general insights into how the dynamic growth and patterning phase, characteristic of the development of many organs, is initiated/ set-up and co-ordinately controlled.

Objectives

I intended to study the epithelial-mesenchymal (e-m) feedback signalling controlling kidney organogenesis by performing a genetic analysis of BMP-Gremlin1 antagonistic interactions.

In performing these studies I took into consideration the known molecular interactions underlying limb bud and metanephric kidney organogenesis.

The first aim of this Ph.D. project was to identify the BMP ligand(s) antagonised by *Grem1* during limb and kidney organogenesis.

The second aim was to investigate whether and how the local BMP antagonism controls initiation and progression of ureter branching morphogenesis.

The third aim was to genetically assess the contributions of BMP4 and BMP7 to the e-m feedback signalling interactions during kidney and limb bud development.

Detailed Description

This project initially focused on the following major questions:

1. Which are the relevant BMP ligand(s) antagonised by *Grem1* during limb and kidney organogenesis? BMP4 is an obvious candidate in the developing kidney, as others have provided some evidence that this BMP ligand is involved in early metanephric organogenesis. This issue was genetically addressed by generating double mutant embryos (or mice) lacking both *Grem* and *Bmp4*. Of particular interest was to define

and study if inactivation of one and/or both alleles of *Bmp4* in addition to *Gremlin* improves or worsens kidney and/or limb organogenesis. Not only the phenotypes, but also the disrupted or restored underlying molecular cascades were to be analysed as the group has done previously for other double compound mutant embryos (te Welscher et al., 2002). The conditional *Bmp4* allele allows the inactivation of this gene in a tissue and stage-specific manner to analyse both its spatial and temporal requirement in single and double mutant mouse embryos. All the required *Cre* transgenic mouse strains for performing this genetic analysis were available. As well as a conditional *Bmp4* allele, a *Bmp7* loss-of-function was available to assess its role during kidney development in combination with *Gremlin1*.

2. Does local BMP antagonism control branching morphogenesis? In addition to sophisticated mouse genetics, the available culture system for mouse embryonic kidneys is a tool to locally perturb BMP-antagonist interactions in two ways:

Either by recombination of wild-type with mutant tissue following separation of the epithelial and mesenchymal compartments or by engraftment of small cell aggregates expressing either specific BMPs or *Grem1* (Zuniga et al., 1999). Moreover, the invading and branching ureter epithelia can be made to express GFP by crossing the *Hoxb7*-GFP transgene into the desired genetic makeups.

3. Are *Grem1* and *Bmp7* interactions essential for kidney organogenesis?

Grem1/Bmp7 genetic studies were elaborated to investigate the underlying molecular interactions. The question is whether *Bmp7* inactivation can improve or worsens the *Grem1* phenotype. Moreover, *Bmp4/Bmp7* compound mutant mouse/embryos can generate insight into the role of those BMP ligands during metanephric kidney development.

VI. MATERIAL AND METHODS

Genetic analysis of the GREM1–BMP4 interactions (studies performed together with Odysse Michos and Jean-Denis Bénazet)

All animal experiments were performed in accordance with Swiss law and were approved by the regional veterinary authorities.

Grem1 and Bmp4 mouse strains and research approach

The genetic analysis was performed using different mouse strains carrying either conditional or constitutive loss-of-function alleles. *Grem1* is located on mouse chromosome 2, while *Bmp4* is located on mouse chromosome 14. Some studies were executed using a *Hoxb7* transgene inserted into mouse chromosome 11.

The *Grem1–Bmp4* genetic analysis was performed with mice carrying the *Grem1*^Δ null allele (Michos et al., 2004). *Grem1*^Δ mice were crossed with mice carrying the *Bmp4*^Δ allele. The *Bmp4* gene was inactivated in the germline by inter-crossing the floxed *Bmp4*^{loxP-lacZ} allele (Kulesa and Hogan, 2002) with the *Cre* deleter mouse strain (Schwenk et al., 1995). The resulting *Bmp4*^{Δ-lacZ} allele was used to generate compound mutant mice for analysis in a mixed 129/C57BL6 background. Compound mutants carrying the *Hoxb7-GFP* transgene to mark the ureteric epithelium (Srinivas et al., 1999) were also used for analysis. The primer pairs used for genotyping all wild-type and mutant alleles are listed in Table 1. Embryonic tissue, preferentially the head or extra-

embryonic membranes, was used for genotyping embryos and tail tip or ear punch biopsies, were used to genotype mice at weaning age.

Bmp4 spatiotemporal conditional inactivation

A Tamoxifen (TM)-inducible form of the P1 phage-derived integrase Cre was used to recombine genes at specific time points during embryonic development using loxP target sites. Hayashi and MacMahon generated the *Cre-ERTM* transgenic mouse line by fusing Cre and a mutated form of the ligand binding domain of the estrogen receptor (ER) that renders Cre activity tamoxifen (TM) inducible (Hayashi and McMahon, 2002). Wide spread expression in embryos and mice was obtained by putting *Cre-ERTM* under control of the cytomegalovirus immediate-early enhancer and the chicken β -actin promoter/enhancer (CAGG) (Niwa et al., 1991). Females carrying one *Bmp4^Δ* allele were crossed with *Cre-ERTM* males to generate *Bmp4^{Δ/+}; Cre-ER^{TM/+}* males. Females homozygous for the conditional *Bmp4^{loxP-lacZ}* were crossed with these *Bmp4^{Δ/+}; Cre-ER^{TM/+}* males. Pregnant females received an intraperitoneal (IP) injection with tamoxifen and/or embryos were collected and kidney rudiments cultured in the presence of 4OH-tamoxifen.

Reagents:

Tamoxifen preparation for IP injection:

A stock solution of 100 mg/ml TM (Sigma) in ethanol (pure grade) was diluted in corn oil (Sigma) to achieve a 20 mg/ml final concentration. 40 mg/ml of progesterone (Sigma) was added to attenuate the abortive effects of TM. An emulsion was obtained after 30 minutes of sonication and 150 μ l of TM-

progesterone solution was injected intraperitoneally into pregnant females (3 mg TM/mouse) at the embryonic days indicated (E8.75-E9.5).

4OH-tamoxifen preparation for kidney cultures:

A stock solution of 100 mg/ml 4OH-TM (Sigma) was prepared in ethanol. The stock solution was then diluted to 100 µg/ml and 100ng/ml and stored in aliquots at 20°C.

Genetic analysis of GREM1–BMP7 interactions

Both *Grem1* and *Bmp7* are located on the mouse chromosome 2, therefore the following genetic approach was required. Mice carrying the *Grem1*^Δ null allele (Michos et al., 2004) were crossed with *Bmp7*^Δ null mice (Karsenty et al., 1996) and their offspring was crossed with wild-type 129 mice. The resulting F2 offspring were screened for mice carrying both mutations in *cis* due to germline recombination. *Grem1*^{Δ/Δ}; *Bmp7*^{Δ/Δ} double homozygous embryos were generated by inter-crossing males carrying both mutations in *cis* with females carrying both mutations either in *cis* and *trans*. To generate single mutant *Grem1*^{Δ/Δ} or *Bmp7*^{Δ/Δ} embryos/mice carrying the respective Δ null alleles were inter-crossed. The same inter-crosses were used to obtain newborn mice for analysis. The genetic background influence was assessed and the results are in Table 1. The primers listed in Table 2 were used for genotyping.

Table 1 – Assessment of the background effect in the *Grem1*; *Bmp7* analysis.

Genotypes	2 kidneys	1 Kidney	0 kidneys	Total
<i>Grem1</i> ; <i>Bmp7</i> x <i>Grem1</i> ; <i>Bmp7</i>				
<i>Grem1</i> ^{ΔΔ}	0	1 (10%)	9 (90%)	10
<i>Grem1</i> ^{ΔΔ} ; <i>Bmp7</i> ^{Δ/+}	0	1 (2,4%)	14 (93%)	15
<i>Grem1</i> x <i>Grem1</i> ; <i>Bmp7</i>				
<i>Grem1</i> ^{ΔΔ}	0	0	7 (100%)	7
<i>Grem1</i> ^{ΔΔ} ; <i>Bmp7</i> ^{Δ/+}	0	1 (17%)	5 (83%)	6

Table 2 – Primers used for PCR genotyping of mice and embryos.

Gene	Forward Primer	Reverse Primer	Allele
<i>Grem1</i>	ATGAATCGCACCCGCATACACTG	TCCAAGTCGATGGATATGCAACG	Wt
	GGCACATGGCTGAATATCGACGG	AAGCGCCTCCCCTACCCGGTA	null
<i>Bmp4</i>	GTGTGTGTAGGGTGTGAGGGAGAAA	CCCGGTCTCAGGTATCAAACACTAGCA	Wt/f
	ATGAATCGCACCCGCATACACTG	ATGAATCGCACCCGCATACACTG	null
<i>Bmp7</i>	TTGTGCTGTGTAGACTGGGTG	TTTGTAGGAGTGGTAGGGTGC	Wt
	TGTTCTCCTCTTCCTCATCTCC	ACCCTTTCCAAATCCTCAGC	null
<i>Hoxb7</i>	AGCGCGATCACATGGTCCTG	ACGATCCTGAGACTTCCACACT	tg
<i>Cre</i>	GCCTGCATTACCGGTCGATGCAACGA	GTGGCAGATGGCGCGGCA ACACCA TT	tg

Molecular and morphological analysis of embryos and organs

Embryos were accurately staged by determining their somite numbers. After embryonic day 12, the somite numbers were no longer considered, unless there was an obvious developmental delay. The kidney rudiments were dissected with approximately 2/3 of the Wolffian duct. Whole-mount and section RNA *in situ* hybridisation, immunohistochemistry (IHC) and detection of β -galactosidase activity were performed.

Paraffin embedding and histological sections of embryos and kidney rudiments were performed as follows:

Paraffin embedding

After embryo collection or organ dissection, samples were fixed overnight (O/N) with 4%PFA in PBS at 4°C.

Embryos were gradually dehydrated using a serial dilution of EtOH in dH₂O. The ethanol serial washes were done either on ice or in the 4°C room:

PBS 2 X 10 minutes

30% EtOH 3 X 20 minutes

50% EtOH 3 X 20 minutes

70% EtOH 3 X 20 minutes

Samples can be stored for a long time in 70% EtOH at 4°C before sectioning. Next day, the samples in 70% EtOH were allowed to warm up to room

temperature (RT) and the protocol proceeded with several washes and incubation periods towards paraffin wax embedding:

100% EtOH 3 X 20 minutes at RT

100% xylene 3 X 15 minutes at RT

Incubation in paraffin wax: xylene (1:1) 30 minutes at 60°C

Incubation in paraffin wax 3 X 60 minutes, 60°C

Embryos were transferred to embedding molds with fresh paraffin wax. The paraffin was kept warm on a heating plate to correctly orientate the samples. Paraffin was then allowed to become hard O/N, RT. The paraffin blocks were kept at 4°C before sectioning.

Coating slides with 3-triethoxysilylpropylamine (TESPA)

Pre-cleaned glass slides of high enough quality for both *in situ* and immunohistochemical techniques were used. For *in situ* hybridization, the slides were treated with diethyl pyrocarbonate (DEPC) to destroy RNases. The slides were coated with TESPA (Sigma-Aldrich) for tight adherence of sections, which ensured that they did not detach during subsequent hybridisation and extensive washing.

Slides were coated using histology glass tanks and slides supports as follows (washes at RT):

1 minute in 2N HCl

1 minute in milliQ water

1 minute in 100% acetone (pure)

1 minute in TESP/acetone (1:1)

1 minute 100% acetone

1 minute 95%EtOH

1 minute 50% EtOH

1 minute 30% EtOH

3 X 1 minute in milliQ water

The slides were dried O/N in a 42°C oven and stored at 4°C in boxes.

Histological sectioning of paraffin-embedded samples

Sections were prepared at the Department of Histology, Anatomy Institute of the University of Basel. For histological analysis, 7-10 µm sections were prepared from the paraffin-embedded samples fixed in 4% PFA. Dewaxed sections were either stained with haematoxylin and eosin or periodic acid schiff (PAS) to reveal the brush border (microvilli) of the distal and proximal tubules. The sections that were prepared for *in situ* hybridization or IHC were stored at 4°C.

Whole-mount in situ hybridization - modified from David Wilkson's protocol (Wilkinson, 1992)

Embryos and dissected kidney rudiments were collected in PBS and fixed O/N in 4% paraformaldehyde (PFA Sigma in PBS) and dehydrated using an increasing methanol series and stored in methanol at -20°C. The dehydration and all the following procedures, except the proteinase K treatment, were performed using a rocking platform shaker. Early embryos or kidney rudiments were stored and handled in 2 ml Eppendorf tubes or multi-well plates. Following

their genotyping and matching of developmental stages, embryos were rehydrated using a reverse methanol into PBT series (PBT: PBS with 0.1% Tween 20). Embryos/organs were bleached for 15 minutes using H₂O₂ (Sigma) in PBT and washed 3 X 5 minutes in PBT. Embryos were digested using 10 µg/ml Proteinase K (mesenchymal treatment) in PBT according to the following Table:

Developmental Stage	Incubation Time
38-40 somites (E10.75)	5 minutes
41-45 somites (E11.0)	6-7 minutes
46-50 somites (E11.5)	8-10 minutes
51-55 somites (E11.75)	11 minutes
E12.5	12 minutes
E13.5 – E15.5	15 minutes

E10.75 – E11.5 kidneys cultured for 48 hours were digested with proteinase K for 6 minutes only. Proteinase K was inhibited by rinsing the slides for 5 min in glycine/PBT (2 mg/ml) solution. The samples were then rinsed twice in PBT and fixed 20 minutes in 4% PFA, PBS, 0.2% glutaraldehyde (Sigma). After rinsing twice for 5 minutes in PBT, embryos were pre-hybridized 3 hours at 65°C with 2 ml of hybridization buffer. After this pre-hybridization, the solution was replaced by hybridization solution (prewarmed to 70°C) containing 10 µl/ml of digoxigenin-labelled RNA probe. The hybridization was incubated O/N at 70°C in an oven with a rotor.

After O/N incubation, embryos were changed into 2X SSC in a graded manner by replacing the hybridization probe solution with hybridization buffer and a

graded 2X SSC series at 70°C. After incubating twice for 30 minutes with 2X SSC/0.1% CHAPS at 70°C, an RNase A (20 mg/ml in 2X SSC, 0.1% CHAPS) digestion was performed for 45 minutes at 37°C to remove non-specific single stranded RNA molecules. Samples were washed twice for 10 minutes with 100 mM maleic acid, 150 mM NaCl pH 7.5 at room temperature and then twice at 70°C with the same solution. After two final washes in PBS and 5 minutes in PBT at room temperature, samples were blocked for 2-3 hours in 10% sheep serum, 1% bovine serum albumin (BSA) in PBT before adding the anti-digoxigenin antibody (Fab fragments Roche). The antibody solution was prepared by heat inactivating 3 mg/ml of embryo powder in PBT for 30 minutes at 70°C and quenching on ice. 1 µl/ml anti-digoxigenin antibody (Fab fragments Roche), 10 mg/ml BSA and 10% inactivated sheep serum were added to the embryo powder in PBT solution and it was kept rocking at 4°C for 2-3 hours to pre-absorb the antibody. The antibody solution was then centrifuged at 10,000 rotations per minute (RPM) for 10 minutes and the supernatant diluted 1:1 with blocking solution. The blocking solution was then replaced by the antibody solution and the samples were incubated overnight at 4°C.

Next day, embryos were washed 5 X 45 minutes with PBT, 0.1% BSA, twice 30 minutes with PBT and 3 X 10 minutes in NTMT. The signal was then revealed by incubating the samples in the dark with BM purple solution (Roche) at room temperature. The coloration process was visually monitored and stopped in NTMT followed by 3 washes with PBT. For long-term stabilization of the staining, the samples were stored in 4% PFA in PBS at 4°C.

Reagents:**Hybridization buffer:**

50% formamide (deionized, extra pure)

5X SSC pH 4.5 (from a 20x stock: 3 M NaCl , 0.3 M tri-sodium citrate dehydrate)

2X Blocking Reagent (Roche)

0.1% Tween 20

0.5% CHAPS

5 mM EDTA 50

50 µg/ml yeast tRNA

50 µg/ml heparin

NTMT:

100 mM NaCl

100 mM Tris HCl pH 9.5

50 mM MgCl₂

0.1% Tween 20

β-Galactosidase staining of embryos and kidney rudiments

Samples were isolated, staged on a petri dish and transferred into 2 ml *Eppendorf* tubes containing ice-cold PBS. All samples must be kept ice-cold to preserve β-Gal activity. PBS was replaced by fixative solution and samples were fixed during 25 minutes at 4°C on a rocking platform. Samples were rinsed 3 times for 5 minutes in PBS at RT. Solutions X, K3 and K4 were brought to RT away from the light during the

samples PBS washes. PBS was then replaced by staining solution and samples were stained at 37°C in a rotating oven (protected from light). The staining reaction requires from several hours to overnight periods. The reaction was stopped by RT PBS washes and samples stored in 4% PFA in PBS. If stained samples were to be used for *in situ* hybridization, samples had to be fixed in 4% PFA in PBS for at least 4 hours at 4°C and dehydrated with the regular MetOH/PBT series.

Reagents:

Fixing solution

37% Formaldehyde	1.35 ml
25% Gluteraldehyde	400 µl
10%NP40 (Igepal)	100 µl
1% Sodium deoxycholate	500 µl

Add PBD to 50 ml final volume

Staining solution for embryos up to E12.5

Solution X (X-gal 40 mg/ml)	625 µl
*Solution K3 (500 mM K ₃ Fe(CN ₆))	25 µl
*Solution K4 (500 mM K ₄ Fe(CN ₆))	25 µl

10% NP40	50 μ l
----------	------------

MgCl ₂ 1M	20 μ l
----------------------	------------

Add PBS to 50 ml

Staining solution for embryos E13.5 or older

Solution X (X-gal 40 mg/ml)	625 μ l
-----------------------------	-------------

*Solution K3 (500 mM K ₃ Fe(CN ₆))	25 μ l
---	------------

*Solution K4 (500 mM K ₄ Fe(CN ₆))	25 μ l
---	------------

10% NP40	50 μ l
----------	------------

MgCl ₂ 1M	20 μ l
----------------------	------------

1% Sodium deoxycholate	500 μ l
------------------------	-------------

Add PBS to 50 ml

*For genes that are highly expressed used 10x as much.

Stock solutions

X-Gal dissolved in dimethyl formamide at 40 mg/ml, store at -20°C

500 mM potassium ferricyanide (K3) in PBS (3.3 g in 20 ml PBS, store in 1 ml aliquots at -20°C and do not re-freeze).

500 mM potassium ferricyanide (K4) in PBS (4.2 g in 20 ml PBS, store in 1 ml aliquots at -20°C and do not re-freeze).

Immunohistochemistry (IHC) assays

Samples were isolated, staged and transferred into 10 ml glass vials containing cold PBS. The solution was then replaced by freshly made 4% PFA in PBS and the vials were put at 4°C on a rocking platform for overnight fixation. After fixation, samples were processed according to the previously described procedures for "Paraffin Embedding".

PODOCALYXIN and CYTOKERATIN Double Immunostaining

Immunostaining for PODOCALYXIN reveals the C-shaped aggregates of podocytes of the renal glomeruli (Schmidt-Ott et al., 2006). In addition, CYTOKERATIN detection reveals the ureteric bud branches and collecting system epithelia. The simultaneous detection of these markers was a good tool to assess the kidneys integrity.

Dewaxed sections slides were boiled at 120°C for 90 seconds in 10 mM Sodium Citrate ($C_6H_5Na_3O_7 \cdot 2H_2O$ – Merck) for antigen retrieval. Slides were immediately removed from the pressure cooker and let to cool off at room temperature for 30 minutes. After being rinsed in tap water and washed twice for 5 minutes with 0.1% Triton-10 in PBS, the sections were pre-blocked one hour with PBS, 0.1% Triton-10, 10% donkey serum, 0,2% BSA at RT. After washing sections three times with PBS, 0.1% Triton-10, the sections were incubated with the primary antibody solution overnight at 4°C.

Primary antibody solution in PBS, 0.1% Triton-10:

Polyclonal goat anti-mouse Podocalyxin (R&D Systems) 1:50

Monoclonal mouse anti-pan Cytokeratin (Sigma) 1:50

The next day, the antibody solution was removed and the sections were washed with PBS, 0.1% Triton-10 for three hours (6 X 30 minutes washes). The antibody was recovered because it can be re-used once. The PBS, 0.1% Triton-10 was replaced by the secondary antibody and the sections were incubated for one hour at RT in the dark.

Secondary antibody solution in PBS, 0.1% Triton-10:

Cy2 (green) donkey anti-mouse IgG (Amersham) 1:200

Cy3 (red) donkey anti-goat IgG (Amersham) 1:100

The sections were washed with PBS, 0.1% Triton-10 for two hours (4 X 30 minutes). A counterstain with Hoechst 33258 (5 mg/ml) was performed for 5 minutes to reveal the nuclei followed by a PBS wash for 5 minutes more. The slides were then mounted with Mowiol (Calbiochem).

Reagents:

Mowiol preparation

1. Weigh 6 g glycerol (water-free) into a 50 ml Falcon Tube
2. Add 2.4 g of Mowiol 4-88 (Calbiochem)3. Mix very well
4. Add 6 ml of H₂O
5. Mix for 2 hours at RT
6. Add 12 ml of 0.2 M Tris HCl pH 8.5
7. Incubate solution at 53°C until everything is completely in solution, stir occasionally
8. Spin at 4.000 to 5.000 RPM for 20 minutes at RT
9. Aliquot clear supernatant into glass vials and store at -20°C until used
10. Use a defrosted aliquot for mounting, do not refreeze

Kidney rudiment cultures

Kidney primordia culture

Kidney primordia were isolated from somite-staged wild-type and mutant embryos. Kidney rudiments were cultured in DMEM (Dulbecco's Modified Eagle Medium) + GlutamaxTM-I (Gibco) supplemented with 10% foetal bovine serum (Invitrogen) and 0.5% penicillin-streptomycin (Invitrogen) on Nucleopore filters (0.1 µm pore size, Corning) as previously described (Lin et al., 2001) with the following modifications. Experiments were performed using E10.75-11.25 (38-44 somites) embryos instead of the classic T-shape stages (E11.5, 48-50 somites). It is important to realise that it is not possible to efficiently rescue

kidney primordia from *Grem1*-deficient embryos older than E11.25. A piece of Gelfoam (Pfizer) was soaked in medium and the Nucleopore filter with the kidney primordia was placed on top in a 6-well plate and incubated in a humidified atmosphere at 37°C with 5% CO₂. Mouse recombinant GREM1 (R&D Systems – catalogue number 956-GR) was added to the culture medium at 2-5 µg/ml and changed every 48 hours. Noggin-conditioned medium was produced using the B3-CHO cell line (Smith et al., 1993) and used at a dilution of 1:4. Rat recombinant GDNF (R&D Systems - catalogue number 512-GF) was used at 100 ng/ml final concentration. After culture, the kidney primordia were fixed in 4% paraformaldehyde (PFA) and processed for molecular analysis.

Semi-quantitative RT-PCR analysis

Kidney rudiments were collected either directly or after 48 hours in culture into RNA-later (Ambion). RNA was isolated from four kidney rudiments per genotype using the RNeasy kit (Qiagen) and reverse transcribed using Superscript III (Invitrogen). The cDNA contents of all samples were normalised for their *β-actin* (*Actb* – Mouse Genome Informatics) transcripts (primer sequences: forward 5'-ACACTGTGCCCATCTACGAGG-3'; reverse 5' CATGGATGCCACAGGATTCC-3').

The relative levels of *Gdnf* and *Grem1* transcripts were determined using established primers [*Gdnf* (Towers et al., 1998); *Grem1*(Zuniga et al., 2004)] located in two different exons to avoid potential amplification of genomic DNA:

- *Gdnf* forward primer: 5'- CGCTGACCAGTGACTCCAATATGC -3'
- *Gdnf* reverse primer: 5'- ACATTGTCTCGGCCGATTCACAGG -3'

The PCR products were separated on 1.8% agarose gels and visualised by ethidium bromide staining. Digital images were acquired to determine the relative expression levels using the LI-COR Odyssey Imaging Software (version 2.0). Three completely independent series of experiments were performed to assess *Gdnf* expression.

Affymetrix gene chip microarray analysis

To investigate which genes were involved in the restoration of the *Grem1*^{ΔΔ} kidney phenotype, a microarray analysis experiment was designed to allow us to compare the wild-type, *Grem1*^{ΔΔ} and *Grem1*^{ΔΔ}; *Bmp4*^{Δ/+} kidney rudiments. A high resolution expression analysis, comprising more than 750,000 unique 25-mer oligonucleotides constituting more than 28,000 gene-level probe sets, was performed using GeneChip® Mouse Gene 1.0 ST Arrays (Affymetrix).

Kidney rudiments collection, gender determination and RNA isolation

Kidney rudiments were collected from E11.25-11.5 (47-48 somites) embryos and put into RNA-later (Ambion). Embryos heads were isolated and extracted genomic DNA used to determine the genotype and gender of the embryos (heads were split in half for posterior independent analysis if required). Sex determination was performed using the Sex-determining Region Y (*Sry*), which is a sex-determining gene on the Y chromosome in the therians (placental mammals and marsupials (Wallis et al., 2008) and *Myogenin* (*Myog*) was used as an internal control as described in (McClive and Sinclair, 2001). Triplicates of each genotype of interest (wild-type, *Grem1*^{ΔΔ} and *Grem1*^{ΔΔ}; *Bmp4*^{Δ/+}) were then processed for analysis.

The primers used to determine the embryo's gender were:

- Sry forward primer: 5'- TCATGAGACTGCCAACCACAG -3'
- Sry reverse primer: 5'- CATGACCACCACCACCACCAA -3'
- Myog forward primer: 5'- TTACGTCCATCGTGGACAGC -3'
- Myog reverse primer: 5'- TGGGCTGGGTGTTAGTCTTA -3'

RNA isolation and analysis

Male kidney rudiments stored in RNA-later were processed for RNA extraction. RNA isolation was performed using the Qiagen Mini Kit. RNA was extracted using *RNeasy* Mini Spin Columns (Qiagen) using the Qiagen recommended protocol. RNA fragment length degradation was assessed using an Agilent Bioanalyzer. An average of 3µg of total RNA was extracted. 5µl RNA samples with a concentration of 60 ng/ µl of RNA were given to the Friedrich Miescher Institute Functional Genomics department for microarray hybridization, posterior data mining and analysis.

Affymetrix Genechip® hybridization and scanning

The regular Affymetrix "GeneChip® Whole Transcript (WT) Sense Target Labelling Assay" was followed using 240 ng of the kidneys rudiments RNA from the different genotypes. Briefly, double-stranded cDNA was synthesized with random hexamers tagged with a T7 promoter sequence. The double-stranded cDNA was subsequently used as a template and amplified by T7 RNA polymerase producing many copies of antisense cRNA. In the second cycle of cDNA synthesis, random hexamers were used to prime reverse transcription of the cRNA from the first cycle to produce single-stranded DNA in the sense

orientation. The synthesized cRNA was used for hybridization to a single array. One Affymetrix Mouse Gene 1.0 ST Array was used per genotype (one kidney rudiments pair per genotype). Chips were hybridized for 17 hours at 45°C using a GeneChip® Fluidics Station 450 and GeneChip®s were scanned with the GeneChip® Scanner 3000.

Genedata Expressionist Microarray data mining and Ingenuity® (Ingenuity Systems Inc.) pathway analysis

Genedata Expressionist® was used and different statistical analysis tools were applied to generate reliable and reproducible results. After verifying the expression values per chip/experiment, an N-Way ANOVA was applied to the dataset. To reduce the probability of analysing hits, GeneChip® probes that hybridized with the cRNAs) that were due to biological variability and experimental imprecision, a P-VALUE $p < 0.05$ was defined (it indicates a statistical significance over 95%). Once the primary data was filtered the analysis proceeded comparing the statistically validated targets from the different genotypes samples. “Side-by-side” comparisons were done between pairs of different genotypes. After performing the Genedata Expressionist® data mining, the list of hybridized probes (hits) was used with Ingenuity®. Pairwise comparisons were made as follows: wild-type versus *Grem1*^{Δ/Δ}, *Grem1*^{Δ/Δ}; *Bmp4*^{Δ/+} versus *Grem1*^{Δ/Δ} and *Grem1*^{Δ/Δ}; *Bmp4*^{Δ/+} versus wild-type. The “Top Networks” and “Top Bio Functions” were assessed and based on that analysis a new putative network of genes was designed and used for genetic and molecular analysis.

VII. REDUCTION OF BMP4 ACTIVITY BY GREMLIN1 ENABLES URETERIC BUD OUTGROWTH AND GDNF/WNT11 FEEDBACK SIGNALING DURING KIDNEY BRANCHING MORPHOGENESIS

PUBLICATION:

Odyssé Michos*, Alexandre Gonçalves*, Javier Lopez-Rios, Eva Tiecke, Florence Naillat, Konstantin Beier, Antonella Galli, Seppo Vainio and Rolf Zeller. **Reduction of BMP4 activity by gremlin 1 enables ureteric bud outgrowth and GDNF/WNT11 feedback signalling during kidney branching morphogenesis.** * These authors contributed equally to this work. *Development* 134, 2397-2405 (2007).

Summary

Antagonists act to restrict and negatively modulate the activity of secreted signals during progression of embryogenesis. In mouse embryos lacking the extra-cellular BMP antagonist Gremlin1 (*Grem1*), metanephric development is disrupted at the stage of initiating ureteric bud outgrowth. Treatment of mutant kidney rudiments in culture with recombinant Gremlin1 protein induces additional epithelial buds and restores outgrowth and branching. All epithelial buds express *Wnt11*, and *Gdnf* is significantly upregulated in the surrounding mesenchyme, indicating that epithelial-mesenchymal (e-m) feedback signalling is restored. In the wild type, *Bmp4* is expressed by the mesenchyme enveloping the Wolffian duct and ureteric bud and *Grem1* is upregulated in the

mesenchyme around the nascent ureteric bud prior to initiation of its outgrowth. In agreement, BMP activity is reduced locally as revealed by lower levels of nuclear pSMAD protein in the mesenchyme. By contrast, in *Grem1*-deficient kidney rudiments, pSMAD proteins are detected in many cell nuclei in the metanephric mesenchyme, indicative of excessive BMP signal transduction. Indeed, genetic lowering of BMP4 levels in *Grem1*-deficient mouse embryos completely restores ureteric bud outgrowth and branching morphogenesis. The reduction of BMP4 levels in *Grem1* mutant embryos enables normal progression of renal development and restores adult kidney morphology and functions. This study establishes that initiation of metanephric kidney development requires the reduction of BMP4 activity by the antagonist Gremlin 1 in the mesenchyme, which in turn enables ureteric bud outgrowth and establishment of autoregulatory GDNF/WNT11 feedback signalling.

Introduction

Mammalian kidney organogenesis is regulated by reciprocal epithelial-mesenchymal (e-m) signalling interactions that involve inductive signalling between ureteric bud epithelium and metanephric mesenchyme (Saxen, 1987; Yu et al., 2004). In mouse embryos, the ureteric bud forms around embryonic day (E) 10.5 as an epithelial swelling in the caudal-most part of the Wolffian duct. Development of the definitive kidney is initiated when the ureteric bud elongates to invade and induce the metanephric mesenchyme. In turn, the induced metanephric mesenchyme produces signals that initiate nephrogenesis.

During ureteric bud outgrowth, the epithelial tip region thickens to form an ampulla just prior to appearance of the first epithelial branch (Shakya et al., 2005). In addition, this process induces condensation of the metanephric mesenchyme, which is the first morphological sign of nephrogenesis (Saxen, 1987). Many of the human congenital anomalies of the kidney and urinary tract (CAKUT) are caused by defects in these early inductive events, but their aetiology remains poorly understood (Batourina et al., 2002; Pope et al., 1999).

During the last decade, significant parts of the molecular networks and e-m feedback signalling interactions that regulate mammalian kidney organogenesis have been identified (Costantini and Shakya, 2006; Vainio and Lin, 2002). It is established that ureteric bud formation and the induction of its branching require GDNF (glial cell line derived neurotrophic factor), a secreted growth factor that is expressed by the metanephric mesenchyme. The GDNF ligand interacts with its cognate receptor RET (ret proto-oncogene), which is first expressed by the Wolffian duct and then by the ureteric epithelial tips as branching morphogenesis progresses (Schuchardt et al., 1996). The current view is that establishment of signalling between GDNF, RET and its co-receptor GFR α 1 (glial cell line derived neurotrophic factor family receptor α 1) is essential for ureteric bud formation and initiation of outgrowth and branching (Costantini and Shakya, 2006). As the rostral part of the Wolffian duct initially expresses *Ret*, it is competent to form supernumerary buds and branches upon exposure to GDNF (Shakya et al., 2005). Therefore, a mechanism must exist that restricts ureteric bud formation to the caudal-most part of the Wolffian duct. Indeed, supernumerary epithelial buds form in mouse embryos lacking either SLIT2 or

ROBO2 functions, the SPRY1 intra-cellular antagonist or the FOXC1 transcriptional regulator. Molecular analysis showed that SLIT2 and/or ROBO2 signalling is required to restrict *Gdnf* expression to caudal mesenchyme (Grieshammer et al., 2004). FOXC1 is also required for caudal restriction of *Gdnf* (Kume et al., 2000), but is not a target of SLIT2/ROBO2 signalling (Grieshammer et al., 2004). By contrast, SPRY1, an intra-cellular antagonist of tyrosine kinase receptors, reduces the sensitivity of the Wolffian duct to GDNF, such that only one ureteric bud forms (Basson et al., 2005; Chi et al., 2004). In *Spry1*-deficient mouse embryos, ectopic epithelial buds form and multiple- and hydroureters are formed, which results in phenotypes identical to the human CAKUT syndrome (Basson et al., 2005). However, ectopic expression of *Spry2* in the Wolffian duct sensitises the epithelium to GDNF signalling, which again results in formation of supernumerary epithelial buds (Chi et al., 2004). Hence, the current view is that the interaction of these different signal transduction cascades restricts GDNF expression and activity such that only one ureteric bud forms in the caudal-most part of the Wolffian duct (Basson et al., 2005; Grieshammer et al., 2004). Metanephric kidney development is then initiated by the onset of ureteric bud outgrowth, and invasion and induction of the metanephric mesenchyme under the influence of GDNF-RET signalling (Costantini, 2006).

Wnt11 expression is activated in the epithelial tip of the ureteric bud and WNT11 signalling is in turn required to propagate mesenchymal GDNF signalling, which results in establishment of an autoregulatory e-m feedback signalling loop (Majumdar et al., 2003). In *Wnt11*-deficient mouse embryos, *Gdnf* expression

remains lower and the number of epithelial branches is reduced. Conversely, the disruption of GDNF signal reception in *Ret*-deficient embryos reduces *Wnt11* expression. Therefore, autoregulatory GDNF-WNT11 feedback signalling co-ordinately controls the progression of metanephric branching morphogenesis after initiation of ureteric bud outgrowth (Majumdar et al., 2003). During branching, the ureteric epithelial tips secrete additional signals (e.g. WNT9b) (Carroll et al., 2005), which induce nephrogenesis. Nephrogenesis is regulated by transcriptional activation of another WNT signal, WNT4 in the condensing mesenchyme. Mouse embryos that lack *Wnt4* fail to form metanephric kidneys due to disruption of the mesenchyme to epithelial transition of the nephrogenic precursors (Stark et al., 1994).

Several BMP ligands and their receptors are expressed during metanephric kidney organogenesis, but relatively little is known about their essential roles in these processes as loss-of-function mutations often cause early embryonic lethality. However, genetic inactivation of *Bmp7* in mouse embryos leads to premature depletion of the nephrogenic mesenchyme, which manifests itself in a dysplastic kidney phenotype (Dudley et al., 1995; Luo et al., 1995). A recent study shows that BMP4 can compensate for the lack of *Bmp7* during metanephric kidney development, which indicates that BMPs could potentially replace one another during kidney organogenesis (Oxburgh et al., 2005). Furthermore, a small fraction of mice heterozygous for a *Bmp4* loss-of-function allele display CAKUT-like phenotypes and/or multicystic dysplastic kidneys (Miyazaki et al., 2000). This phenotype is likely caused by defects in ureteric stalk elongation, but treatment of metanephric kidney primordia with

recombinant BMP4 also interferes with epithelial branching morphogenesis in culture, which indicated that BMP4 activity may require dynamic modulation (Miyazaki et al., 2000; Raatikainen-Ahokas et al., 2000). Gremlin 1 (GREM1) is a member of the CAN domain family of extra-cellular BMP antagonists that binds BMP2 and BMP4 with highest affinity in vitro (Hsu et al., 1998). However, the ligands antagonised by GREM1 in vivo during vertebrate embryogenesis remained elusive to date. We recently showed that *Grem1* is expressed by the meso and metanephric mesenchyme and that metanephric kidney organogenesis is disrupted in *Grem1*-deficient mouse embryos, resulting in bilateral renal agenesis and neo-natal lethality (Michos et al., 2004). In particular, metanephric kidney development is blocked at the stage of initiating of ureteric bud outgrowth. However, *Gdnf* expression is initially normal in the metanephric mesenchyme and the epithelium continues to express *Ret*. The block in initiating ureteric bud outgrowth causes progressive loss of *Gdnf* expression and elimination of the metanephric mesenchyme by apoptosis.

In the present study, we established that culturing early *Grem1*-deficient kidney primordia in medium supplemented with recombinant GREM1 restores ureteric bud outgrowth and supernumerary epithelial buds are induced. Multiple epithelial buds invade the metanephric mesenchyme and initiate branching morphogenesis. *Wnt11* expression in the epithelial tips and *Gdnf* expression in the metanephric mesenchyme around the epithelium is restored, which is indicative of establishment of e-m feedback signalling in GREM1-treated mutant kidney primordia. We identify excessive BMP activity in the metanephric mesenchyme around the ureteric bud as the primary signalling defect in *Grem1*-

deficient mouse embryos. As a consequence, the invasion of the mutant metanephric mesenchyme by the ureteric bud and concurrent establishment of the autoregulatory GDNF/WNT11 feedback signalling loop are disrupted. Therefore, it was important to identify the BMP ligand(s) antagonised by GREM1 in the mesenchyme. BMP4 was identified as a relevant BMP signal by its partially overlapping expression with *Grem1* during initiation of ureteric bud outgrowth and by genetic complementation: inactivation of only one copy of the *Bmp4* gene in *Grem1*-deficient mouse embryos completely restores metanephric kidney organogenesis and functions. We conclude that GREM1-mediated reduction of BMP4 activity in the mesenchyme around the nascent ureteric bud is essential to (1) initiate ureteric bud outgrowth and invasion of the metanephric mesenchyme, and (2) enable autoregulatory e-m feedback signalling that regulates the dynamics of epithelial branching morphogenesis.

Results

The BMP antagonist gremlin 1 induces supernumerary epithelial buds and restores invasion and branching in Grem1-deficient kidney primordia.

We have previously shown that metanephric kidney development arrests prior to initiation of ureteric bud outgrowth in *Grem1*-deficient mouse embryos (Michos et al., 2004). To gain insight into the functions of GREM1 during the inductive phase of metanephric kidney organogenesis, wild-type and *Grem1*-deficient metanephric kidney primordia (E11.0-11.25, 40-44 somites; expressing the *Hoxb7*-GFP transgene) (Srinivas et al., 1999) were cultured for up to 96 hours in

the presence or absence of soluble recombinant GREM1 protein. In contrast to wild-type controls (Fig. 1A), the development of *Grem1*-deficient kidney primordia arrests at the ureteric bud stage (Fig. 1B, $n=13/16$). Supplementation of the culture medium with GREM1 (5 $\mu\text{g/ml}$) restores ureteric epithelial outgrowth and branching (Fig. 1C,D; $n=12/16$) and induces several supernumerary epithelial buds (on average two to four; indicated by red asterisks in Fig. 1C,D). Most supernumerary buds appear within 48 hours and by 96 hours the ureteric and ectopic epithelial buds have undergone between two and four branching events (Fig. 1C,D). Epithelial tracings of the GREM1-treated *Grem1* mutants (right-most panels in Fig. 1C,D) reveals that branching of the ureteric bud is delayed by at least 24 hours in comparison to the wild-type (right-most panels in Fig. 1A,E). Ureteric epithelial outgrowth and branching are also restored and ectopic epithelial buds induced when mutant kidneys are cultured in the presence of less recombinant GREM1 (2 $\mu\text{g/ml}$; data not shown) or the unrelated BMP antagonist noggin (see Fig. S1). In wild-type, recombinant GREM1 also induces ectopic epithelial buds (red asterisks) and ectopic branches of the ureteric epithelium (blue asterisks, Fig. 1E). In general, treatment with soluble BMP antagonists induces more ectopic epithelial buds in the rostral part of the mutant Wolffian duct (red asterisks, Fig. 1C,D, and see Fig. S1) than in wild-type kidney primordia (red asterisks, Fig. 1E). Therefore, the potential for ectopic epithelial bud formation appears increased in the mutant, possibly due to the early developmental arrest of *Grem1*-deficient kidney primordia.

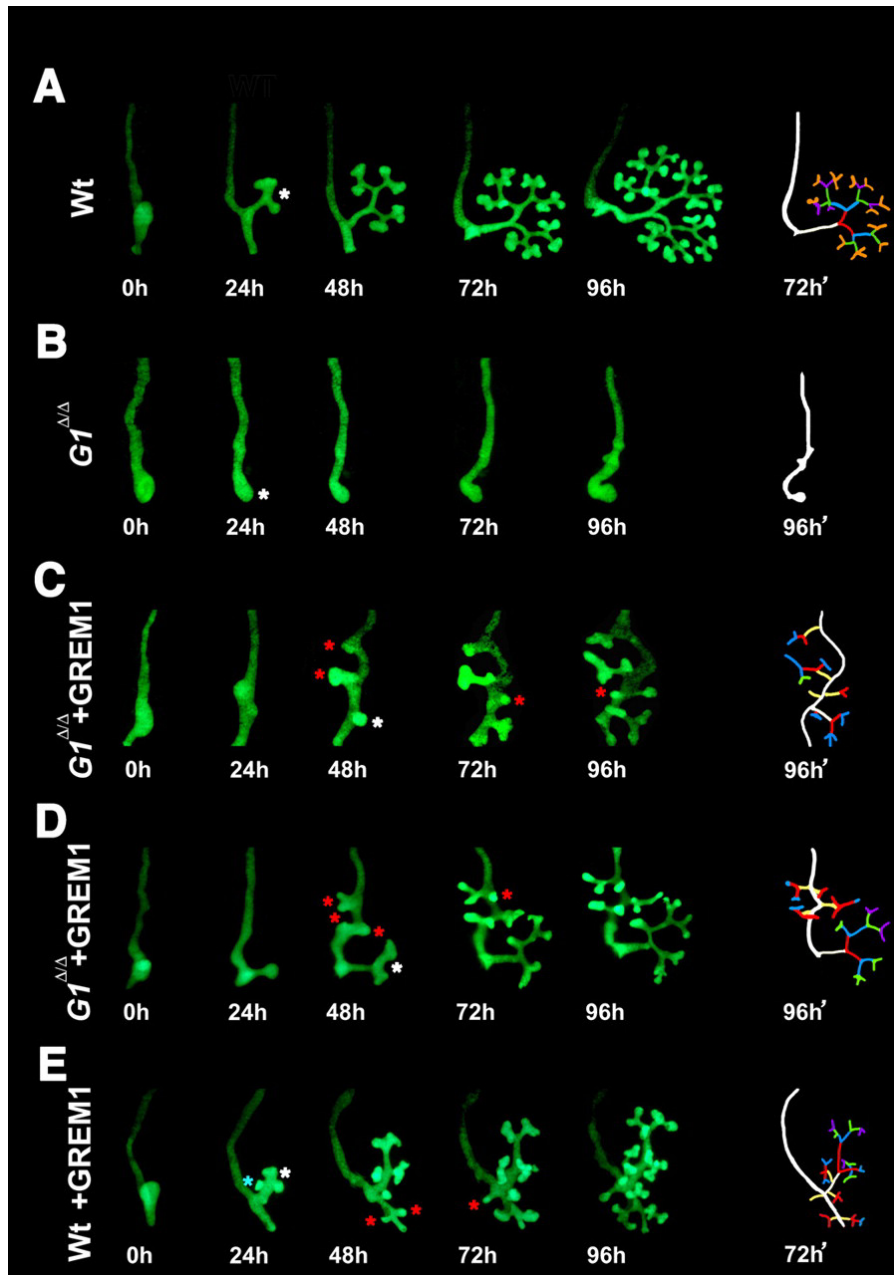


Fig. 1. Recombinant GREM1 protein is able to induce ectopic epithelial buds and restore branching in *Grem1*-deficient kidney primordia. Wild-type and *Grem1*-deficient kidney primordia expressing the *Hoxb7*-GFP transgene in their Wolffian duct and ureteric epithelium (Srinivas et al., 1999) were isolated from mouse embryos of 40-44 somites (E11.0-E11.25) and cultured for up to 96 hours. Panels show from left to right: cultures at 0 hours, 24 hours, 48 hours, 72 hours and 96 hours (time: ± 2 -3 hours). White asterisks indicate ureteric buds, red asterisks indicate ectopic epithelial buds and blue asterisks ectopic branches. The right-most panels are schematic tracings of the Wolffian duct and epithelial branching pattern at the developmental time points indicated (96 hours for *Grem1* mutants; 72 hours for wild type). Wolffian duct and ureteric bud are shown in white; ectopic epithelial buds and/or outgrowth in yellow; first branch in red; second branch in blue; third branch in green; fourth branch in purple; fifth branch (A only) in orange. (A,B) Kidney primordia cultured in control medium. (A) Wild-type control. (B) *Grem1*-deficient metanephros; outgrowth and branching are blocked. (C-E) *Grem1*-deficient (C,D) and wild-type (E) kidney primordia cultured in medium supplemented with recombinant GREM1 (5 μ g/ml). The *Grem1*-deficient metanephric kidney primordia shown in C and D are representative of the variability observed.

In *Grem1*-deficient embryos, *Ret* continues to be expressed by the Wolffian duct and ureteric epithelium. Also *Gdnf* expression is initially normal, but is downregulated progressively and the mutant mesenchyme is eliminated by apoptosis (Michos et al., 2004). By contrast, the expression of *Wnt11* in the mutant ureteric bud epithelium is lower than in the wild-type bud from the beginning and is completely lost by E11.5 (see Fig. S2). Therefore, *Wnt11* and *Gdnf* provide good markers to monitor of e-m feedback signalling in *Grem1*-deficient kidney primordia (Fig. 2). Mutant kidney rudiments (isolated from E10.75-11.0 mouse embryos; 38-40 somites) were cultured for 48 hours to avoid the onset of massive apoptosis (Fig. 2B,E and data not shown) and to allow treatment with recombinant GREM1 to restore ureteric bud outgrowth (white asterisks, Fig. 2C,F) and induce formation of ectopic buds (red asterisks, Fig. 2C,F). Indeed, GREM1 treatment restores *Gdnf* expression in the distal mesenchyme around the invading ureteric bud (white asterisk in Fig. 2C) and expression is also activated around the ectopic buds (red asterisks, Fig. 2C). Semi-quantitative RT-PCR analysis reveals that GREM1 treatment increases *Gdnf* transcript levels by at least twofold (see Fig. S3; 1.9 ± 0.4 , mean \pm s.e.m., $n=3$). In the ureteric epithelium, the expression of *Wnt11* is no longer detected in *Grem1*-deficient kidney primordia after 48 hours (Fig. 2E) in contrast to the wild-type primordia (Fig. 2D). Strikingly, GREM1 treatment of the mutant kidney primordia completely restores *Wnt11* expression in the epithelial tips of the invading ureteric (white asterisk, Fig. 2F) and all ectopic (red asterisks, Fig. 2F) buds. This molecular analysis establishes that recombinant GREM1 is able to restore epithelial WNT11 signalling and thereby autoregulatory e-m feedback signalling and metanephric branching morphogenesis.

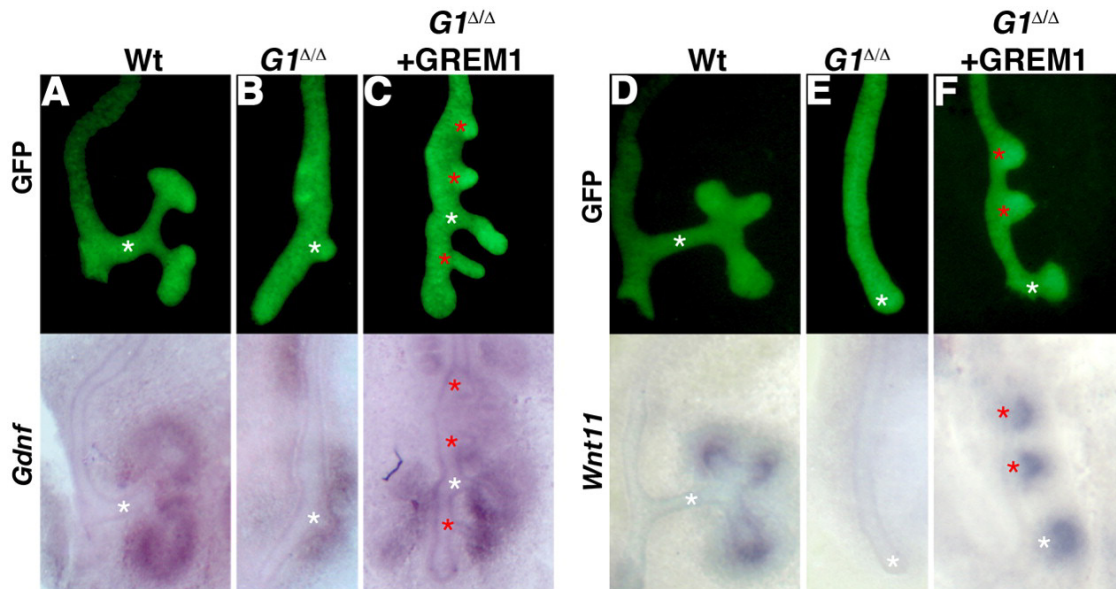


Fig. 2. Treatment with recombinant GREM1 enables upregulation and propagation of *Wnt11* and *Gdnf* expression in *Grem1*-deficient kidney rudiments in culture. Mouse kidney primordia were isolated at E10.75-11.0 (38-42 somites) and cultured for 48 hours either without (A,B,D,E) or in the presence of recombinant GREM1 (5 μ g/ml, C,F). All upper panels show the epithelial branching pattern as revealed by the *Hoxb7*-GFP transgene. Lower panels show transcript distributions as revealed by whole-mount in situ hybridisation. Ureteric buds are indicated by white asterisks, ectopic epithelial buds by red asterisks. (A-C) *Gdnf* expression: (A) wild-type control; (B) *Grem1*-deficient kidney primordia, note the smaller size and remaining *Gdnf* expression; (C) *Grem1*-deficient kidney primordia cultured in the presence of recombinant GREM1. Note the ectopic epithelial buds and *Gdnf* expression in the surrounding mesenchyme. (D-F) *Wnt11* expression (D) wild-type control; (E) *Grem1*-deficient kidney primordia, note the complete loss of *Wnt11* expression; (F) *Grem1*-deficient kidney primordia cultured in the presence of recombinant GREM1. *Wnt11* is expressed in the epithelial tips of both ureteric and ectopic buds.

The responsiveness of the epithelium and mesenchyme in *Grem1*-deficient kidney primordia was further studied as follows: (1) By forced activation of canonical Wnt signal transduction in culture, nephrogenesis is activated (see Fig. S4), thereby establishing that the mutant metanephric mesenchyme remains responsive to inductive signals; (2) By culturing *Grem1*-deficient kidney primordia in an excess of recombinant GDNF (100 ng/ml; Fig. 3) massive epithelial overgrowth and branching are induced along the entire Wolffian duct similar to what occurs in wild type (Fig. 3A,B; see also Shakya et al., 2005). These results indicate that the block to initiate ureteric bud outgrowth and invasion of the mesenchyme is not caused by defective epithelial signal reception, but rather by defects in signalling, i.e. the failure to upregulate *Gdnf* expression in the mesenchyme and/or *Wnt11* in the ureteric epithelium.

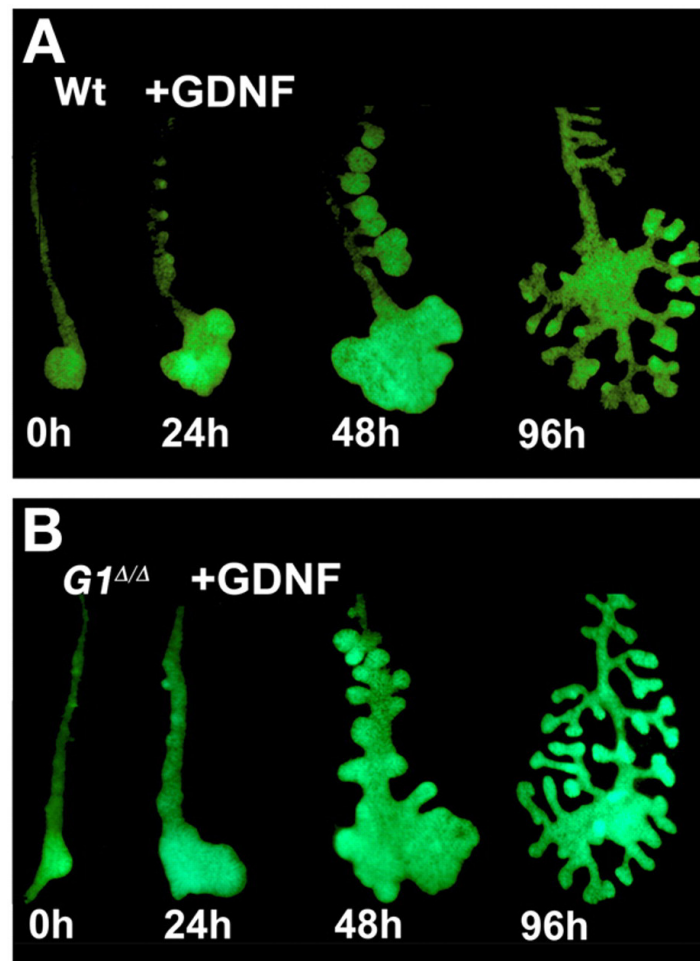


Fig. 3. Recombinant GDNF induces epithelial overgrowth and excessive branching in both wild-type and *Grem1*-deficient mouse metanephric kidney primordia. Kidney primordia (E11.0, 40-42 somites) were cultured for 96 hours in medium supplemented with recombinant GDNF (100 ng/ml). **(A)** Wild-type; note the formation of many epithelial buds along the Wolffian duct and overgrowth of the ureteric epithelium within 24 hours, which results in excessive branching. **(B)** *Grem1*-deficient kidney primordia; note the formation of many epithelial buds, overgrowth and excessive branching similar to the wild type (A).

The Grem1 deficiency causes aberrant nuclear accumulation of pSMAD proteins in the metanephric mesenchyme around the ureteric bud.

The results so far reveal the importance of identifying the primarily affected kidney compartment and relevant BMP ligand(s). With respect to the latter, *Bmp4* (in contrast to *Bmp2* and *Bmp7*) (Michos et al., 2004) is expressed by the mesenchyme along the entire Wolffian duct, including the region where the ureteric bud is forming (Fig. 4C, compare with Fig. 4A, see also Fig. 4G). Therefore, the Wolffian duct and nascent ureteric bud are 'embedded' in *Bmp4*-expressing mesenchyme. By contrast, the nascent metanephric mesenchyme is more or less devoid of *Bmp4* expression during ureteric bud outgrowth and first branching (Fig. 4B,D). Subsequently, *Bmp4* expression is (re-) activated in metanephric mesenchyme enveloping the ureteric stalk, consistent with its proposed functions during stalk elongation (Miyazaki et al., 2000) (and data not shown). Just prior to initiation of ureteric bud outgrowth, the highest levels of *Grem1* transcripts are detected in the mesenchyme around the caudal Wolffian duct and nascent ureteric bud (Fig. 4E,H). Activation of *Grem1* expression does not seem to require GDNF signalling, as *Grem1* remains expressed in the metanephric kidney primordia of *Gdnf* mutant mouse embryos (see Fig. S3). After the first epithelial branching event, *Grem1* expression is highest in the metanephric mesenchyme surrounding the ureteric epithelial tips (Fig. 4F). The transcriptional upregulation of *Grem1* just prior to the onset of ureteric bud outgrowth (Fig. 4E,H) would likely inhibit BMP4 locally and generate a region of low mesenchymal BMP activity. Such regional lowering of mesenchymal BMP

activity likely relieves repression of ureteric bud outgrowth and enables its invasion into the metanephric mesenchyme in response to GDNF signalling.

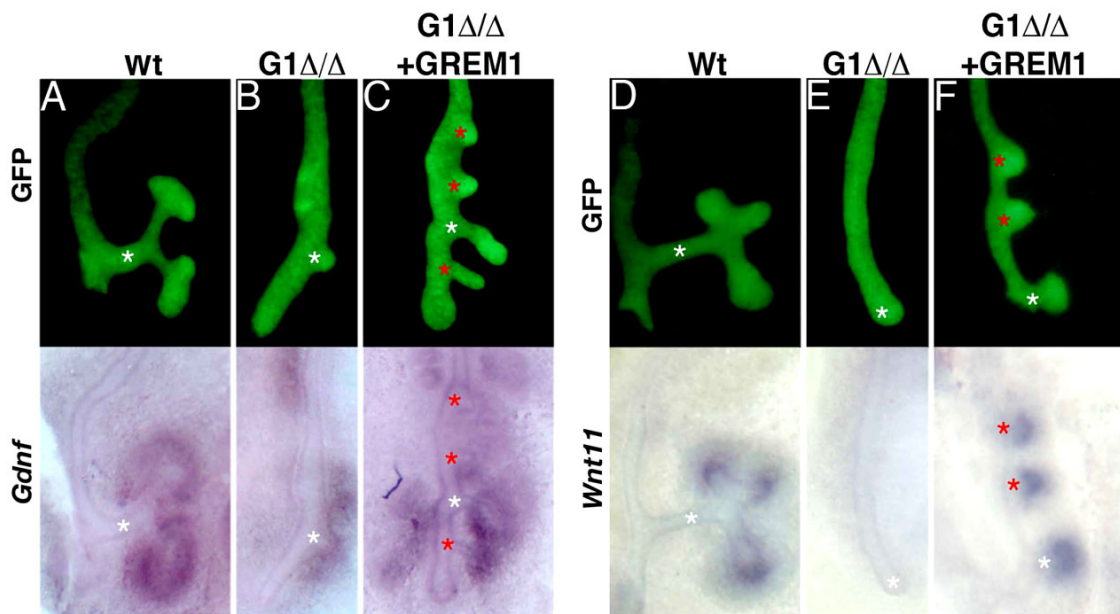


Fig. 4. Dynamic changes in *Grem1* and *Bmp4* expression during initiation of metanephric kidney development in mouse. (A-D) *Bmp4* distribution during initiation of metanephric kidney development. (A,B) GFP reveals the morphology of the nascent ureteric bud at E11.0 (40-42 somites; A) and after the first epithelial branching (E11.5, 48-50 somites; B). Asterisks in B indicate the tips of the ureter branches. (C,D) The *Bmp4* transcript distribution was determined using a *lacZ* reporter gene inserted into the endogenous *Bmp4* transcription unit (*Bmp4:lacZ*) in heterozygous embryos (Kulesa and Hogan, 2002), as detection by whole mount in situ hybridisation is not reliable. (C) At E11.0, *Bmp4:lacZ* is expressed by the mesenchyme surrounding the Wolffian duct (arrow) and ureteric bud (see also G). The dotted circle indicates the position of the ureteric bud (compare with A). (D) By E11.5, the *Bmp4:lacZ* expression is retained in the mesenchyme surrounding the Wolffian duct (arrow), while the metanephric mesenchyme is largely devoid of *Bmp4*. The dotted line indicates the position of the first branch (compare with B). (E,F) *Grem1* expression in the mesenchyme. (E) At E11.0, *Grem1* expression is highest in the mesenchyme around the ureteric bud (indicated by a dotted circle). (F) Subsequently (E11.5), *Grem1* is expressed in the mesenchyme around the tips of first ureteric epithelial branch (indicated by dotted oval). (G,H) Detection of *Bmp4* and *Grem1* transcripts on transverse sections by in situ hybridisation. Sections are oriented with dorsal to the top. Note that the epithelium (indicated by a dotted line) expresses neither *Bmp4* (G) nor *Grem1* (H). (G)

There is abundant *Bmp4* expression in the mesenchyme around the caudal Wolffian duct and ureteric epithelium in agreement with the *Bmp4:lacZ* distribution shown in C. (H) At E10.75 (38 somites), *Grem1* is also expressed in the mesenchyme around the caudal Wolffian duct and ureteric epithelium in agreement with the whole mount in situ hybridisation shown in E. Note that *Bmp4* and *Grem1* are also expressed by the mesenchyme around the hindgut. Hg, hindgut; mm,.; metanephric mesenchyme; wd, Wolffian duct.

To determine if such lowering of BMP signal transduction indeed occurs, the phosphorylation of SMAD proteins (pSMAD1/5/8; established mediators of BMP signal transduction) (Massagué et al., 2005) was analysed in wild-type and *Grem1*-deficient mouse embryos (Fig. 5). During ureteric bud formation in the wild-type, the Wolffian duct and ureteric bud are largely devoid of nuclear pSMAD proteins (brown stained nuclei, Fig. 5A) as revealed by abundant Hoechst fluorescence (light blue nuclei, Fig. 5A). Whereas the pSMAD antigen is abundant in the ventral mesenchyme, only a few pSMAD-positive nuclei are apparent in the metanephric mesenchyme (demarcated region indicated by 'mm' in Fig. 5A). By contrast, a significant fraction of the cells in the corresponding region of *Grem1*-deficient embryos contain pSMAD proteins in their nuclei and the metanephric mesenchyme appears overall less dense (Fig. 5B). These results indicate that BMP signal transduction is lowered in the wild-type metanephric mesenchyme during initiation of ureteric bud outgrowth (Fig. 5A), whereas it remains excessively high in the mutant mesenchyme (Fig. 5B). In the wild type, the nuclear pSMAD levels remain low in both epithelium and condensing metanephric mesenchyme during invasion and first branching (Fig. 5C,E), while they increase in stromal mesenchyme (Fig. 5C,E). This increase is

consistent with a role of BMP4 in ureteric stalk elongation (Miyazaki et al., 2000). In *Grem1* mutant kidneys, the aberrant pSMAD levels persist throughout the mutant metanephric mesenchyme, while the arrested ureteric bud epithelium remains largely devoid of nuclear pSMAD proteins (Fig. 5D,F). The low pSMAD levels in the wild-type metanephric mesenchyme (Fig. 5A,C) overlap well with the area normally expressing *Grem1* (Fig. 4E,F). In summary, the aberrant and persistently high BMP(4) activity in the mutant metanephric mesenchyme reveals a primary defect in *Grem1*-deficient kidney primordia (Fig.5B,D,F) and sharply contrasts with the dynamic changes of BMP activity in the wild type (Fig. 5A,C,E).

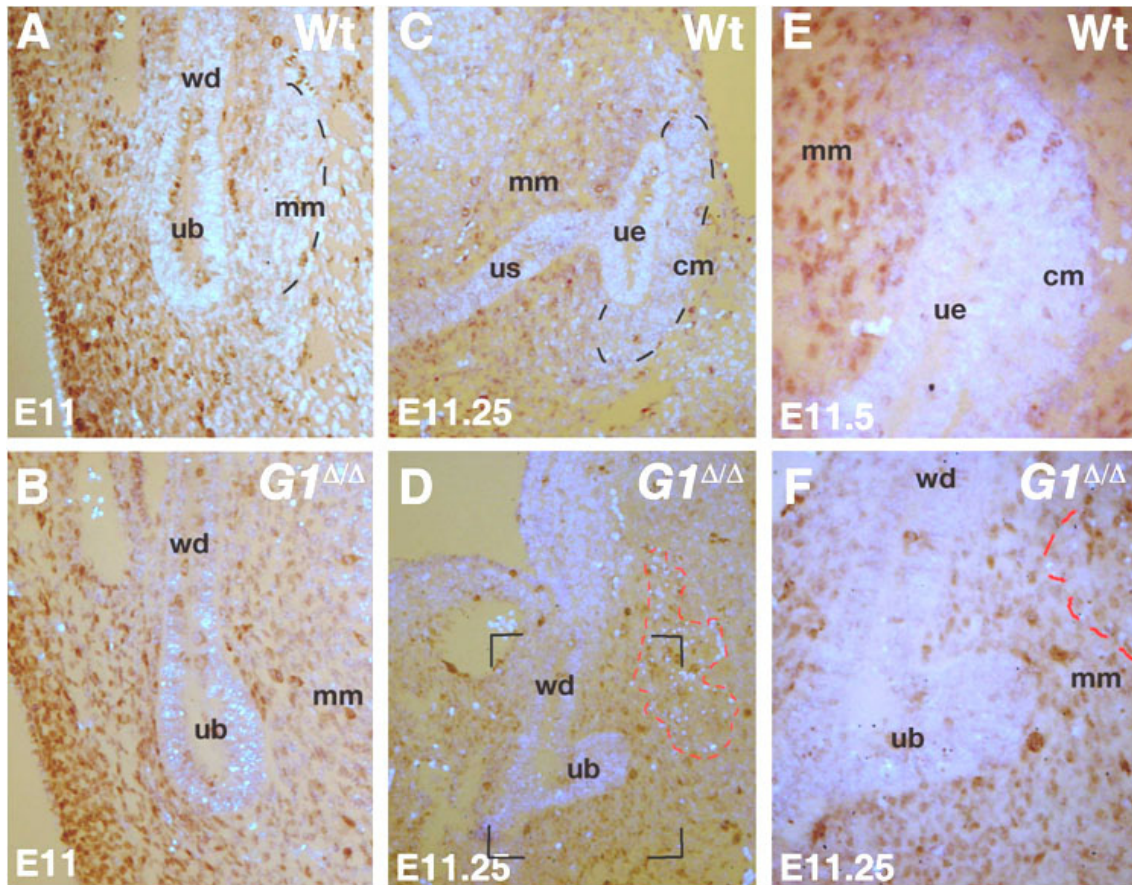


Fig. 5. Detection of phosphorylated SMAD1/5/8 proteins (pSMAD) on tissue sections. The brown precipitate reveals pSMAD-positive nuclei. All sections are counterstained with Hoechst 33258 (light blue fluorescence) to reveal nuclei lacking pSMADs. All sections are sagittal along the primary embryonic axis with ventral to the left and dorsal to the right. Sections shown are representative of the results obtained by analysing serial sections of at least three embryos per genotype. **(A,C,E)** Wild-type mouse embryos at E11.0 (40 somites; A); E11.25 (47 somites; C) and E11.5 (50 somites, enlargement of tip region; E). **(B,D,F)** *Grem1*-deficient embryos at E11.0 (42 somites; B) and E11.25 (48 somites; D), an enlargement of the ureteric bud area in D is shown in F. The area within the red dashed line contains many picnotic nuclei indicative of the onset of cellular apoptosis (D,F). cm, condensing metanephric mesenchyme; mm, metanephric mesenchyme; sm, stromal mesenchyme; ub, ureteric bud; ue, ureteric epithelium (first branch); us, ureteric stalk; wd, Wolffian duct.

Genetic reduction of BMP4 activity in Grem1-deficient mouse embryos rescues metanephric kidney organogenesis and postnatal kidney functions

To test the hypothesis that excess mesenchymal BMP4 activity blocks the initiation of ureteric bud outgrowth, compound mutant embryos and mice carrying both *Grem1* and *Bmp4* loss-of-function mutations were generated. The early lethality of *Bmp4*-deficient mouse embryos (Winnier et al., 1995) is not rescued by additional inactivation of *Grem1*, which precludes analysis of double homozygous embryos. However, inactivation of one copy of the *Bmp4* gene in *Grem1*-deficient ($G1^{\Delta\Delta}$; $B4^{\Delta/+}$) mouse embryos restores ureteric bud morphology (Fig. 6C, compare with Fig. 6A,B). In $G1^{\Delta\Delta}$; $B4^{\Delta/+}$ mutant embryos (Fig. 6C,F,I,L), ureteric bud outgrowth and branching are initiated with kinetics similar to that in the wild type (Fig. 6A,D,G,J). Consistent with this rescue of epithelial outgrowth and branching, the expression of *Gdnf* in the mesenchyme (Fig. 6F,L, compare with Fig. 6E,K) and *Wnt11* in the ureteric bud epithelium are restored (see Fig. S2 and data not shown), which is indicative of intact autoregulatory e-m feedback signalling during branching and normal progression of metanephric branching morphogenesis.

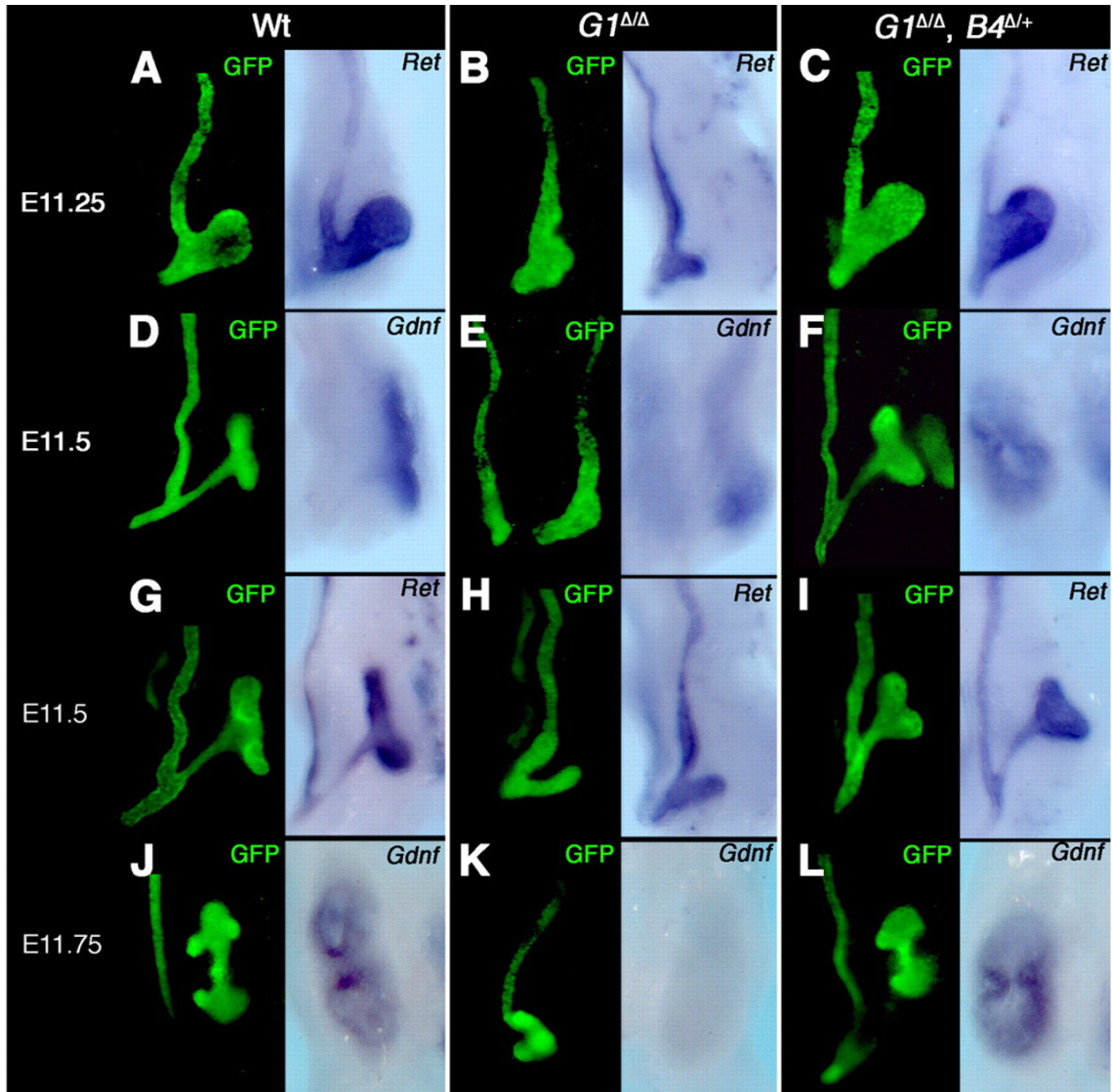


Fig. 6. Genetic inactivation of one copy of the *Bmp4* gene in a *Grem1* mutant background rescues the kinetics of ureteric epithelial growth and branching. Left panels: GFP reveals the morphology of the epithelium before fixation. Right panels: whole-mount in situ detection of the expression of the *Ret* receptor (**A-C,G-I**) and the *Gdnf* ligand (**D-F,J-L**). (**A,D,G,J**) Wild-type metanephric primordia. (**B,E,H,K**) *Grem1* ($G1^{\Delta\Delta}$)-deficient metanephric primordia. Note the complete disruption of ampulla formation (**E,H,K**) and loss of mesenchymal *Gdnf* expression (**K**), whereas *Ret* expression remains in the arrested epithelium (**H**). (**C,F,I,L**) Metanephric primordia of $G1^{\Delta\Delta}; B4^{\Delta/+}$ mouse embryos. Note the rescue of ureteric epithelial outgrowth (**C**), branching (**F,I,L**) and propagation of *Gdnf* expression (**L**).

Indeed, the distribution of the *Pax2* transcript underscores the normal progression of kidney organogenesis in *G1^{ΔΔ}; B4^{Δ/+}* embryos by E14.5 (Fig. 7C, compare with Fig. 7A). By contrast, in *Grem1*-deficient embryos at this stage both kidneys have been eliminated by apoptosis (as revealed by the complete lack of *Pax2* expression; Fig. 7B). All *G1^{ΔΔ}; B4^{Δ/+}* mice are born with two fully developed and functional kidneys (Fig. 7G, compare with Fig. 7D; $n=20$), whereas complete bilateral renal agenesis is observed in about 90% of all *Grem1*-deficient litter mates ($n=22/25$; the other three manifested unilateral renal aplasia). Histological analysis of *G1^{ΔΔ}; B4^{Δ/+}* mice at 1 and 8 months old reveals that their kidneys are morphologically indistinguishable from wild-type kidneys (Fig. 7E-I). No signs of congenital malformations such as CAKUT, glomerulosclerosis or polycystic kidney disease are observed (Fig. 7G,H,I). Taken together, these results show that the genetic reduction of BMP4 activity in *Grem1*-deficient mouse embryos completely restores metanephric kidney organogenesis and functions.

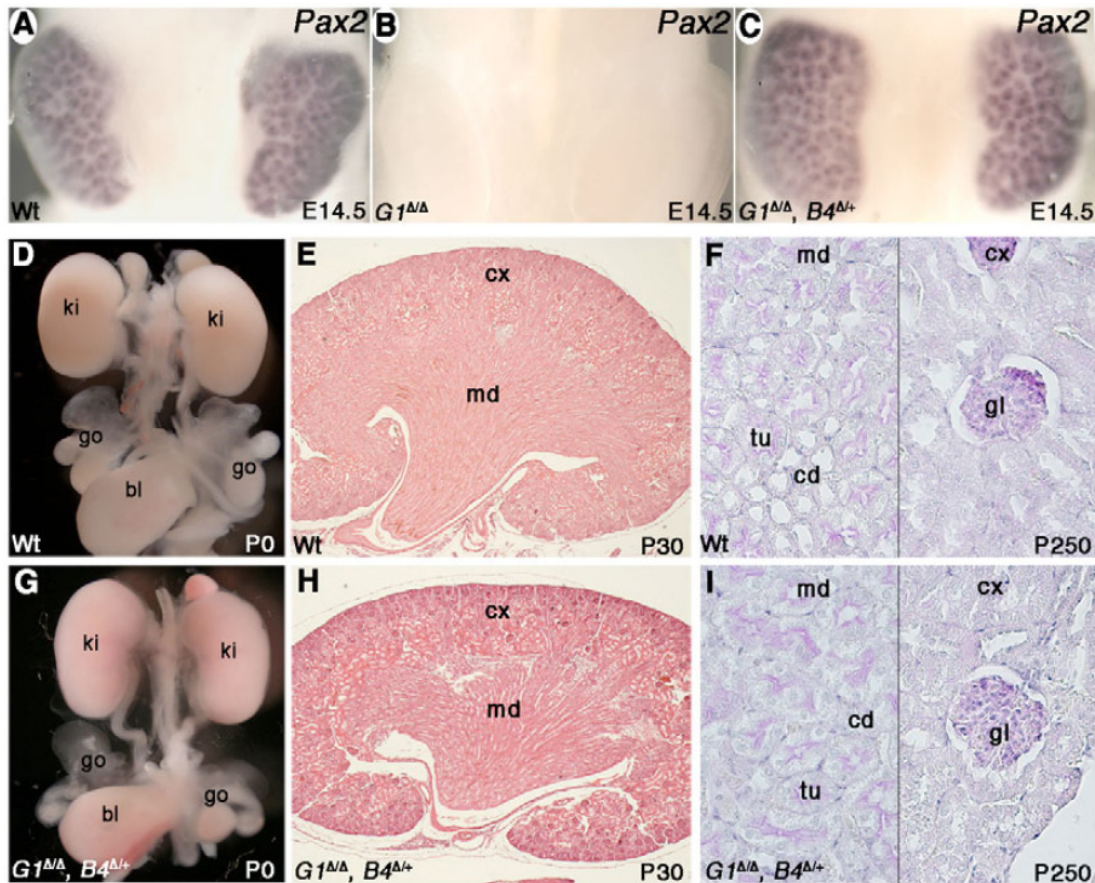


Fig. 7. Inactivation of one copy of the *Bmp4* gene in a *Grem1*-deficient mouse embryo results in formation of two normal kidneys. (A-C) Whole-mount in situ hybridisation to detect *Pax2* expression at E14.5. (A) Wild-type *Pax2* distribution. (B) The absence of *Pax2* expression in a *Grem1*-deficient embryo is due to the complete renal aplasia at this stage. (C) The *Pax2* distribution in kidneys of a *Grem1^{Δ/Δ}; Bmp4^{Δ/+}* embryo is indistinguishable from a wild-type littermate (A). (D) Gross morphology of the wild-type urogenital system at birth (postnatal day P0). (E) Haematoxylin and Eosin staining of a histological section of a wild-type kidney 30 days after birth (P30). (F) PAS staining reveals the morphology of the medulla (collecting ducts) and cortex regions of a wild-type kidney at about 8 months of age (P250). (G) Gross morphology of the urogenital system of a *Grem1^{Δ/Δ}; Bmp4^{Δ/+}* mouse at birth (P0). Note that both kidneys are of normal size and shape (compare with D). (H) Haematoxylin and Eosin staining of a kidney section from a *Grem1^{Δ/Δ}; Bmp4^{Δ/+}* mouse at P30. (I) PAS staining of a kidney from a *Grem1^{Δ/Δ}; Bmp4^{Δ/+}* mouse at P250. Medulla, cortex and glomeruli appear normal. Bl, bladder; cd, collecting duct; cx, cortex; gl, glomerulus; go, gonad; ki, kidney; md, medulla, tu, tubules.

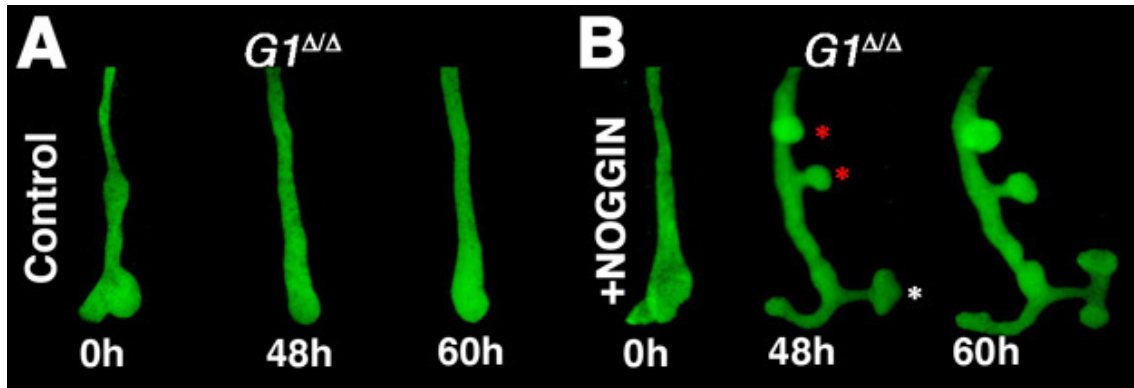
SUPPLEMENTARY FIGURES

Fig. S1. The BMP antagonist noggin induces ectopic epithelial buds, outgrowth and branching in cultured *Grem1*-deficient kidney primordia. **(A)** Culture of a *Grem1*-deficient metanephric primordia in control medium for 60 hours. **(B)** Culture of a *Grem1*-deficient ($G1^{\Delta/\Delta}$) metanephric primordia in noggin-supplemented medium. After 48 hours, several ectopic epithelial buds have formed (red asterisks). The ureteric epithelium (white asterisk) has undergone its first branching by 48 hours and the second branching is initiated after about 60 hours ($n=6$).

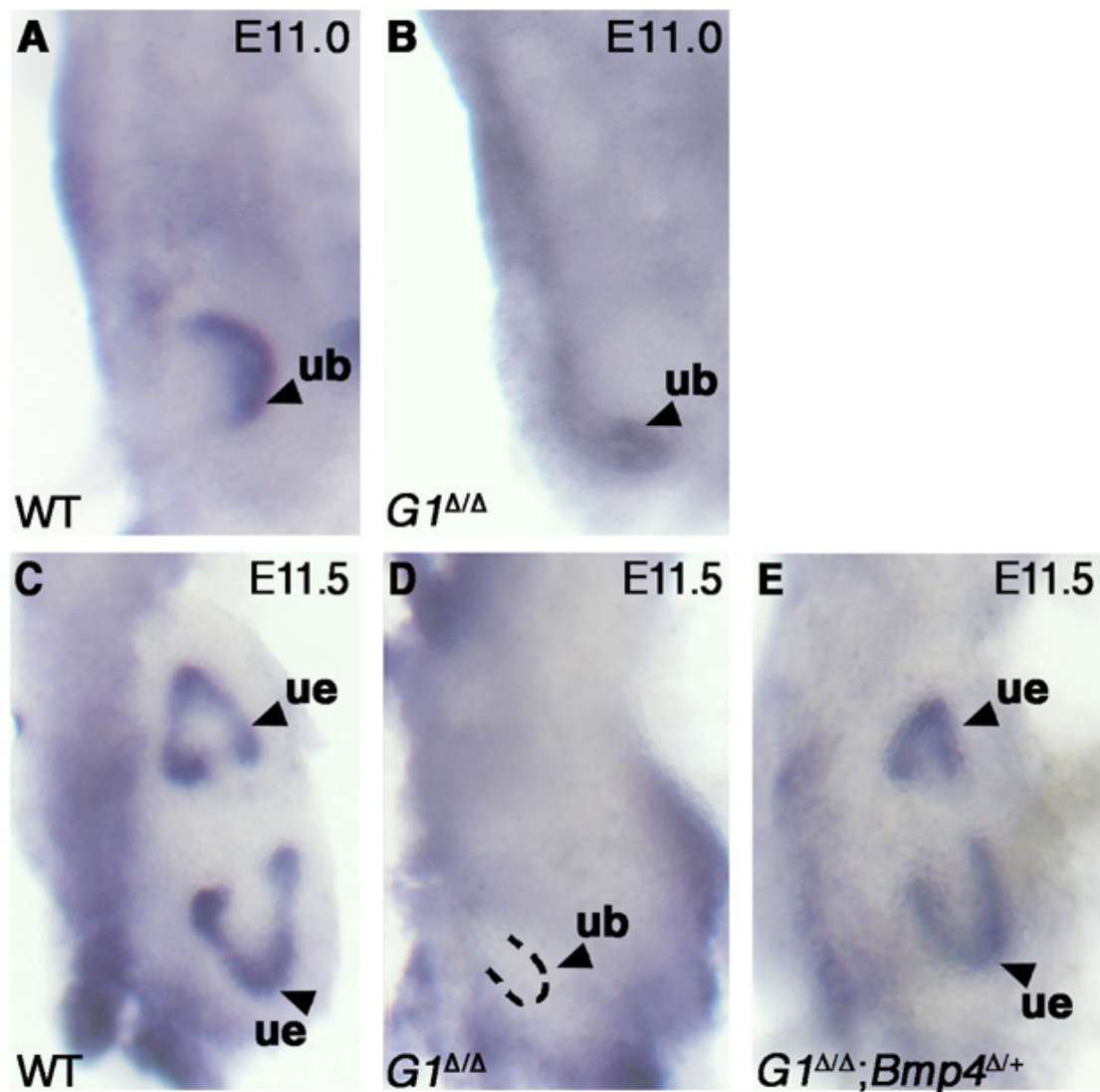


Fig. S2. Expression of *Wnt11* in the ureteric bud epithelium depends on gremlin 1. (A-D) The expression of *Wnt11* is lost from the ureteric bud epithelium of *Grem1*-deficient metanephric kidneys. Detection of *Wnt11* transcripts at E11.0 (A,B) and E11.5 (C,D) in wild-type (A,C) and *Grem1*-deficient (B,D) kidney primordia. The approximate position of the mutant ureteric bud is indicated by a broken line in D. (E) Genetic reduction of *Bmp4* activity in the context of a *Grem1* deficiency (*Grem1*^{Δ/Δ}; *Bmp4*^{Δ/+}) restores *Wnt11* expression. Arrowheads point to the ureteric epithelial tips. ub, ureteric bud; ue, ureteric epithelial tip region expressing *Wnt11* after first branching.

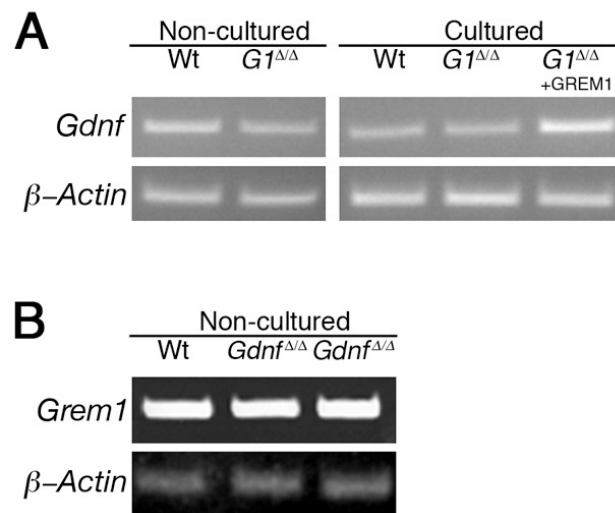


Fig. S3. Semiquantitative RT-PCR analysis *Gdnf* and *Grem1* expression. (A) Determination of the relative *Gdnf* expression levels in wild-type (Wt) and *Grem1*-deficient ($G1^{\Delta\Delta}$) kidney primordia isolated at E10.75-11.0 (38-40 somites). RNA was isolated either at the time of dissection (Non-cultured) or after 48 hours in culture (Cultured) in medium alone or supplemented with recombinant gremlin 1 (5 μ g/ml; lane $G1^{\Delta\Delta}$ +GREM1). Relative *Gdnf* transcript levels (upper row) after normalization for β -Actin mRNA content (lower row). As expected, the relative *Gdnf* levels and kidney primordia sizes are similar when wild-type (Wt) and *Grem1* ($G1^{\Delta\Delta}$)-deficient kidney primordia are isolated at E10.75. After 48 hours in culture, one would expect lower levels of *Gdnf* transcripts in mutant kidneys (see Fig. 2B). However, due to the developmental arrest, the overall size of the mutant kidney primordia is significantly smaller than those of wild-type controls and mutants treated with gremlin 1 ($G1^{\Delta\Delta}$ +GREM1; see Fig. 2B and compare with Fig. 2A,C; and data not shown). The normalization for β -Actin transcript content will also adjust for the smaller overall size; therefore, the relative *Gdnf* transcript levels of untreated mutants appear similar to wild-type controls after 48 hours in culture. Most importantly, treatment of *Grem1* mutants with recombinant gremlin 1 protein ($G1^{\Delta\Delta}$ +GREM1) increases *Gdnf* expression levels about twofold (1.9 ± 0.4 , $n=3$) in comparison with untreated mutants ($G1^{\Delta\Delta}$) and wild-type controls. (B) *Grem1* expression in wild-type and *Gdnf*-deficient kidney primordia isolated at E11.0 (40-44 somites). Note that *Grem1* remains expressed at similar levels in *Gdnf* mutant ($Gdnf^{\Delta\Delta}$) kidney primordia as in wild-type controls (Wt).

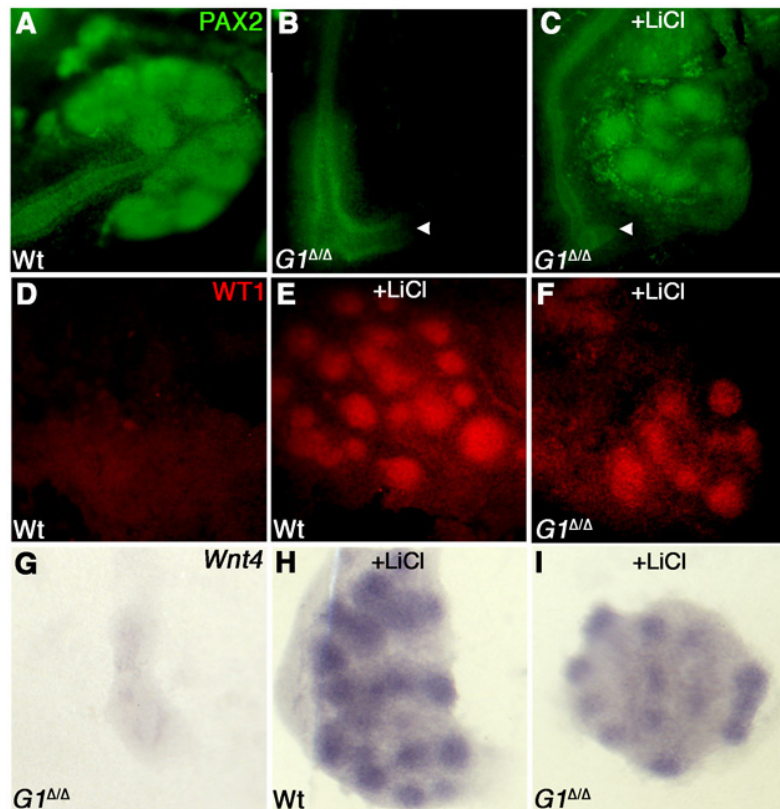


Fig. S4. The metanephric mesenchyme of *Grem1*-deficient embryos remains competent to condense and initiate nephrogenesis. (A-C) Distribution of the PAX2 protein in kidney primordia cultured for 72 hours. (A) PAX2 is present in both the epithelium and condensing mesenchyme of wild-type metanephric kidney primordia. (B) PAX2 is only retained in the epithelium of *Grem1*-deficient metanephric kidney primordia (arrowhead points to the tip of ureteric bud). (C) Culturing *Grem1*-deficient metanephric kidney primordia in the presence of 15 μ M LiCl (+LiCl) induces mesenchymal condensation (Davies et al., 1995; Oxburgh and Robertson, 2002) as revealed by PAX2. LiCl induces nephrogenesis probably by activating canonical Wnt signal transduction (as it acts at the level of GSK3 β) (Klein and Melton, 1996). Note that the ureteric epithelium has neither grown nor branched. Arrowheads (B,C) point to the distal tip of the ureteric bud. (D-F) 15 μ M LiCl induces the isolated metanephric mesenchyme to condense as revealed by activation of the Wilm's tumor-1 (WT1) protein. (D) Isolated wild-type and *Grem1*-deficient (data not shown) mesenchyme cultured without LiCl is eliminated by apoptosis. (E,F) LiCl treatment of both wild-type (E) and *Grem1*-deficient (F) mesenchyme induces the WT1 protein. (G-I) *Wnt4* expression is activated in isolated metanephric mesenchyme cultured with 15 μ M LiCl for 72 hours. (G) *Wnt4* is not detected in mutant mesenchyme cultured without LiCl. (H,I) LiCl treatment induces *Wnt4*

expression in to a similar extent in wild-type (H) and *Grem1*-deficient (I) mesenchyme, which indicates that nephrogenesis has been initiated. For immunodetection of PAX2 and WT1, kidney primordia were incubated overnight in a methanol:DMSO solution (4:1, 4°C) and incubated again overnight with either PAX2 (Covance, 1/500) or WT1 (Santa Cruz, 1/50) primary antibodies diluted in FBS:DMSO (4:1, 4°C). After washing in PBT/FBS/DMSO, samples were incubated overnight with secondary antibodies coupled to specific fluorochromes (Cy3 for WT1 and Cy2 for PAX2; Amersham) and washed extensively the following day.

Discussion

Our study establishes genetically that the extra-cellular BMP antagonist GREM1 is required to reduce BMP4 activity in the mesenchyme surrounding the nascent ureteric bud in mouse embryos. The reduction of BMP4 signal transduction in the metanephric mesenchyme is necessary to initiate ureteric bud outgrowth and establish autoregulatory feedback signalling between GDNF-RET and WNT11, which in turn regulates epithelial branching morphogenesis (Fig. 8). In *Grem1*-deficient kidney primordia, mesenchymal BMP signal transduction is increased, as revealed by the increased nuclear accumulation of pSMAD proteins in the metanephric mesenchyme, which blocks initiation of ureteric bud outgrowth. Indeed, general inhibition of BMP activity in *Grem1*-deficient kidney primordia, by addition of recombinant GREM1, induces supernumerary epithelial buds and restores outgrowth and branching. At the molecular level, GREM1 treatment (re-) activates *Wnt11* expression in the epithelial buds and enables upregulation and propagation of *Gdnf* expression in the mesenchyme. Most importantly, genetic reduction of BMP4 activity in the context of a *Grem1* deficiency completely restores metanephric kidney organogenesis and functions. Therefore, we can conclude that local reduction of BMP4 activity by GREM1 is vital to initiate ureteric bud outgrowth and thereby metanephric kidney organogenesis (Fig. 8).

Formation of the ureteric bud, initiation of its outgrowth and branching appear as distinct processes (Fig. 8). In the metanephros, a single ureteric bud forms in the caudal part of each of the bilateral Wolffian ducts at the level of the mid-hind limb bud. GDNF is essential for ureteric bud formation, as ureteric buds fail to

form in most *Gdnf*-deficient mouse embryos (Pichel et al., 1996). As *Grem1* remains expressed in *Gdnf* mutant metanephric kidney rudiments, the activation of its expression does not depend on GDNF signalling and seems not to require the presence of an intact ureteric bud. Interestingly, recombinant GREM1 is itself able to induce supernumerary epithelial buds in *Grem1*-deficient kidney primordia. These results indicate that in spite of the early developmental arrest, the competence of the rostral Wolffian duct to form supernumerary epithelial buds remains intact in *Grem1*-deficient embryos. In wild-type embryos, the signalling interactions mediated by SLIT2/ROBO2 and FOXC1 restrict *Gdnf* expression to the caudal Wolffian duct (see Introduction and references therein). We provide evidence that BMP4 signalling by the mesenchyme enveloping the Wolffian duct is part of a safeguard mechanism that inhibits formation of supernumerary epithelial buds (Fig. 8A). Local upregulation of *Grem1* expression reduces pSMAD-mediated BMP signal transduction in the mesenchyme and relieves this repression around the ureteric bud, which enables ureteric bud outgrowth and invasion of the metanephric mesenchyme (Fig. 8B). Taken together, the successful initiation of ureteric bud outgrowth likely requires both antagonism of BMP4 by GREM1 in mesenchyme and signalling by GDNF from the metanephric mesenchyme to RET in the ureteric epithelium (Fig. 8A,B).

Subsequently, autoregulatory feedback signalling between GDNF in the mesenchyme and WNT11 in the epithelial tips is established to regulate branching morphogenesis (Fig. 8C; Majumdar et al., 2003). As GREM1 is required for upregulation of *Wnt11* in the ureteric epithelium and *Gdnf*

expression in the mesenchyme, it appears to be crucial for establishment of e-m feedback signalling (Fig. 8C).

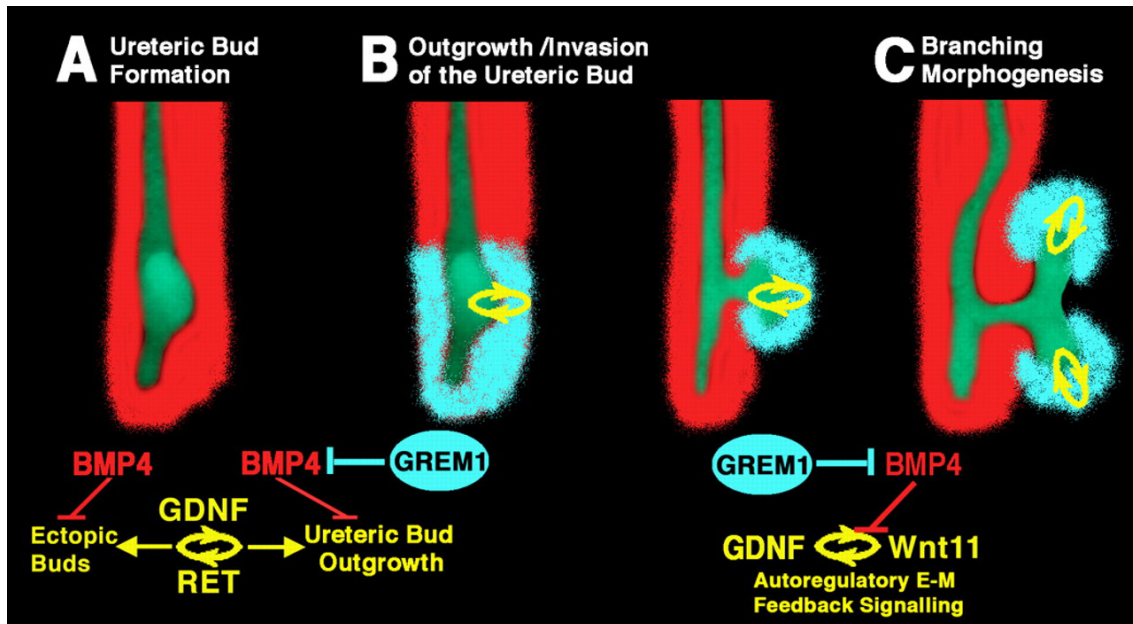


Fig. 8. Reduction of BMP4 activity by gremlin 1 in the mesenchyme around the ureteric bud is essential to enable ureteric epithelial outgrowth, GDNF-RET and WNT11-mediated e-m feedback signalling and branching morphogenesis. (A) In mouse, the ureteric bud forms in the caudal-most part of the Wolffian duct under the influence of GDNF-RET signalling. During this inductive period, *Bmp4* is expressed by the mesenchyme enveloping the Wolffian duct. High levels of mesenchymal BMP4 activity inhibit the formation of ectopic epithelial buds and epithelial branching at this stage (prior to E11.0). At this early stage only low levels of *Grem1* transcripts are detected (not shown). (B) Expression of the BMP antagonist *Grem1* is upregulated in the mesenchyme around the nascent ureteric bud thereby locally reducing BMP4 signal transduction (around E11.75-11.0). This reduction of BMP4 activity by GREM1 enables initiation of ureteric bud outgrowth and its invasion into the metanephric mesenchyme. (C) GREM1 is required to maintain and propagate expression of *Wnt11* in the ureteric epithelial tip(s) and *Gdnf* in the mesenchyme via e-m feedback signalling. For details see Discussion.

As BMP signal transduction is increased in the metanephric mesenchyme of *Grem1*-deficient embryos, one might expect a direct effect of GREM1 and/or BMP4 on mesenchymal *Gdnf* expression. However, treatment of isolated metanephric mesenchyme with either GREM1 or BMP4 did not alter *Gdnf* expression significantly within 18-24 hours (O.M. and R.Z., unpublished). Therefore, we favour an alternative explanation, by which the primary defect (elevated BMP4 activity) in the *Grem1*-deficient metanephric mesenchyme blocks initiation of ureteric epithelial outgrowth and signalling as evidenced by the loss of *Wnt11* expression. GREM1-mediated reduction of BMP activity in the mesenchyme may act via epithelial signalling to propagate mesenchymal *Gdnf* expression, analogous to the requirement of GREM1 for *Shh* expression in the limb bud mesenchyme (see below). Further (genetic) studies are required to understand how excess BMP signal transduction in the mesenchyme blocks initiation of ureteric bud outgrowth. In agreement with our studies, others have already shown that (1) addition of recombinant BMPs to metanephric kidney primordia in culture partially inhibits epithelial branching morphogenesis (Bush et al., 2004; Piscione et al., 1997), and (2) overexpression of the BMP receptor type 1A (ALK3; also known as BMPR1A-Mouse Genome Informatics) in the ureteric epithelium causes renal aplasia or dysplasia in a fraction of mice (Hu et al., 2003).

Last but not least, the present study reveals striking mechanistic similarities in the way GREM1-mediated e-m feedback signalling controls limb and kidney organogenesis. During limb bud development, GREM1-mediated BMP4 antagonism is key to establishing and propagating the feedback signalling loop

between SHH (expressed by the posterior mesenchyme) and FGF (in the apical ectodermal ridge, AER), which enables progression of limb bud morphogenesis (Michos et al., 2004; Panman et al., 2006; Zuniga et al., 1999). Our previous studies showed that GREM1 is not required to initiate SHH signalling by the limb bud organiser in the posterior mesenchyme, but is essential to initiate the dynamic phase of SHH/FGF e-m feedback signalling. In particular, GREM1-mediated SHH/FGF feedback signalling regulates the temporally and spatially coordinated propagation of both signalling centres during limb bud outgrowth and patterning (Panman et al., 2006). Similarly, GREM1 is not required to activate GDNF signalling in the metanephric mesenchyme and for formation of the ureteric bud, but for initiation of epithelial outgrowth and establishment of autoregulatory GDNF/WNT11 e-m feedback signalling. In both the limb and kidney primordia, GREM1 acts in the mesenchyme to reduce BMP4 signal transduction and thereby relieve the inhibitory effect on the ureteric and AER epithelium (this study and J.D. Bénazet and R. Z., unpublished). As a consequence, the expression of *Wnt11* in the ureteric bud and *Fgfs* in AER are upregulated and this epithelial signalling in turn propagates GDNF in the metanephric, and SHH in the limb bud, mesenchyme, respectively.

VIII. GENETIC ANALYSIS OF THE BMP7-GREMLIN1 INTERACTIONS DURING KIDNEY EPITHELIAL BRANCHING

Summary

Molecular and genetic studies revealed a requirement of Gremlin1 (*Grem1*)-mediated antagonism of Bone Morphogenetic Protein 4 (BMP4) activity for initiation of metanephric kidney organogenesis. GREM1 in the caudal-most part of the metanephric mesenchyme inhibits BMP4 locally to enable GDNF/RET/Wnt11 feedback signalling. *In vitro* culture of kidney rudiments with GREM1 induces ectopic ureteric buds (UB). Temporally controlled inactivation of *Bmp4* *in vivo* by tamoxifen induced recombination (see Appendix 1) suggested that BMP signalling inhibits formation of ectopic UBs. However, ectopic UBs are a response to localised inactivation of *Bmp4* unlike the effects of general BMP antagonism, achieved by recombinant GREM1 application *in vitro*. These results suggest that several BMP family members might function in at least a partially overlapping manner in this process. Indeed, genetic inactivation of *Bone morphogenetic Protein 7* (*Bmp7*) in a *Grem1*-deficient background restores the initiation of UB outgrowth and epithelial branching. These studies reveal a self-propagating system for progression of kidney development as revealed by the onset of nephrogenesis. Analysis of *Six2* expression reveals the partial restoration of the *Grem1* deficient phenotype but is not sufficient to rescue the dysplastic *Bmp7*^{ΔΔ} deficiency. This was confirmed using the kidney glomeruli marker PODOCALYXIN and the collecting system epithelia marker CYTOKERATIN. The comparison of *Grem1*; *Bmp4* and *Grem1*;

Bmp7 compound mutants indicates that *Six2* is normally regulated by both BMPs. These results indicate that GREM1 mediated BMP antagonism reduces overall BMP activity in a spatially restricted manner rather than only affecting either BMP4 or BMP7. The local reduction of BMP signalling permits initiation of UB outgrowth while BMP4 is then specifically required for UB stalk elongation (Miyazaki et al., 2000) and BMP7 for expansion of *SIX2* positive progenitors (Self et al., 2006).

Introduction

Genetic studies revealed that the BMP7 null mutation in mice develops defects in the skeleton, kidney and eye (Jena et al., 1997). *Bmp7* expression is initiated during gastrulation at around E7.5. The metanephric mesenchyme (MM) expresses high levels of *Bmp7* at the time of inductive interaction with the ureteric bud (UB) and at later stages it is expressed in the developing glomeruli, distal tubules and collecting ducts. BMP7 inhibits cell proliferation and induces cell differentiation. In the kidney, *Bmp7*-null mice present well formed proximal convoluted tubules but formation of distal convoluted tubules is disrupted (Godin et al., 1999). Distal convoluted tubules are responsible for Ca^{2+} absorption hence ossification defects are expected (Berry and Floyd C, 1989). Furthermore, the few surviving *Bmp7*^{Δ/Δ} newborn mice develop unilateral or bilateral polycystic kidneys and die shortly after birth. Most importantly, BMP7 is required to ensure the survival and proliferative expansion of the nephrogenic progenitors in the metanephric mesenchyme (Dudley et al., 1995).

Oxburgh and colleagues (Oxburgh et al., 2005) showed that BMP4 can substitute for loss of BMP7 during kidney development. Receptor occupancy by either BMP4 or BMP7 activates the same signalling pathways in the kidney. BMP type-I receptors *Alk2* (activin receptor-like kinase-2) and *Alk3* (activin receptor-like kinase-3) knock-out mice display similar phenotypes. They are both embryonic lethal, *Alk2* by E7.5 and *Alk3* at around E9.5, and animals carrying any of the transgenes present a normal nephron number (Martinez et al., 2002; Mishina et al., 1995; Mishina et al., 1999). However, another finding puzzled the previous assumption that both receptors were equivalent. The renal aplasia/dysgenesis or medullary dysplasia in mutants over-expressing ALK3 throughout the ureteric epithelium was not expected, but it is possibly due to differential transducing activities depending of the combination of ligands during early development (Cain et al., 2008; Hu et al., 2003).

To investigate which are the relevant BMP ligand(s) antagonised by *Grem1* during kidney and limb organogenesis we have undertaken different research strategies. We showed that GREM1 is required to modulate BMP signalling and that the genetic reduction of *Bmp4* is sufficient to restore kidney development in a *Grem1* -deficient background (Michos et al., 2007). Furthermore, we have shown that GREM1-mediated BMP4 antagonism is part of the SHH/GREM1/FGF signalling feedback loops which provides limb development with robustness (Bénazet et al., 2009). This study also revealed that GREM1 also antagonises BMP7 during limb bud development albeit less efficiently.

Indeed, the genetic inactivation of *Bmp7* restores kidney development in the context of the *Grem1* deficiency. However, unlike *Bmp4*, both *Bmp7* allele

copies must be inactivated to restore initiation of branching morphogenesis. At a later stage, it is known that loss of *Bmp7* results in depletion of the nephrogenic progenitor pool. We now reveal that the genetic inactivation of *Grem1* in a *Bmp7* null background improves the nephron defects.

This analysis reveals that unlike in *Grem1*^{ΔΔ}; *Bmp4*^{Δ/+} embryos only initiation and early UB branching morphogenesis are restored in embryos lacking both *Grem1* and *Bmp7*, while nephrogenesis as a whole is still impaired.

Results

Complete genetic inactivation of Bmp7 restores the failure to initiate branching morphogenesis in Grem1 deficient kidneys

We previously demonstrated that GREM1 mediated antagonism of BMP4 is required to initiate branching morphogenesis.

To analyse the BMP7-GREM1 interaction during kidney organogenesis it was important to consider the following two issues: 1) is the reduction of *Bmp7* activity sufficient to restore the *Grem1*^{ΔΔ} phenotype (failure to induce UB outgrowth) and 2) is the reduction of the *Grem1* activity able to restore the *Bmp7* loss-of-function phenotype (depletion of nephrogenic progenitors).

To address the first issue, an allelic series of *Bmp7* loss-of-function mutation in a *Grem1* deficient background was analysed (Fig1 and Fig.S1). As shown, *Grem1* deficient mice display bilateral renal aplasia, which is fully penetrant in a mixed F1 129/C57BL6 genetic background (Michos et al., 2007). However, if

the C57Bl6 component is increased, the *Grem1* phenotype can vary from none to two kidneys – which reveals the importance of genetic background for the renal phenotypes. It suggests that BMP activity is tightly regulated during kidney development.

In both *Grem1* and *Bmp7* heterozygous embryos/mice kidney development was not affected and the same was observed in the trans-heterozygous (data not shown). In contrast, a 50% reduction of *Bmp7* in a *Grem1*^{Δ/Δ} background (*Grem1*^{Δ/Δ}; *Bmp7*^{Δ/+}) displayed a phenotypic variability (Table1).

Table 1 - Kidney agenesis - Genetic analysis of *Grem1*; *Bmp7* compound mutant newborn mice.

Genotypes	2 kidneys	1 Kidney	0 kidneys	Total
<i>Grem1</i> ^{Δ/Δ}	0	1 (10%)	9 (90%)	10
<i>Grem1</i> ^{Δ/Δ} ; <i>Bmp7</i> ^{Δ/+}	1 (5,0%)	2 (10%)	17 (85%)	20
<i>Grem1</i> ^{Δ/Δ} ; <i>Bmp7</i> ^{Δ/Δ}	8 (89%)	1 (11%)	0	9
<i>Grem1</i> ^{Δ/+} ; <i>Bmp7</i> ^{Δ/Δ}	14 (93%)	1 (2,4%)	0	15
<i>Bmp7</i> ^{Δ/Δ}	5 (100%)	0	0	5

The observed abnormalities in *Grem1*^{Δ/Δ}; *Bmp7*^{Δ/+} newborn mice varied from complete kidney agenesis (17 out 20) to the formation of 2 hypoplastic kidneys (1 out of 20). By doing the appropriate genetic crosses we were able to exclude that variability in penetrance of the renal agenesis was a mere genetic background effect (see Materials and Methods). In conclusion, in most of the *Grem1*^{Δ/Δ}; *Bmp7*^{Δ/+} mice the renal agenesis is not rescued in contrast to normal

progression of kidney development in *Grem1*^{ΔΔ}; *Bmp4*^{Δ/+} mice. Analysis of the hypoplastic kidneys formed at low frequency in *Grem1*^{ΔΔ}; *Bmp7*^{Δ/+} (Sup. Fig. 1A) revealed their striking similarity to *Grem1*^{ΔΔ}; *Bmp7*^{ΔΔ} kidneys (Fig. 2D-F).

As reducing *Bmp7* activity by 50% was not sufficient to restore kidney development, we anticipated that complete inactivation of *Bmp7* is necessary. Indeed, the majority of all (89%) *Grem1*^{ΔΔ}; *Bmp7*^{ΔΔ} newborn mice displayed two hypoplastic kidneys (Fig. 1E, F and Table 1) in comparison to wild-types (Fig. 1A, B). Although no hydronephroses were observed, the reduced kidney size may be due to the premature loss of nephrogenic progenitors which is responsible for the *Bmp7*^{ΔΔ} phenotype (Dudley et al., 1995). Histological sections indeed reveal the much thinner cortex region (indicated with **Cx**) and fewer glomeruli in *Grem1*^{ΔΔ}; *Bmp7*^{ΔΔ} in comparison to the wild-type mice (Fig. 1B, C and Fig. 1F, G). This indicates that genetic inactivation of *Bmp7* does restore the early *Grem1* defect in initiation of UB outgrowth and mesenchymal apoptosis due to excess of BMP signalling, but fails to restore the depletion of mesenchymal progenitors due to lack of *Bmp7*. However, comparison of *Bmp7*^{ΔΔ} kidneys to *Grem1*^{ΔΔ}; *Bmp7*^{ΔΔ} kidneys (Fig. 1A-D and Fig. 1I-L) reveals that hydronephroses formation was prevented and that the cortex region was slightly enlarged resulting in a bigger kidney size in double mutants (compare the kidneys and respective sections – Fig. 1A, B, C and Fig. 1I, J, K). However, the major phenotype due to the importance of *Bmp7* as a mesenchymal survival factor (Godin et al., 1998) was not completely restored. Hence this direct genetic comparison indicates that the GREM1/BMP7 interactions are possibly different from the GREM1/BMP4 antagonistic interactions.

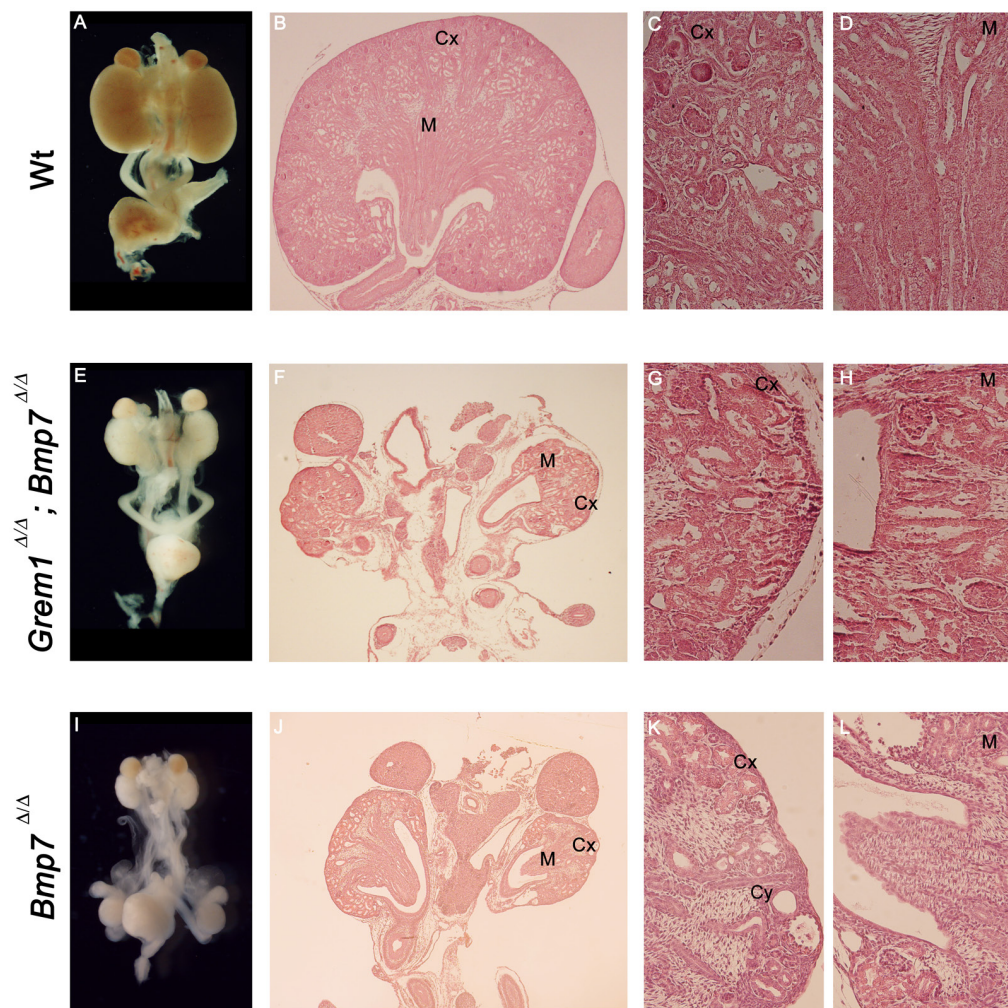


Fig. 1. Inactivation of both *Bmp7* alleles restores the *Grem1*^{ΔΔ} kidney agenesis phenotype but not the *Bmp7*^{ΔΔ} phenotype resulting in depletion of nephrogenic progenitors. (A, E, I) Gross morphology of the urogenital system at birth. (B, F, J) Haematoxylin and Eosin staining of histological sections of urogenital ridges from newborn mice. (C, G, K) Magnification of the kidney cortex regions. (D, H, L) Magnification of the medullar region. The *Grem1*^{ΔΔ}; *Bmp7*^{ΔΔ} urogenital ridge displays two hypoplastic kidneys (compare E with A). The double-mutant kidney sections reveal the morphology of the hypoplastic small kidneys (F – compare with B). Magnification of the cortex area (G) reveals a thin cortex with scarce glomeruli and the medulla (H) is abnormal and poorly defined – compare to the wild-type sections (panels C and D). *Bmp7*^{ΔΔ} kidneys (I) more severely affected as they are even more reduced in size in comparison to wild-type and double mutant kidneys (A). A detailed magnification of section J shows that the cortex is severely depleted as only a few glomeruli are detected and cysts are apparent. Note that the *Grem1*^{ΔΔ}; *Bmp7*^{ΔΔ} (E-H) are bigger than the *Bmp7*^{ΔΔ} kidneys (I-L) and less affected by cysts. Magnifications: kidney ridges 1.25x ; sections gross morphology: 4x ; sections high magnification: 40x. Cx, cortex; Cy, cyst; M, medulla

Inactivation of Grem1 improves glomeruli and collecting duct formation in Bmp7 deficient kidneys

To examine the formation of glomeruli and the collecting duct system, an immune detection assay was performed using the podocyte marker PODOCALYXIN (red) (Schmidt-Ott et al., 2006) and the anti-pan CYTOKERATINS 1, 5, 6, 8 (green) that marks the epithelium of the collecting ducts (Fig.2; Achtstatter et al., 1985).

In wild-type sections, PODOCALYXIN and CYTOKERATIN (Fig. 2A-C) revealed the normal glomerular morphology and number (red) and the epithelial tree of the collecting duct system (green). Comparing wild-types to *Grem1^{ΔΔ}; Bmp7^{ΔΔ}* kidneys (Fig. 2D-F) revealed the major defects. There is an overall decrease in the number of glomeruli and some cysts were readily observed in the cortex region, because they are delineated by epithelial cells (compare Fig. 2D with Fig. 2A). CYTOKERATIN staining showed that the fewer glomeruli that formed are properly connected to the collecting duct system (Fig. 2D-F), in agreement with normal urine secretion observed in some of the newborn mice. In contrast, *Bmp7^{ΔΔ}* kidneys are severely malformed as previously described (Fig. 2G-I; Dudley et al., 1995). They appear smaller than the *Grem1^{ΔΔ}; Bmp7^{ΔΔ}* kidneys and fewer normal looking glomeruli are formed (Fig. 2G and Fig. 2D). The cortex region is further reduced and the reduced nephrogenic area is poorly defined as some epithelial ducts seem to invade the cortex, indicative of a severely dysplastic phenotype. The *Bmp7* deficient kidney displays a larger number of cysts. Moreover, abnormal glomeruli, indicative of a glomerulosclerosis phenotype, were detected with PODOCALYXIN with a

higher incidence in *Bmp7* deficient than double mutant kidneys. Both gross morphology (Fig. 1 and Sup. Fig.1) and immunohistochemistry (Fig. 2) analysis indicate that additional inactivation of *Grem1* is able to partially restore the kidneys phenotype caused by the *Bmp7* deficiency, which indicates that *Grem1* modulation of BMP signalling is also required for robust nephron and ureter branching at later stages.

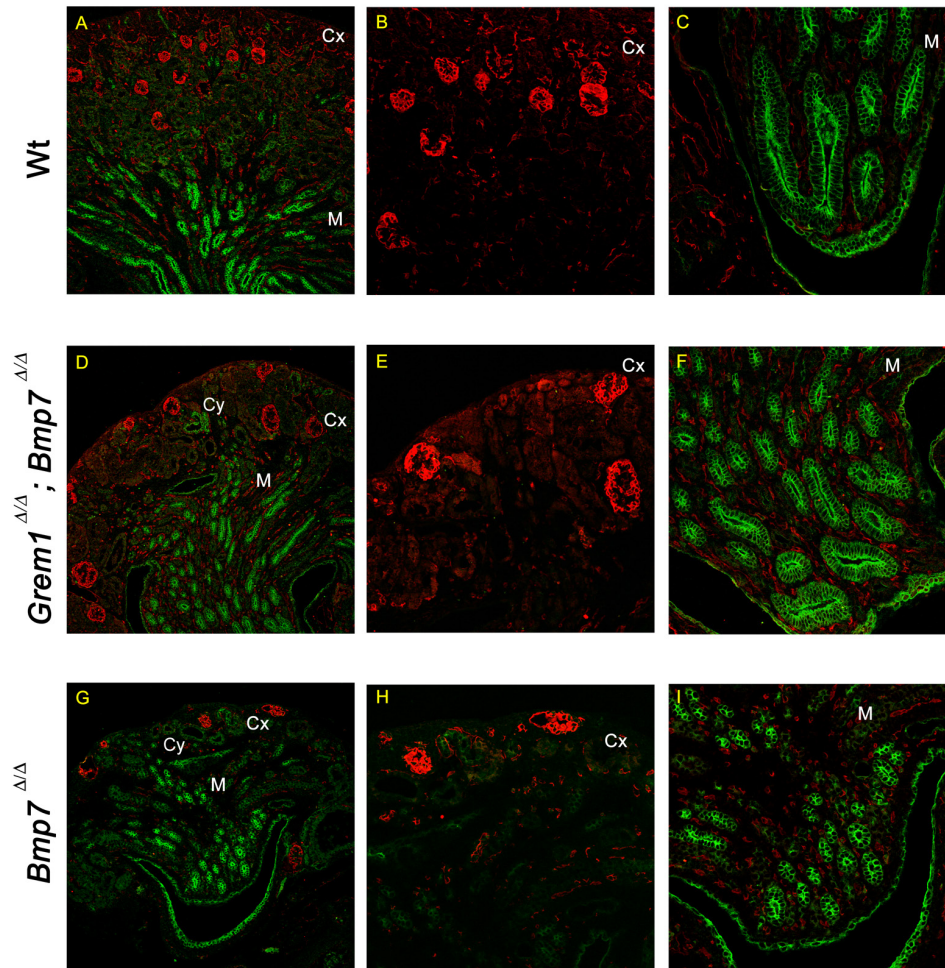


Fig. 2. Detection of PODOCALYXIN (red) to assess glomerular morphology and CYTOKERATIN (green) to reveal the collecting system. (A, D, G) Detection of PODOCALYXIN (red) and CYTOKERATIN (green) in newborn kidneys sections. **(B, E, H)** Magnification of PODOCALYXIN distribution in the cortex region. **(C, F, I)** Magnification of the medullar region showing the CYTOKERATIN distribution. *Grem1*^{ΔΔ}; *Bmp7*^{ΔΔ} kidneys are smaller than wild-types (compare **A** and **D**) and show less glomeruli, evidenced by podocytes positive for PODOCALYXIN (**A, B** and **D, E**). The *Bmp7*^{ΔΔ} kidney is even more hypoplastic than the *Grem1*^{ΔΔ}; *Bmp7*^{ΔΔ}, with a thinner nephrogenic region and less glomeruli – note the abnormal, collapsed morphology of some glomeruli (**D, E** and **G, H**). Both *Grem1*^{ΔΔ}; *Bmp7*^{ΔΔ} and *Bmp7*^{ΔΔ} kidneys develop cysts that are better visualized by CYTOKERATIN detection (**D** and **G**). The epithelial collecting duct system was labelled with CYTOKERATIN and reveals that the collecting duct trees are reduced, but potentially functional in the mutant kidneys (**D, F, G** and **I**). Confocal microscope magnifications: **A, D, G** 10x ; **B, C, E, F, H, I** 20x. Cx, cortex; Cy, cyst; M, medulla.

Inactivation of Bmp7 in Grem1^{ΔΔ} kidney rudiments restores the GDNF/Ret/Wnt11 feedback signalling loop and onset of nephrogenesis

To gain insight into the extent of restoration of kidney development we performed a comparative molecular analysis of the Gdnf/Ret/Wnt11 feedback signalling loop in *Grem1*; *Bmp7* deficient mouse embryos (Fig.3A-H). Furthermore, we also investigated whether the metanephric mesenchyme was competent to undergo nephrogenesis by analysing the expression of *Pax2* (Fig.3I-L) at E11.5.

Ret expression was detected both along the Wolffian duct and in the epithelial tips of the invading and branching ureteric bud (Fig.3A-D). At E11.5 *Grem1^{ΔΔ}* kidney rudiments already undergo apoptosis (Michos et al., 2004) and *Ret* expression is already lost (Fig. 3B – compare with wild-type panel A). These results show that complete inactivation of *Bmp7* restores the *Grem1*-null phenotype (Fig. 3C). *Bmp7* inactivation not only triggered initiation of epithelial branching but also prevented the metanephric mesenchyme to undergo apoptosis. Indeed, *Wnt11* was also expressed by branching ureteric bud tips (Fig. 3E, G, H). Although *Gdnf* expression was not analysed, these results indicate that complete Gdnf/Ret/Wnt11 feedback signalling is restored in the *Grem1^{ΔΔ}*; *Bmp7^{ΔΔ}* kidneys. *Wnt11* is only up-regulated following activation of the RET receptor by the GDNF ligand (Majumdar et al., 2003), which in turn permits propagation of epithelial-mesenchymal interactions and branching morphogenesis. In contrast, *Wnt11* was not detected in the *Grem1* deficient while it was properly expressed in *Bmp7^{ΔΔ}* embryonic kidneys (Fig. 3F and H). *Pax2* transcripts were expressed normally in the Wolffian duct of all genotypes

except *Grem1*^{Δ/Δ} embryos (Fig. 3I-L). The mesenchymal expression in the induced metanephric mesenchyme, indicative of the onset of nephrogenesis, was observed in the double mutant kidneys (Fig.3K – compare with panel I) and *Bmp7*^{Δ/Δ} (Fig. 1L), but not *Grem1* deficient kidney rudiments.

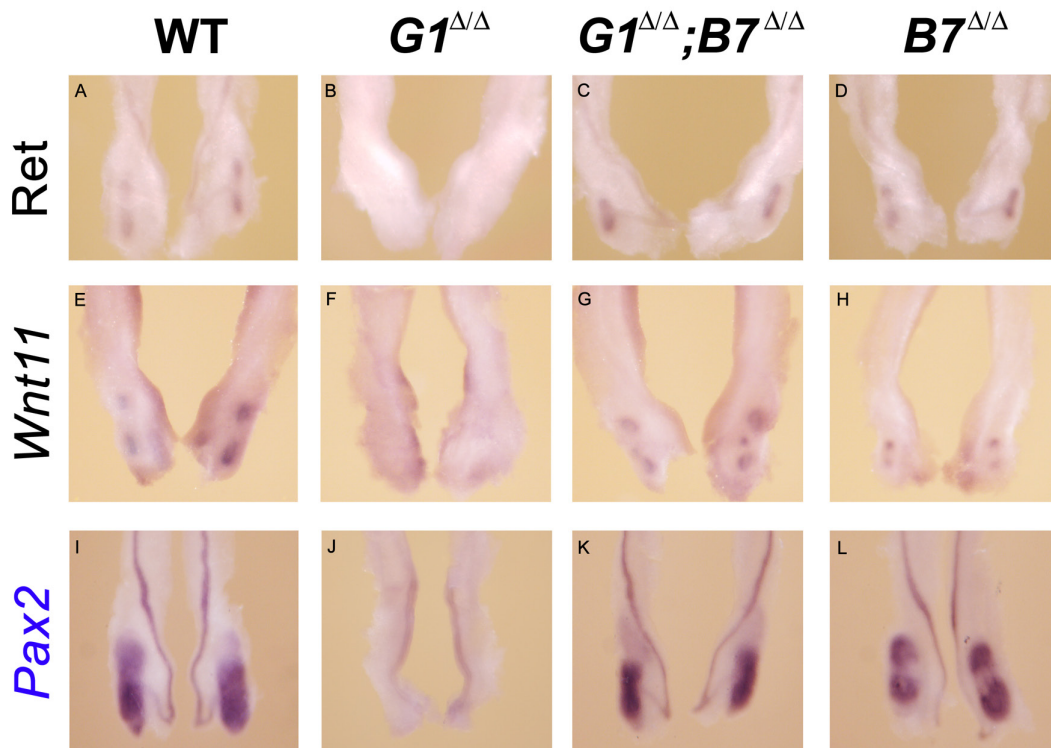


Fig. 3. Complete inactivation of *Bmp7* in a *Grem1* deficient background restores the GDNF/*Ret*/*Wnt11* feedback signalling loop and epithelial branching morphogenesis.

In situ hybridization with *Ret* (A-D), *Wnt11* (E-H) and *Pax2* (I-L) using mouse embryonic kidneys at E11.5-11.75 (49-54 somites). *Ret* expression was detected in the Wolffian duct epithelia of all samples. *Ret* transcripts were observed in tips of the branching epithelial ureteric bud (A, C, D) but not identified in *Grem1*^{Δ/Δ} kidney rudiments (B). Inactivation of *Bmp7* in *Grem1*^{Δ/Δ} embryos restores branching morphogenesis as shown by up-regulation of *Ret* (compare B with C). *Bmp7* deficient embryonic kidneys display normal *Ret* expression (D). *Wnt11* expression analysis (E-H) parallels *Ret* levels. Normal *Wnt11* expression is observed in *Grem1*^{Δ/Δ}, *Bmp7*^{Δ/Δ} (G) and in

the *Bmp7^{ΔΔ}* kidney rudiments (H) but absent from *Grem1^{ΔΔ}* early kidneys (F). *Pax2* expression was normal in the mesenchyme surrounding the Wolffian duct and the induced metanephric mesenchyme of the wild-type (I), *Grem1^{ΔΔ}*; *Bmp7^{ΔΔ}* (J) and *Bmp7^{ΔΔ}* kidney rudiments (L). *Pax2* transcripts are lost from *Grem1^{ΔΔ}* embryonic kidneys (J) due to apoptosis of the metanephric mesenchyme (Torres et al., 1995).

*Six2 positive nephrogenic progenitors are partially restored in *Grem1^{ΔΔ}*; *Bmp7^{ΔΔ}* embryos*

It has been shown that *Six2* marks the nephron progenitor cell population in the metanephric mesenchyme (Kobayashi et al., 2008). Therefore *Six2* was used to reveal the pool of nephrogenic progenitors in the different mutant genotypes. The *Six2 in situ* hybridization of E11.5 kidney rudiments revealed its rather unaltered expression in all relevant genotypes (Fig. 4A-D). In *Grem1^{ΔΔ}* embryonic kidneys *Six2* was only slightly down-regulated (compare Fig. 4A with Fig. 4B), which appeared restored to wild-type levels in *Grem1^{ΔΔ}*; *Bmp7^{ΔΔ}* (Fig. 4A, C). At this early stage, *Six2* transcripts levels were also normal in *Bmp7^{ΔΔ}* embryonic kidneys (Fig. 4D – compare with the wild-type in panel A). As previous studies showed that the *Bmp7* loss-of-function phenotype only becomes evident around E13.5 (Jena et al., 1997), such stage and later kidney rudiments were also analysed. Indeed, branching morphogenesis is altered in *Bmp7^{ΔΔ}* embryos by E13.5 (Fig. 4D) and *Six2* transcript levels are lower (compare with the wild-type in panel E). It is also evident that the metanephric mesenchyme, where *Six2* is normally expressed, appears rather reduced possibly due to the defects in branching morphogenesis. A very similar

reduction is seen in *Grem1*^{ΔΔ}; *Bmp7*^{ΔΔ} kidneys (Fig. 4G). In contrast *Six2* expression is lost in *Grem1*^{ΔΔ} kidney rudiments due to apoptosis (Fig. 4F). The analysis of the E14.5 kidney rudiments (Fig. 4I-L) confirmed these alterations. Residual *Six2* expression was observed in *Grem1*^{ΔΔ}; *Bmp7*^{ΔΔ} kidneys (Fig. 4K) in contrast to *Grem1* deficient kidneys (Fig. 4J). *Bmp7*^{ΔΔ} kidneys appeared smaller and *Six2* was only weakly detected (Fig. 4L).

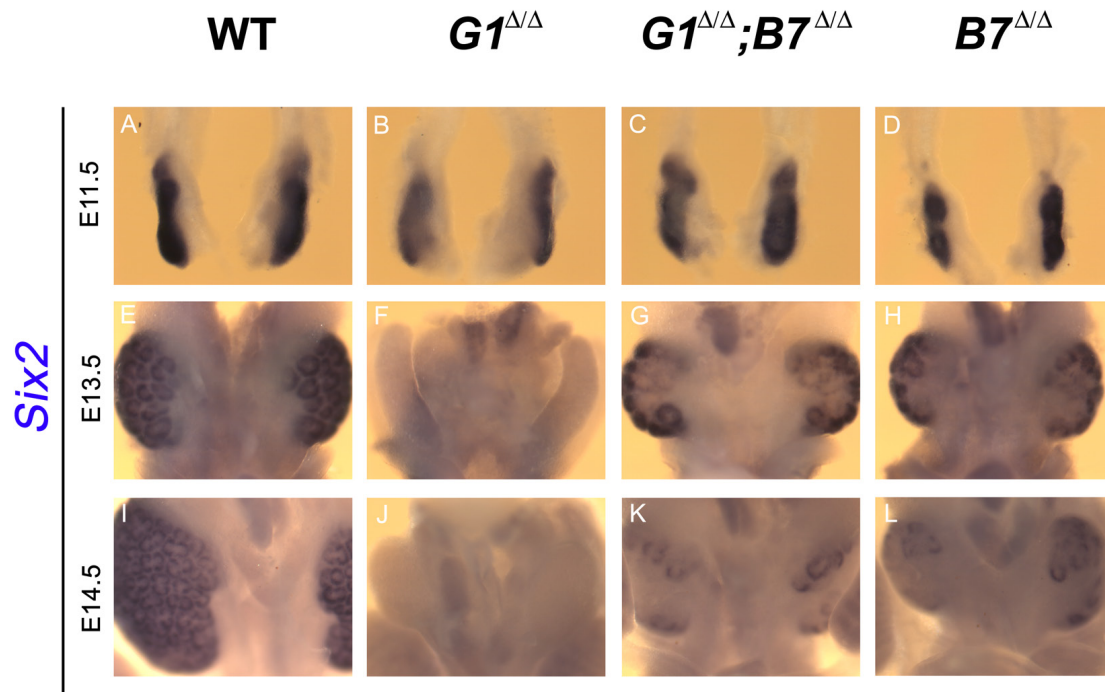


Fig. 4. *Six2* expression in metanephric nephron progenitors highlights the partial restoration of kidney development in *Grem1*^{ΔΔ} embryos by *Bmp7* inactivation.

Six2 whole-mount *in situ* hybridization reveals the *Grem1* and *Bmp7* inactivation phenotypes. Kidney rudiments isolated at E11.5 (**A-D**) show rather normal *Six2* expression. While expression is slightly decreased in *Grem1*^{ΔΔ} kidneys (compare with wild-type in panel **A**) the double mutants (**C**) show close to normal expression. The *Bmp7* deficient embryonic kidneys also express *Six2* at normal levels (**D**). By E13.5 *Grem1* deficient kidneys have been eliminated by

apoptosis (F) but in *Grem1^{ΔΔ}; Bmp7^{ΔΔ}* embryos *Six2* expression was reduced but not lost (G). *Bmp7^{ΔΔ}* kidneys (H) express similar *Six2* levels as the *Grem1^{ΔΔ}; Bmp7^{ΔΔ}* kidneys. By E14.5 the *Grem1^{ΔΔ}; Bmp7^{ΔΔ}* embryonic kidneys (K) are bigger than the *Bmp7^{ΔΔ}* (L), but clearly smaller than wild-types (I). In both mutant genotypes *Six2* expression levels are very much reduced.

Comparative analysis of the Grem1, Bmp4 and Bmp7 expression patterns during early kidney development

In summary the genetic and molecular analysis suggests that GREM1 regulates the activity of different BMP ligands during kidney development (see also chapter VII). Therefore the spatiotemporal expression patterns of *Grem1*, *Bmp4* and *Bmp7* during early kidney development was assessed (Fig. 5). The epithelial expression of the *Hoxb7*- GFP transgene marks the Wolffian duct and the ureteric epithelium (Fig. 5A-D). *Grem1* is expressed at rather low levels (Fig. 5E-H). By E10.5 the expression is detected in the mesenchyme adjacent to the Wolffian duct and around the emerging epithelial ureteric bud (Fig. 5E). As development proceeds, the expression is maintained around the Wolffian duct and *Grem1* transcripts remain around the ureteric bud at the ampullae stage (Fig. 5F). Subsequently it becomes restricted to the metanephric mesenchyme around the ureteric bud tips (Fig. 5G, H). To detect *Bmp4* expression levels in embryonic kidneys we took advantage of the presence of the *LacZ* gene inserted into the *Bmp4* locus and whose expression is under the control of the *Bmp4* promoter. Interestingly, *Bmp4* expression was low whenever *Grem1* expression was high (compare Fig. 5I-L with Fig. 5E-H). In contrast *Bmp7*

expression (Fig. 5M-P) appear to overlap at least partially with the one of *Grem1* (compare Fig- 5E-H with panels M-P).

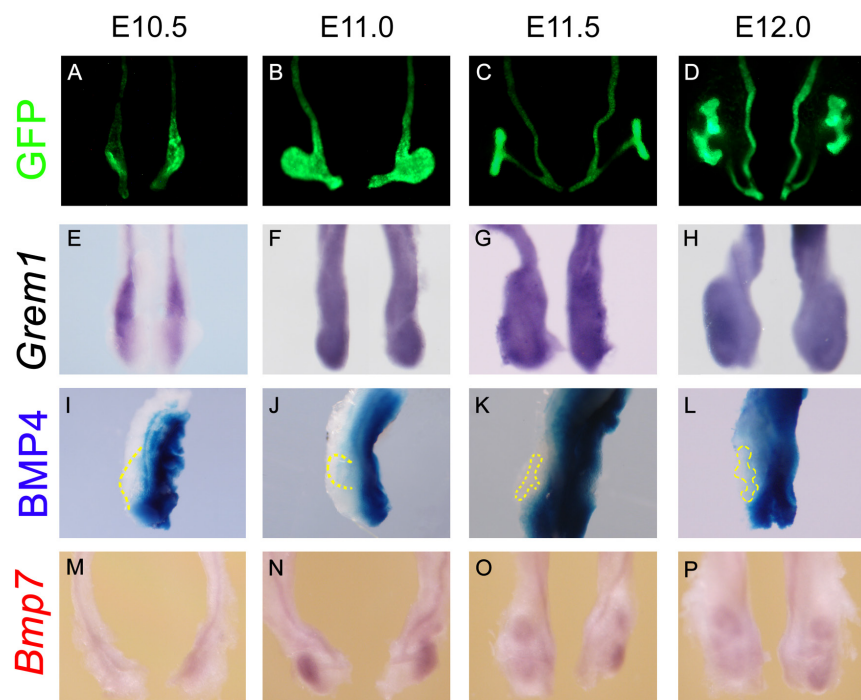


Fig. 5. Spatiotemporal analysis of *Grem1*, *Bmp4* and *Bmp7* expression during early kidney development. Embryonic kidney rudiments were isolated between E10.5 to E12.0. Kidney pairs from embryos carrying the *Hoxb7*-GFP transgene (heterozygous) were used to visualise the ureteric epithelial system (**A-D**). Wild-type embryos were used for *Grem1* and *Bmp7* *in situ* hybridization (**E-H** and **M-P** respectively). *Bmp4* expression was assessed by X-gal staining of kidneys carrying the *Bmp4* ^{Δ -lacZ} allele (**I-L**). *Grem1* transcripts were detected in the metanephric mesenchyme and mesenchymal cells surrounding the Wolffian duct (**E-H**). As the ureteric bud is emerging from the Wolffian duct and elongates to form the ampullae, *Grem1* expression becomes stronger around the ureteric bud tip (**E-F**). Once epithelial branching occurs, *Grem1* is detected in the metanephric mesenchyme around the tips of the branched ureteric

epithelium (**G-H**) – note that *Grem1* expression is maintained in the mesenchyme surrounding the Wolffian duct. β -galactosidase activity reveals the *Bmp4* transcript distribution (**I-L**). *Bmp4* expression is detected in the ventral mesenchyme of the kidney rudiments and delineates the Wolffian duct. The mesenchyme surrounding the ureteric bud lacks *Bmp4* (**I**), as it gives rise to the ampullae (**J**), and branches (**K-L**). *Bmp7* transcripts are expressed in a pattern similar to *Grem1* transcripts (compare **M-P** with **E-P**). *Bmp7* is expressed by the mesenchymal cells adjacent to the Wolffian duct and in the metanephric mesenchyme. At the earlier stages (**M-N**) *Bmp7* expression is more pronounced in the metanephric mesenchyme. *Bmp7* transcripts are also detected in the metanephric mesenchyme surrounding the branched ureteric tips and the expression is maintained around the Wolffian duct (**O-P**).

Discussion

The main aim of the present study was to genetically analyse the GREM1/BMP7 interactions. It was important to assess if GREM1 antagonises also BMP7 which had previously been shown to be also required for normal kidney development (Godin et al., 1998; Jena et al., 1997).

In contrast to *Bmp4* (Michos et al., 2007), *Bmp7* must be completely inactivated to restore the disruption of UB outgrowth in *Grem1* deficient kidneys. In particular, RET signalling is restored in double mutant embryonic kidneys, which suggested that GDNF/RET signalling was re-established. This was confirmed by restricted *Wnt11* expression in *Grem1^{ΔΔ}; Bmp7^{ΔΔ}* kidney rudiments. If both *Ret* and *Wnt11* are normally expressed, then the GDNF/RET/WNT11 signalling loop must be restored as it is required to propagate branching morphogenesis (Majumdar et al., 2003). Furthermore, normal induction of kidney development was further supported by the restored *Pax2* expression, both in the epithelia and condensing mesenchyme. These results, together with the fact that PAX2 is required for activation of GDNF via enhanced RET activity (Brophy et al., 2001; Brophy et al., 2003), show that the kidney rudiments are competent to initiate ureteric bud branching morphogenesis.

Furthermore, *Six2* expression is restored at early stages in the *Grem1^{ΔΔ}; Bmp7^{ΔΔ}* kidney rudiments indicative of survival of the mesenchymal nephron progenitors in contrast to *Grem1* mutants. In fact also the premature depletion of these progenitors in *Bmp7^{ΔΔ}* mutants is partially restored in double mutants.

Although *Grem1*; *Bmp7* double mutant kidneys display a hypoplastic phenotype due to the fact that at later stages, the *Six2* expression is also lost similarly to *Bmp7* deficient kidneys. However, morphogenesis of *Grem1*^{ΔΔ}; *Bmp7*^{ΔΔ} kidneys is improved in comparison to *Bmp7* deficient kidneys. First of all, hydroureter formation is suppressed in double mutant kidneys. Second, fewer and smaller cysts were observed in *Grem1*^{ΔΔ}; *Bmp7*^{ΔΔ} kidneys. Thirdly, the thickness of the cortex is increased and morphologically more normal glomeruli form. Based on these details we may state that *Grem1* inactivation does improve the *Bmp7* deficiency even at more advanced stages.

I propose that not GREM1 mediated antagonism of a particular BMP ligand, but spatiotemporally controlled reduction of BMP activity is key to initiation and progression of kidney morphogenesis. This study reveals an early function for *Bmp7* as it is clearly co-expressed with *Grem1* and its activity must be negatively regulated by GREM1 as revealed by the excess of BMP signal transduction in *Grem1* deficient embryonic kidneys. The possible GREM1/BMP7 agonistic interaction might be a consequence of heterodimer formation. In *Xenopus* BMP4-BMP7 heterodimers have a potent mesoderm inducing capability, which is stronger than the one of BMP4 and BMP7 homodimers respectively (Suzuki et al., 1997). It has also been suggested that BMP4-BMP7 heterodimers exist in the mouse as mice heterozygous for both *Bmp4* and *Bmp7* display minor skeletal defects (Katagiri et al., 1998). Although the existence of BMP4-BMP7 heterodimers has not been demonstrated *in vivo*, this partially shows why GREM1 also antagonises BMP7 at an early stage. This could be similar to the situation in limb buds, where additional inactivation of

Bmp7 also contributes to restoration of digit development in *Grem1*^{Δ/Δ} embryos (Bénazet et al., 2009). Considering that *Grem1* and *Bmp7* are spatiotemporally co-expressed in the early kidney metanephric mesenchyme, it is plausible that, while BMP4-BMP7 heterodimers are antagonised by GREM1, BMP7 homodimers are not. As I have already indicated, GREM1 preferentially antagonizes BMP4. Hence, the antagonistic effect GREM1 exerts on the BMP4 homodimers and potential BMP4-BMP7 heterodimers might favour the BMP7 homodimers to exert their function on e.g. *Six2* positive nephrogenic progenitors

Another major finding was that *Grem1* inactivation prevents to some extent the glomerulosclerosis, hydronephrosis and cyst formation observed in *Bmp7* deficient embryonic kidneys. However, the impairment of kidney organogenesis in *Grem1; Bmp7* double mutant embryos is a likely consequence of *Six2* down-regulation. *Six2* deficient kidneys lose their nephron progenitor pool by apoptosis, revealing the essential role of *Six2* in maintaining the metanephric mesenchyme in an undifferentiated state (Self et al., 2006). This results in premature nephrogenesis and small kidney size due to the metanephric mesenchyme cell death.

In summary this study provides a first glimpse into the intricate regulation of BMP activity (as the sum of BMP4 and BMP7 activities) during initiation and progression of metanephric kidney organogenesis.

IX. CONCLUSION AND OUTLOOK

This section aims to combine the main outcomes described in the different chapters. None of them should be considered as independent studies, but rather as an effort to achieve the main goal of this thesis, namely to analyse the BMP-Gremlin1 antagonistic interactions.

GREM1 is a crucial renal BMP signalling antagonist, required for initiation of ureteric bud (UB) outgrowth and epithelial branching morphogenesis (Michos et al., 2007). The BMP signalling activity, with particular emphasis on BMP4, is regulated by GREM1 in a precise spatiotemporal context. *Grem1* deficient kidney rudiments cultured with recombinant GREM1 displayed a restoration of UB outgrowth and epithelial branching. Both *Gdnf* mesenchymal expression and *Wnt11* expression at the epithelial tips were restored by culturing *Grem1* deficient kidney rudiments with recombinant GREM1. Genetic and molecular studies have shown that reduction of BMP4 activity by GREM1 enables the epithelial-mesenchymal GDNF/WNT11 feedback signalling loop essential for UB initial outgrowth and epithelial branching. These studies provided insight into the mechanisms that mediate the first steps required for metanephric mesenchyme invasion by the UB, which is the first step in metanephric kidney development.

However also BMP7 activity is modulated by GREM1 as complete inactivation of *Bmp7* in a *Grem1* deficient background also permits initiation of ureteric bud outgrowth and epithelial branching morphogenesis. Furthermore, the *Grem1*

inactivation is not sufficient to restore the depletion of *Six2* positive mesenchymal progenitors which characterize the *Bmp7* deficient hypoplastic kidney phenotype. As aspects of collecting duct morphogenesis were restored, *Grem1* may normally also function after initiation of UB outgrowth in structures such as the collecting ducts system and the glomeruli. Moreover, at least at an early stage, GREM1-BMP7 interactions may not be merely antagonistic. The BMP7 activity may actually benefit from a BMP4 zone generated by GREM1 mediated BMP4 antagonism via formation of alternative BMP heterodimers, which may alter receptor-ligand interactions (as previously suggested by BMP7 and BMP2 co-localization analysis (Lyons et al., 1995).

Recently, miRNAs binding sites were identified in the *Grem1* promoter, which reveals another level of regulating *Grem1* expression (Walsh et al., 2008). *Grem1* is not only expressed during onset of kidney development but also during renal injury (McMahon et al., 2000; Walsh et al., 2008). Therefore, the regulation of *Grem1* expression during normal kidney development, which is largely unknown, and renal injury must be analysed in detail.

While these genetic studies reveal that GREM1 antagonises BMP4 to a larger extent than BMP7 or BMP2 during limb and kidney development (Bénazet et al., 2009) it appears as a key gate keeper of overall BMP activities during the development of these structures. These results may also be relevant to developing novel tissue engineering strategies.

APPENDIX 1. TM-CRE MEDIATED INACTIVATION OF BMP4 DURING KIDNEY DEVELOPMENT

Introduction

GREM1-mediated inhibition of BMP4 activity in the metanephric mesenchyme is required for initiation of UB outgrowth and subsequent branching morphogenesis. Furthermore, it has also been shown that GREM1 treatment of cultured kidney rudiments leads to the formation of ectopic UBs (Michos et al., 2007). The observed phenotype was possibly due to the abnormal overall down-regulation of BMP signalling. I wanted to address the following questions: 1) was the ectopic bud formation the result of direct antagonism of BMP4 as suggested by the analysis of *Grem1*; *Bmp4* compound mutant embryos and; 2) were the supernumerary ectopic UBs able to initiate branching morphogenesis. To investigate these issues, *Bmp4* was completely inactivated using tamoxifen-CRE mediated gene inactivation.

Methods and Aims

Tamoxifen-CRE mediated gene inactivation provided results for both limb and kidney development. This appendix will focus on the investigation of *Bmp4* inactivation during early metanephric kidney development. The methods are described in the 'Material and Methods' chapter. Early inactivation of *Bmp4* *in vivo* was accomplished by injecting tamoxifen into pregnant *Bmp4*^{ff} females mated previously with *Bmp4*^{Δ/+}; *Tm-Cre*^{+/+} males. To assess the TM-Cre mediated inactivation in all embryonic tissues, pregnant *Bmp4*^{ff} females were

injected with tamoxifen and embryos were collected 15-20 hours later for β -galactosidase staining. Injection at around E9.25 – E9.5 resulted in complete recombination before 33 somites - (Sup. Fig.1C – compare with Sup. Fig.1B). Pregnant females were injected when embryos had developed to about E8.75 to E9.5. Embryos were collected at E11.5 and kidneys isolated for molecular analysis. Mice of the same genotypes were also used to collect kidney rudiments to be used for 4OH-TM mediated inactivation of *Bmp4* in culture. Embryonic kidneys were cultured for 48 hours prior to molecular analysis.

Results

Bmp4 was conditionally inactivated using a uniformly expressed TM-Cre line. 4OH-TM tamoxifen mediated inactivation of *Bmp4* in culture reveals effects on kidney branching morphogenesis (Fig. 1A'-E'). *Ret* is expressed by the UB tips, which allowed us to trace the resulting branching pattern (Fig. 1A-E). A schematic representation (Fig. 1A' to 1E') reveals that *Bmp4^{f/+}* and *Bmp4^{Ac/+}*; *Tm^{f/+}* kidney rudiments (Fig.1A-B) develop with normal branching pattern as expected. Reduction of BMP4 activity as is the case in *Bmp4^{Δf}* kidney rudiments allows branching morphogenesis to progress normally but the elongation of the ureteric bud is affected (compare Fig.1C and Sup. Fig. 1A-C with Fig. 1A, B). Complete inactivation of *Bmp4* in *Bmp4^{ΔAc}*; *Tm^{f/+}* kidneys (Fig. 1D, E) resulted in formation of ectopic UBs (Fig. 1D' and E'). Inactivation of *Bmp4* also caused variable branching such that the endogenous ureteric bud (red) of the kidney rudiment in Fig. 1D' only branched once in contrast to the

one shown in Fig. 1E' (branched 3 times). Furthermore, ectopic buds emerged from the Wolffian duct of both *Bmp4*^{Δ/Δc}; *Tm*^{t/+} kidneys. Only one ectopic ureteric bud formed in one (Fig. 1E') while several formed in the other case (Fig. 1D'). This might be due to the fact that one embryo (Fig. 1D) was significantly younger (41 somites) than the other (Fig. 1E ; 49 somites). *Bmp4* inactivation at earlier stages might therefore promote formation of more ectopic UBs. No ectopic UBs were seen in controls and embryonic kidneys cultured **without** 4OH-tamoxifen (compare Fig. 1D, E to Fig. 2D, E). Furthermore, culture of *Bmp4*^{Δf} kidney rudiments in medium with 4OH-tamoxifen did not cause formation of ectopic buds (Fig. 1C and Fig. 2A, B).

To study the effects of *in vivo* *Bmp4* inactivation during early metanephric kidney development, pregnant *Bmp4*^{Δf} females were injected with tamoxifen around E9.5-E9.75 and embryos were collected 48 hours later. Initial analysis revealed about 50% lethality of the *Bmp4*^{Δ/Δc}; *Tm*^{t/+} embryos while the overall lethality was about 23% (Table 1). Analysis of *Ret* expression showed that an ectopic UB emerged from the Wolffian duct in 1 out of 2 *Bmp4*^{Δ/Δc}; *Tm*^{t/+} embryos (Fig. 1I, J) while this was never the case in controls. Similarly, analysis of *Pax2* revealed ectopic UBs in *Bmp4*^{Δ/Δc}; *Tm*^{t/+} in 1 of 2 kidney rudiments (Fig. 1N ,O). I also noted that the formation of ectopic buds (Fig. 1J, O) was paralleled by developmental retardation of kidney development.

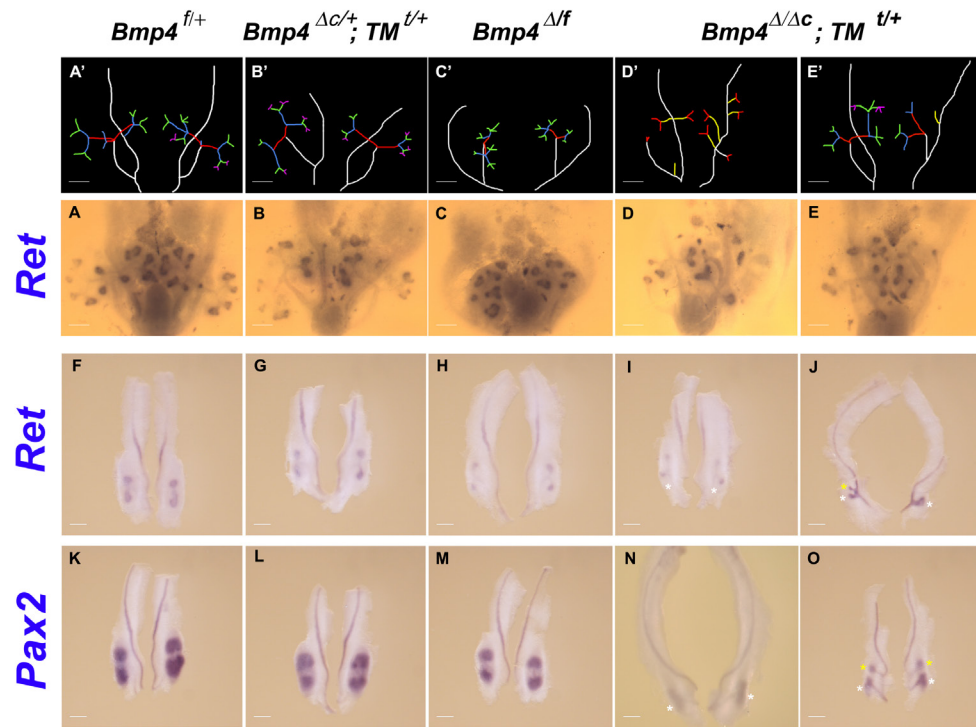


Fig.1. *Bmp4* inactivation mediated by tamoxifen induced recombination reveals the BMP4 early requirement towards ureteric bud elongation and branching morphogenesis, highlighted by the *Ret* and *Pax2* endogenous and ectopic expression domains.

Mouse embryonic kidneys collected at E11.25-11.5 (41-49 somites) and cultured with 4OH-TM during 48 hours (A-E). Upper panels represent the schematic tracings of the Wolffian duct and ureteric epithelium. Wolffian duct and endogenous ureteric bud (white) and ectopic ureteric buds (yellow) – the first branch in red; second branch in blue; third branch in green; fourth branch in purple (A'- E'). Mouse kidney rudiments isolated from tamoxifen injected females at E11.5. White asterisks indicate endogenous ureteric buds and the yellow asterisks the ectopic epithelial buds

(F – O). *Ret* expression is detected along the Wolffian duct and tips of the ureteric buds (F-J) while *Pax2* expression is detected in the mesenchyme surrounding the Wolffian duct and metanephric mesenchyme around the ureteric bud epithelia (K-O). Note the ectopic epithelial bud tip expressing *Ret* (J) and the *Pax2* expression in the metanephric mesenchyme surrounding the ectopic ureteric buds. (O). From all viable *Bmp4*^{ΔΔc}; *Tm*^{t/t} embryos (17), 10 were used for the present analysis and displayed ectopic buds in 50% of the cases. Scale bars, 200μm.

Genotypes	Collected Embryos	Viable Embryos	Genotype Specific Lethality
<i>Bmp4</i> ^{Δ/Δ^c} ; <i>Tm</i> ^{t/+}	35	17	50%
<i>Bmp4</i> ^{Δ^f}	38	31	18%
<i>Bmp4</i> ^{Δ^{c/+}} ; <i>Tm</i> ^{t/+}	53	44	17%
<i>Bmp4</i> ^{f/+}	38	34	11%
Total	164	126 (77%)	

Table 1 – Genetic analysis of TM mediated *Bmp4* inactivation. The embryonic viability upon tamoxifen injection was 77% while the remnant 23% may be attributed to the technique itself or/and to the embryonic development variability that lead to an early *Bmp4* inactivation still at a critical stage. Note that *Bmp4*^{Δ/Δ^c} ; *Tm*^{t/+} lethality was 51% while the *Bmp4*^{Δ^f} was only 18%. The overall 11% lethality observed in the *Bmp4*^{f/+} embryos can be recognized as the tamoxifen injection derived mortality.

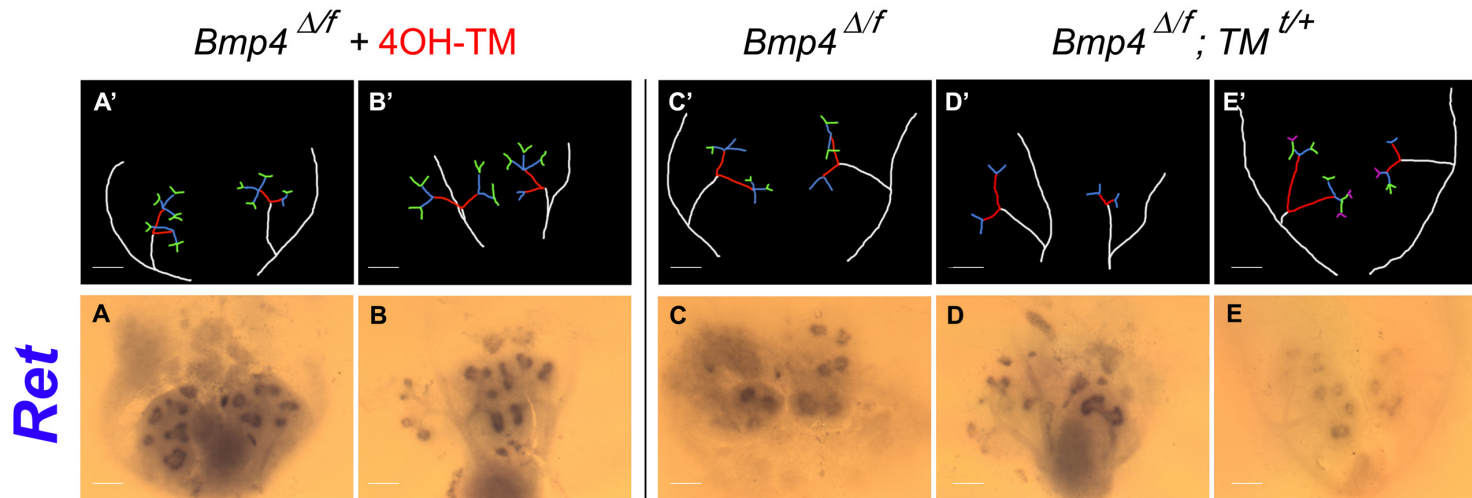
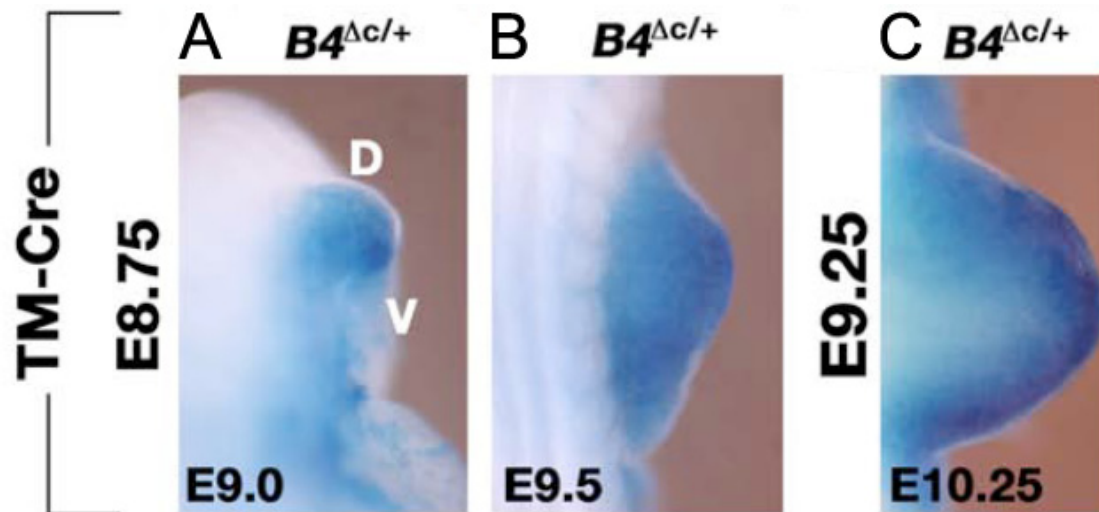


Fig.2. Cultured $Bmp4^{\Delta/f}$ kidney rudiments never displayed the formation of supernumerary ectopic ureteric buds.

Mouse embryonic kidneys collected at E11.25-11.5 (41-49 somites), obtained from littermate embryos displayed in figure 1. The *Ret in situ* hybridization allowed the identification of the ureteric bud tips (**A-E**). Compare the kidney rudiments cultured for 48 hours with 4OH-TM (**A, B**) with the control culture without 4OH-TM (**C-E**). Note that the $Bmp4^{\Delta/f}; TM^{t/+}$ kidneys do not display any abnormal ectopic ureteric buds. Upper panels represent the schematic tracings of the Wolffian duct and ureteric epithelium. Wolffian duct and endogenous ureteric bud (white) and ectopic ureteric buds (yellow) – the first branch in red; second branch in blue; third branch in green (**A'- E'**). Scale bars, 200 μ m.

Conclusion

Both *in vivo* and *in vitro* tamoxifen mediated *Bmp4* inactivation revealed its requirement for restriction of UB formation to one site. Although ectopic UB were only observed in 50% of the embryonic kidneys, culturing of kidney rudiments with recombinant GREM1 resulted in formation of supernumerary ectopic UBs in 75% of all cases (12 out of 16) (see chapter VII). Therefore, it is safe to conclude that the GREM1-mediated reduction of BMP4 activity results in formation of ectopic buds along the Wolffian duct. None of the observed ectopic buds resulting from *Bmp4* inactivation initiated proper branching morphogenesis, which differs from the effects of treatment with GREM1.



Sup. Fig.1. Cre recombinase mediated inactivation of *Bmp4* (*B4*) is monitored by activation of the *LacZ* cassette.

LacZ staining to monitor TM-Cre mediated inactivation of the *Bmp4*^{loxP-lacZ} allele in the entire embryo. Embryos were harvested 15-20hrs after one tamoxifen injection into pregnant mothers at about E8.75. Embryo dorsal view at the level of the forelimb (**A-C**). Recombination appears complete prior to E9.0 (22 somites, panel **B** – compare with **A**). (**C**) TM injection at around E9.25 results in complete recombination prior to E10.25 (33 somites). D: dorsal; V: ventral (from Bénazet et al., 2009).

APPENDIX 2. MICROARRAY ANALYSIS OF THE GREM1-BMP4 ANTAGONISTIC INTERACTIONS

Introduction

The kidney agenesis phenotype caused by inactivation of *Grem1* can be restored by additional inactivation of one *Bmp4* allele. However, further studies were required to understand how excessive BMP signalling blocks UB outgrowth and how restoration of UB outgrowth is molecularly controlled. To gain insight into those events, a microarray gene expression analysis was performed. Microarray technology measures transcript levels in cells of a particular tissue and is often used to identify genes functioning in a particular tissue/process. The microarray analysis of *Grem1*^{Δ/Δ} and *Grem1*^{Δ/Δ}; *Bmp4*^{Δ/+} kidney rudiments identified molecular novel components of the morpho-regulatory mechanisms controlling branching.

Methods and Aims

The microarray analysis aimed to assess transcript levels at a very precise developmental stage, between the UB ampullae and T-shape stages. Kidneys were isolated at 47-48 somites stage, before nephrogenesis had started. The gender of all embryos was determined to circumvent sex specific fluctuations in gene expression. The selection of male samples was unbiased and mainly the consequence of both developmental stage and gender availability. RNA was isolated from the collected kidney rudiments and processed according the

standard GeneChip® protocol. Upon scanning of the hybridized chips, data were statistically validated using the Genedata Expressionist® analysis programme. Expression values were normalized and N-Way ANOVA tests filtered results with a p-value of ≤ 0.05 (95% confidence). To further restrict the analysis but retain the already validated results, a minimal fold change filter was applied. The resulting list, after removal of the internal GeneChip® controls, was used for Ingenuity® pathway analysis. A modified BMP pathway was built by integrating the discovered pathways nodes intersecting with the BMP signalling pathway based on the biological relationships. Select genes were then verified by *in situ* hybridization analysis.

Results

The N-Way ANOVA 0.05 p-value restriction resulted in a list of 411 differentially hybridizing transcripts. This transcripts list was used for Ingenuity® pathway analysis. The BMP signaling network was used as a scaffold and the network was expanded to discover potentially affected pathways due to altered BMP signalling (Fig. 1). The genes list identified by the Ingenuity® BMP pathway analyses is shown in Table 1. Analysing *Grem1*^{Δ/Δ} versus wild-type kidneys allowed me to focus my attention on the underlying molecules and signalling complexes (Fig. 1 – colour ellipses highlight the molecular modules).

The direct relationship between GREM1 and BMP4 was immediately recognized (Fig. 1 – blue ellipse) and the identified genes behaviours correspond to the already known interactions. *Grem1* expression was still

detected in the *Grem1*^{Δ/Δ} samples because the *Grem1* knock-out targeted exon 2 specifically (Michos et al., 2004) while Affymetrix GeneChip array probes cover the entire gene. The GDNF/RET signalling pathway was also evidenced (Fig.1 – yellow ellipse) and although *Ret* was not shown as significantly changed, *Gfra1*, the co-receptor, was identified as altered. *Gfra1* was down-regulated to 0.69-fold in the *Grem1*^{Δ/Δ} kidney rudiments. Conversely, *Gfra1* was up-regulated to 1.6 fold *Grem1*^{Δ/Δ}; *Bmp4*^{Δ/+} kidney rudiments when compared to *Grem1* deficient kidney rudiments.

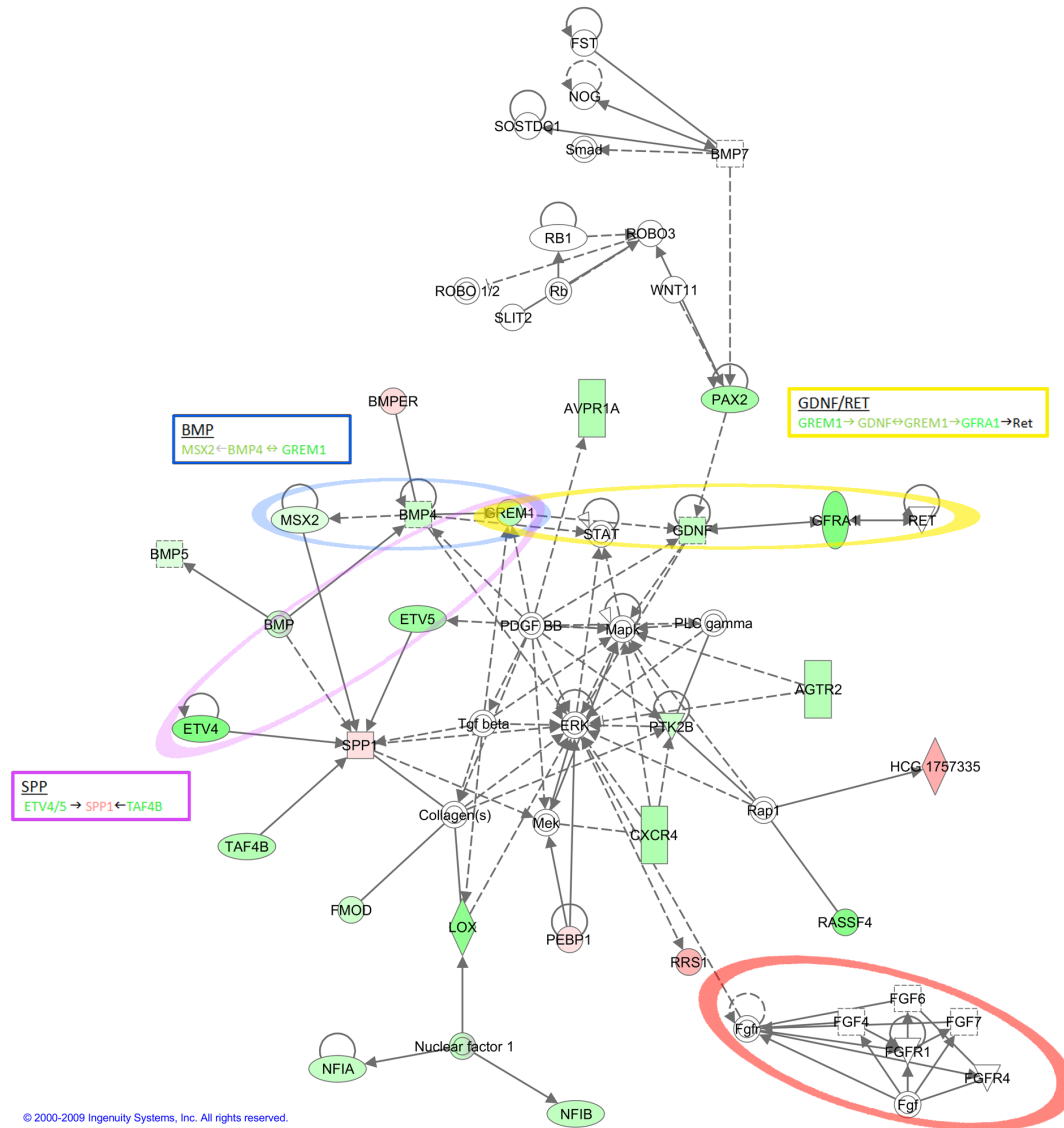
Although the FGFR interactions, highlighted by the red ellipse (Fig. 1), did not show any variation in expression levels, indirect transcriptional alterations were. Expression of the *Etv4* and *Etv5* transcription factors transcriptionally regulated by FGFs in several organs including the kidney (Firnberg and Neubüser, 2002; Liu et al., 2003; Lu et al., 2009) is altered. *Etv4* and *Etv5* are down-regulated in *Grem1*^{Δ/Δ} kidney rudiments 0.68 and 0.75 fold respectively (Table 1) while *Etv4* is up-regulated 1.48 fold in *Grem1*^{Δ/Δ}; *Bmp4*^{Δ/+} kidney rudiments. In contrast, *Etv5* is restored to wild-type expression levels (1,08 fold) in *Grem1*^{Δ/Δ}; *Bmp4*^{Δ/+} kidney rudiments.

Six2 is down-regulated 0.67-fold in *Grem1*^{Δ/Δ} in comparison to wild-type expression kidney rudiments. A 1.91-fold up-regulation was detected in the *Grem1*^{Δ/Δ}; *Bmp4*^{Δ/+} in comparison to *Grem1*^{Δ/Δ}, while a 1.29 fold change was observed in comparison to wild-type kidney rudiments (Fig. 2B).

Both *Etv4* and *Six2* expression patterns were assessed by mRNA *in situ* hybridization and confirmed the microarray analysis (Fig. 2A, compare with the

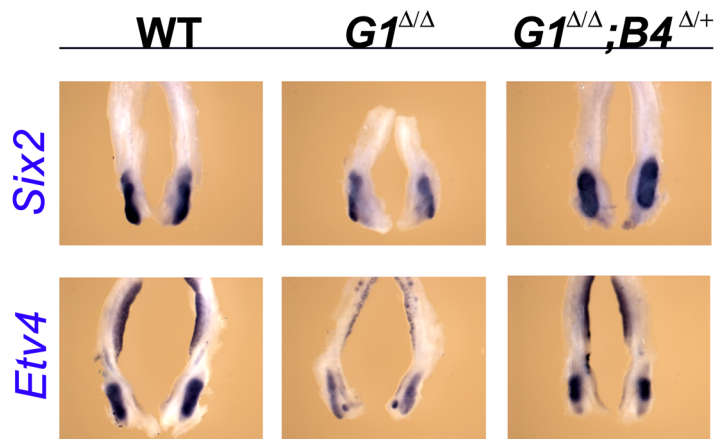
expression values in B). *Six2* expression is slightly reduced in *Grem1*^{Δ/Δ} while it was clearly up-regulated in *Grem1*^{Δ/Δ}; *Bmp4*^{Δ/+} kidney rudiments. *Etv4* was clearly down-regulated in *Grem1* deficient kidneys and up-regulated following additional inactivation of one *Bmp4* allele.

Several other genes identified by the microarray analysis have not yet been analysed further.



© 2000-2009 Ingenuity Systems, Inc. All rights reserved.

Fig.1. Network analysis of the alterations in gene expression between *Grem1*^{Δ/Δ} and wild-type kidney rudiments. The Ingenuity® canonical BMP pathway network was expanded to discover potentially linked pathways. The network is displayed graphically as nodes (genes/gene products) and edges. Intensity of the node colour indicates the degree of up-regulation (red) or down-regulation (green). Node shapes represent the functional class of the gene products (square, cytokine; vertical oval, transmembrane receptor; rectangle, nuclear receptor; diamond, enzyme; rhomboid, transporter; hexagon, translation factor; horizontal oval, transcription factor; and circle, other). Edges labels indicate relationships: — binding only; → acts on. The length of an edge reflects the node-to-node relationship. Dotted edges represent indirect interactions. The coloured ellipses indicate different signalling modules responding to the alterations in BMP signalling. BMP signalling in blue, GDNF/Ret in yellow, ETV4/5 in purple and FGF in red.

A**B**

Genes	Fold change $Grem1^{\Delta/\Delta}$ / WT	Fold change $Grem1^{\Delta/\Delta};Bmp4^{\Delta/+}$ / $Grem1^{\Delta/\Delta}$	Fold change $Grem1^{\Delta/\Delta};Bmp4^{\Delta/+}$ / WT
<i>Six2</i>	0,670397306	1,927665542	1,292301786
<i>Etv4</i>	0,6844401	1,482473035	1,014663992

Fig.2. Whole-mount *in situ* detection of the *Six2* and *Etv4* mRNAs validates the microarray transcripts identification criteria.

Mouse embryonic kidneys collected at E11.5 (48-51 somites). **(A)** *Six2* expression is detected in the metanephric mesenchyme around the epithelial ureteric bud while *Etv4* is expressed in the ureteric bud epithelia and metanephric mesenchyme (the gonads also express *Etv4* whose detection is weakly observed along the Wolffian duct epithelia as well). **(B)** *Six2* and *Etv4* expression intensity values and fold-change variation among the different genotypes. Note that while it is obvious that *Etv4* is down-regulated and restored, *Six2* down-regulation is not so obvious but the up-regulation is clear and possibly due to the expansion of the metanephric mesenchyme compartment.

Conclusion

The microarray analysis of genes altered in *Grem1*^{Δ/Δ} and restored in *Grem1*^{Δ/Δ}; *Bmp*^{Δ/+} kidney rudiments provided evidence for interconnected pathways. The immediate examination yielded surprisingly few altered genes. The second important finding was the identification of *Six2* and *Etv4/5* as altered genes. The identification of *Six2* correlates with the depletion of nephrogenic progenitors in *Grem1*^{Δ/Δ} embryonic kidneys, in agreement with the fact that *Six2* is required to regulate the nephron progenitor pool within the metanephric mesenchyme (Kobayashi et al., 2008). The identification of the *Etv4/5* transcription factors correlates with their recently demonstrated requirement for kidney branching morphogenesis, downstream of GDNF-Ret signalling (Lu et al., 2009).

Genes	WT	<i>Grem1^{ΔΔ}</i>	<i>Grem^{ΔΔ},Bmp4^{Δ/+}</i>	Fold change <i>Grem1^{ΔΔ}</i> / WT	Fold change <i>Grem^{ΔΔ},Bmp4^{Δ/+}</i> / <i>Grem1^{ΔΔ}</i>	Fold change <i>Grem^{ΔΔ},Bmp4^{Δ/+}</i> / Wt
Agtr2	528,6041	423,9591	416,1042	0,802035209	0,981472505	0,787175506
Avpr1a	98,41199	78,33794	83,89924	0,796020282	1,070991144	0,852530672
Bmp4	621,0085	532,8455	373,1586	0,858032539	0,700312942	0,600891292
Bmp5	520,4172	493,9408	410,9665	0,949124664	0,832015699	0,789686621
Bmper	676,3885	734,0994	578,9975	1,085322119	0,788718122	0,856013223
Cxcr4	458,8655	360,5381	469,4916	0,785716294	1,302196911	1,02315733
Etv4	141,2644	96,68702	143,3359	0,6844401	1,482473035	1,014663992
Etv5	267,4216	201,5314	217,9943	0,753609282	1,081689007	0,815170876
Fmod	177,7714	152,641	136,3835	0,858636429	0,893491919	0,76718471
Gdnf	162,9293	135,6146	170,591	0,832352438	1,257910284	1,047024691
Gfra1	322,0566	221,1384	354,3294	0,686644521	1,602297023	1,100208473
Grem1	119,4658	96,53632	94,60455	0,808066576	0,97998919	0,791896509
HCG 1757335 (Rap1a)	399,8005	481,2827	484,4134	1,203807149	1,006504909	1,211637804
Msx2	105,9559	100,29	83,52566	0,946525866	0,83284136	0,78830589
NfIA	360,0708	300,7293	259,1877	0,835194912	0,861863809	0,719824268
NfIB	1103,947	914,6273	867,8156	0,828506532	0,948818825	0,786102594
Pax2	205,4109	157,0658	223,278	0,764641993	1,42155708	1,086982239
Pdgf	117,1343	101,2776	87,77714	0,864628038	0,86669846	0,749371789
Pebp1	688,5453	717,0482	865,3643	1,041395824	1,20684258	1,256800823
Ptk2b	135,2831	116,3346	106,5724	0,859934463	0,916085154	0,787773196
Rap1	399,8005	481,2827	484,4134	1,203807149	1,006504909	1,211637804
Rassf4	135,0365	94,11868	108,4451	0,696986963	1,152216542	0,803079908
Rrs1	234,9687	278,8754	295,2354	1,18686191	1,058664192	1,256488205
Ssp1	84,90002	88,09121	68,85815	1,037587624	0,781668795	0,811049868
Tatf4b	92,66903	73,92025	85,89431	0,797680196	1,161986195	0,926893375

Table 1: Genes identified in the Ingenuity® BMP signalling pathway analysis. All genotype classes and relative fold changes were considered.

X. ACKNOWLEDGEMENTS

When the final acknowledgments are written, it is always unfair not to be able to give enough emphasis to the real importance someone had. For that I must apologize and ask for your understanding.

I deeply thank Rolf Zeller for the enormous patience he had with his stubborn, and sometimes hard to deal with, Portuguese Ph.D. student. It was quite a risk to offer a Ph.D. student position to someone who had never worked with mice or kidneys. I honourably embraced the challenge and the least I can say is that it really changed my life. The opportunity to participate in several different projects was an excellent way to get to know the research field as a whole and not just as small niche. His role was not only played inside the lab but in other tough situations away from science.

Aimée could never be forgotten. Always present at the right moment when it really matters. Something not to forget either is the bet I already won... I will finish my Ph.D. studies, without having bought a Mac. Moreover, she was the first victim having to teach me how to make NOGGIN expressing cells.

Odyssé was “just” the one who presented me the kidney development research field. We did have some hard times but when we look back at it we always celebrate it with joy. Now that he’s away I can only say I am proud to see his achievements.

I must definitely thank to Joaquín León for introducing me to science. He was the first pushing me to accept new challenges and helped me out making up my

mind on my first big decision. He has shown me that science can be hard but that makes it fun.

Markus Affolter has been a driving force to see how a kidney branches. We shall spend some time on it afterwards. Meanwhile I will have to convincingly show how a ureteric bud branches... I don't really think it's a default mechanism. I would like to thank to Prof. Dr. Antonius Rolink for being the chairman of the thesis committee as he promptly accepted my request with such short notice.

I also thank "Fundação para a Ciência e Tecnologia" for offering me a Ph.D. fellowship to support my Ph.D. studies (SFRH/BD/24301/2005).

Regarding to Anto "Potter"... it was quite important to have someone working regardless of the time of the day or night. The way she used her magic to make our life away from family bearable was just one of her great qualities. This thesis would not have been possible without the coffee breaks and the nice moments spent at her balcony. I am still waiting to receive the pictures from little Antoné and Odynella.

To my curling-challenged friend Javier, I must thank for his constant presence and wise scientific knowledge. Furthermore, it was an honour to spend great quality family time with Guille and Gretel. Moreover, I will never forget his terrible kart driving abilities.

As for Prof. Bénazet... Jean-Denis has been a great lab companion. Despite his deadly appetite for mice, we spent some great moments at Mr. Pickwick. Something still engraved in my mind is the time we went shopping to start composing my old apartment.

I could not forget to mention Rushi for the good times we had. I really hope Spain was a good starting point towards something big. No matter what, I will always remember you when I eat a döner kebab.

Kit was the person who picked me up at the airport. Her Mac Donald's craving appetite is legendary. Just a word of caution... I am not Magellan, my head is still in place and I did not forget that coffee we still didn't have.

I must thank Nadège for showing me how to properly work with mice. Her organizational skills were contagious and that helped me keeping track of what I have done.

Simone, for historical reasons, is a name omnipresent in my still short scientific life. It was nice to have good company in the dark side of the lab and being able to join the Friday discussions allowed me to acquire more knowledge.

The tireless Dimitri was a good example that good and efficient work can be achieved through hard work. All the invisible work was crucial.

That brings us to Susie... without her the lab wouldn't work. I must also thank for the thousands of TESPAs slides we have done together.

Sometimes Catherine seemed like my mirror reflex. Her non-limb work has further shown it is possible to work on different research fields in the same lab. Her suggestions were always well taken although some haven't yet been completely fulfilled.

To Alex I must thank for something I believe I'm almost the only one to use. The *in situ* probes list has been quite useful. Moreover, a lot of invisible work is constantly being made but it must also be acknowledged.

As for *little* Marco... what can I say? Sometimes he remembers me, many years ago. Many times being one of the last or the last to leave the lab. Coming during

the weekends... yes, we did have some nice scientific and none scientific discussions.

Eva was someone that actively participated in several aspects of my Ph.D.. Having to put up with my temper while performing the kidney paper last experiments was not easy. She did help me to model my temper in some rather stressful situations.

Regarding Emanuele... he's the one who makes me put everything in perspective. Nothing is ever finished and we are always learning... if we ever forget this we must really think about what we are doing.

The effort Konstantin has made to provide us with good histology sections was very important. Having Isabelle and Irena working with "my" precious kidneys was crucial during my PhD.

Not mentioning Chris would be almost like trying to start my car without a key. Life in Basel would not have been possible without her support (you're reading this and you know it's absolutely true). I hope you manage to visit Lisbon soon and I would be delighted to show it to you.

Concerning the microarray work I must thank Ed. He always made everything look easy and his work at FMI was essential. I cannot forget to mention Philippe for helping me with the RNAs final processing step at the Pharmazentrum.

A "small" parenthesis must be made to mention Zé, without him I would still be in Lisbon because I would not have fought for a good scientific future. Furthermore, the precious help from Moisés Mallo could not be forgotten either. His special talent was crucial to apply for a better position.

Now comes the hard part... to acknowledge family. We cannot mention one without thinking about them all.

To my mother and father I can only thank for EVERYTHING. I hope you consider this thesis a good proof of your good work as parents despite all difficulties. I dedicate this thesis to my family for the enormous effort and constant help. Every single one has played a particular role during my Swiss venture.

I want to thank my future wife Marina for all the help, support and sacrifice during all these years. It has been a long journey since high school but it's almost done (or about to begin). It's amazing how things turned out.

The last acknowledgments must be given to my heroic mice. Without them nothing would have been possible. My personal motto during these last 5 years has always been... 'Mice command life'.

To the Portuguese speakers:

Quero agradecer à minha mãe e ao meu pai por TUDO. Espero que considerem esta tese uma prova do vosso bom trabalho como pais apesar de todas as dificuldades. Dedico esta tese a toda a minha família pelo imenso esforço e ajuda constantes. Todos desempenharam um papel importante na minha aventura Suíça.

Quero agradecer à minha futura esposa Marina por toda a ajuda, apoio e sacrifício ao longo de todos estes anos (já lá vão alguns). Tem sido uma longa caminhada desde o liceu mas já está quase (ou prestes a começar). É incrível como tudo funcionou.

XI. REFERENCES

- Achtstatter, T., R. Moll, B. Moore, and W. Franke. 1985. Cytokeratin polypeptide patterns of different epithelia of the human male urogenital tract: immunofluorescence and gel electrophoretic studies. *J. Histochem. Cytochem.* 33:415-426.
- Aono, A., M. Hazama, K. Notoya, S. Taketomi, H. Yamasaki, R. Tsukuda, S. Sasaki, and Y. Fujisawa. 1995. Potent Ectopic Bone-Inducing Activity of Bone Morphogenetic Protein-4/7 Heterodimer. *Biochemical and Biophysical Research Communications.* 210:670-677.
- Attisano, L., and J.L. Wrana. 1998. Mads and Smads in TGF[β] signalling. *Current Opinion in Cell Biology.* 10:188-194.
- Balemans, W., and W. Van Hul. 2002. Extracellular Regulation of BMP Signaling in Vertebrates: A Cocktail of Modulators. *Developmental Biology.* 250:231-250.
- Ballard, S.L., J. Jarolimova, and K.A. Wharton. 2010. Gbb/BMP signaling is required to maintain energy homeostasis in *Drosophila*. *Developmental Biology.* 337:375-385.
- Basson, M.A., S. Akbulut, J. Watson-Johnson, R. Simon, T.J. Carroll, R. Shakya, I. Gross, G.R. Martin, T. Lufkin, A.P. McMahon, P.D. Wilson, F.D. Costantini, I.J. Mason, and J.D. Licht. 2005. Sprouty1 is a critical regulator of GDNF/RET-mediated kidney induction. *Developmental Cell.* 8:229-239.
- Batourina, E., C. Choi, N. Paragas, N. Bello, T. Hensle, F.D. Costantini, A. Schuchardt, R.L. Bacallao, and C.L. Mendelsohn. 2002. Distal ureter

- morphogenesis depends on epithelial cell remodeling mediated by vitamin A and Ret. *Nature Genetics*. 32:109-115.
- Bell, H.L., and M. Gooz. 2010. ADAM-17 Is Activated by the Mitogenic Protein Kinase ERK in a Model of Kidney Fibrosis. *The American Journal of the Medical Sciences*. Publish Ahead of Print:10.1097/MAJ.0b013e3181cb4487.
- Bénazet, J.-D., M. Bischofberger, E. Tiecke, A. Goncalves, J.F. Martin, A. Zuniga, F. Naef, and R. Zeller. 2009. A Self-Regulatory System of Interlinked Signaling Feedback Loops Controls Mouse Limb Patterning. *Science*. 323:1050-1053.
- Berry, C.A., and R. Floyd C. 1989. Electroneutral NaCl absorption in the proximal tubule: Mechanisms of apical Na-coupled transport. *Kidney Int*. 36:403-411.
- Brophy, P.D., L. Ostrom, K.M. Lang, and G.R. Dressler. 2001. Regulation of ureteric bud outgrowth by Pax2-dependent activation of the glial derived neurotrophic factor gene. *Development*. 128:4747-4756.
- Brophy, P.D., S. Patel, J.C. Clarke, and G.R. Dressler. 2003. PAX2 enhances RET activation. *Pediatric Research*. 53:331.
- Brunet, L.J., J.A. McMahon, A.P. McMahon, and R.M. Harland. 1998. Noggin, Cartilage Morphogenesis, and Joint Formation in the Mammalian Skeleton. *Science*. 280:1455-1457.
- Bush, K.T., H. Sakurai, D.L. Steer, M.O. Leonard, R.V. Sampogna, T.N. Meyer, C. Schwesinger, J.Z. Qiao, and S.K. Nigam. 2004. TGF-beta superfamily members modulate growth, branching, shaping, and patterning of the ureteric bud. *Developmental Biology*. 266:285-298.

- Cain, J.E., S. Hartwig, J.F. Bertram, and N.D. Rosenblum. 2008. Bone morphogenetic protein signaling in the developing kidney: present and future. *Differentiation*. 76:831-842.
- Cao, X., and D. Chen. 2005. The BMP signaling and in vivo bone formation. *Gene*. 357:1-8.
- Capdevila, J., T. Tsukui, C.R. Esteban, V. Zappavigna, and J.C.I. Belmonte. 1999. Control of Vertebrate Limb Outgrowth by the Proximal Factor Meis2 and Distal Antagonism of BMPs by Gremlin. *Molecular Cell*. 4:839-849.
- Carroll, T.J., J.S. Park, S. Hayashi, A. Majumdar, and A.P. McMahon. 2005. Wnt9b plays a central role in the regulation of mesenchymal to epithelial transitions underlying organogenesis of the mammalian urogenital system. *Developmental Cell*. 9:283-292.
- Carvajal, G., A. Droguett, M.E. Burgos, C. Aros, L. Ardiles, C. Flores, D. Carpio, M. Ruiz-Ortega, J. Egido, and S. Mezzano. 2008. Gremlin: A novel mediator of epithelial mesenchymal transition and fibrosis in chronic allograft nephropathy. *Transplantation Proceedings*. 40:734-739.
- Challen, G., B. Gardiner, G. Caruana, X. Kostoulas, G. Martinez, M. Crowe, D.F. Taylor, J. Bertram, M. Little, and S.M. Grimmond. 2005. Temporal and spatial transcriptional programs in murine kidney development. *Physiol. Genomics*. 23:159-171.
- Chandramouli, S., C.Y. Yu, P. Yusoff, D.-H. Lao, H.F. Leong, K. Mizuno, and G.R. Guy. 2008. Tesk1 Interacts with Spry2 to Abrogate Its Inhibition of ERK Phosphorylation Downstream of Receptor Tyrosine Kinase Signaling. *Journal of Biological Chemistry*. 283:1679-1691.

- Chi, L.J., S.B. Zhang, Y.F. Lin, R. Prunskaitė-Hyyryläinen, R. Vuolteenaho, P. Itaranta, and S. Vainio. 2004. Sprouty proteins regulate ureteric branching by coordinating reciprocal epithelial Wnt11, mesenchymal Gdnf and stromal Fgf7 signalling during kidney development. *Development*. 131:3345-3356.
- Chi, X., O. Michos, R. Shakya, P. Riccio, H. Enomoto, J.D. Licht, N. Asai, M. Takahashi, N. Ohgami, M. Kato, C. Mendelsohn, and F. Costantini. 2009. Ret-Dependent Cell Rearrangements in the Wolffian Duct Epithelium Initiate Ureteric Bud Morphogenesis. *Developmental Cell*. 17:199-209.
- Clevers, H. 2006. Wnt/[beta]-Catenin Signaling in Development and Disease. *Cell*. 127:469-480.
- Conley, C.A., R. Silburn, M.A. Singer, A. Ralston, D. Rohwer-Nutter, D.J. Olson, W. Gelbart, and S.S. Blair. 2000. Crossveinless 2 contains cysteine-rich domains and is required for high levels of BMP-like activity during the formation of the cross veins in *Drosophila*. *Development*. 127:3947-3959.
- Costantini, F. 2006. Renal branching morphogenesis: concepts, questions, and recent advances. *Differentiation*. 74:402-421.
- Costantini, F., and R. Shakya. 2006. GDNF/Ret signaling and the development of the kidney. *Bioessays*. 28:117-127.
- Cui, Y., R. Hackenmiller, L. Berg, F.o. Jean, T. Nakayama, G. Thomas, and J.L. Christian. 2001. The activity and signaling range of mature BMP-4 is regulated by sequential cleavage at two sites within the prodomain of the precursor. *Genes & Development*. 15:2797-2802.
- Daluiski, A., T. Engstrand, M.E. Bahamonde, L.W. Gamer, E. Agius, S.L. Stevenson, K. Cox, V. Rosen, and K.M. Lyons. 2001. Bone

- morphogenetic protein-3 is a negative regulator of bone density. *Nat Genet.* 27:84-88.
- Derynck, R., W.M. Gelbart, R.M. Harland, C.-H. Heldin, S.E. Kern, J. Massagué, D.A. Melton, M. Mlodzik, R.W. Padgett, A.B. Roberts, J. Smith, G.H. Thomsen, B. Vogelstein, and X.-F. Wang. 1996. Nomenclature: Vertebrate Mediators of TGF[β] Family Signals. *Cell.* 87:173-173.
- Derynck, R., and Y.E. Zhang. 2003. Smad-dependent and Smad-independent pathways in TGF-[β] family signalling. *Nature.* 425:577-584.
- Dressler, G.R. 2002. Tubulogenesis in the developing mammalian kidney. *Trends in Cell Biology.* 12:390-395.
- Dressler, G.R. 2006. The Cellular Basis of Kidney Development. *Annual Review of Cell and Developmental Biology.* 22:509-529.
- Dressler, G.R., U. Deutsch, K. Chowdhury, H.O. Nornes, and P. Gruss. 1990. PAX2, A NEW MURINE PAIRED-BOX-CONTAINING GENE AND ITS EXPRESSION IN THE DEVELOPING EXCRETORY SYSTEM. *Development.* 109:787-795.
- Dudley, A.T., K.M. Lyons, and E.J. Robertson. 1995. A REQUIREMENT FOR BONE MORPHOGENETIC PROTEIN-7 DURING DEVELOPMENT OF THE MAMMALIAN KIDNEY AND EYE. *Genes & Development.* 9:2795-2807.
- Dudley, A.T., and E.J. Robertson. 1997. Overlapping expression domains of bone morphogenetic protein family members potentially account for limited tissue defects in BMP7 deficient embryos. *Developmental Dynamics.* 208:349-362.

- Dunn, N.R., G.E. Winnier, L.K. Hargett, J.J. Schrick, A.B. Fogo, and B.L.M. Hogan. 1997. Haploinsufficient Phenotypes in *Bmp4* Heterozygous Null Mice and Modification by Mutations in *Gli3* and *Alx4*. *Developmental Biology*. 188:235-247.
- Firnberg, N., and A. Neubüser. 2002. FGF Signaling Regulates Expression of *Tbx2*, *Erm*, *Pea3*, and *Pax3* in the Early Nasal Region. *Developmental Biology*. 247:237-250.
- Fukagawa, M., N. Suzuki, B.L.M. Hogan, and C.M. Jones. 1994. Embryonic Expression of Mouse Bone Morphogenetic Protein-1 (BMP-1), Which Is Related to the *Drosophila* Dorsoventral Gene *tolloid* and Encodes a Putative Astacin Metalloendopeptidase. *Developmental Biology*. 163:175-183.
- Godin, R.E., E.J. Robertson, and A.T. Dudley. 1999. Role of BMP family members during kidney development. *International Journal of Developmental Biology*. 43:405-411.
- Godin, R.E., N.T. Takaesu, E.J. Robertson, and A.T. Dudley. 1998. Regulation of BMP7 expression during kidney development. *Development*. 125:3473-3482.
- Greenwald, J., J. Groppe, P. Gray, E. Wiater, W. Kwiatkowski, W. Vale, and S. Choe. 2003. The BMP7/ActRII Extracellular Domain Complex Provides New Insights into the Cooperative Nature of Receptor Assembly. *Molecular Cell*. 11:605-617.
- Grieshammer, U., L. Ma, A.S. Plump, F. Wang, M. Tessier-Lavigne, and G.R. Martin. 2004. SLIT2-mediated ROBO2 signaling restricts kidney induction to a single site. *Developmental Cell*. 6:709-717.

- Hartman, H.A., H.L. Lai, and L.T. Patterson. 2007. Cessation of renal morphogenesis in mice. *Developmental Biology*. 310:379-387.
- Hartwig, S., M.-C. Hu, C. Cella, T. Piscione, J. Filmus, and N.D. Rosenblum. 2005. Glypican-3 modulates inhibitory Bmp2-Smad signaling to control renal development in vivo. *Mechanisms of Development*. 122:928-938.
- Hayashi, S., and A.P. McMahon. 2002. Efficient recombination in diverse tissues by a tamoxifen-inducible form of Cre: A tool for temporally regulated gene activation/inactivation in the mouse. *Developmental Biology*. 244:305-318.
- Hogan, B.L.M. 1996. Bone morphogenetic proteins in development. *Current Opinion in Genetics & Development*. 6:432-438.
- Hoodless, P.A., T. Haerry, S. Abdollah, M. Stapleton, M.B. O'Connor, L. Attisano, and J.L. Wrana. 1996. MADR1, a MAD-Related Protein That Functions in BMP2 Signaling Pathways. *Cell*. 85:489-500.
- Hsu, D.R., A.N. Economides, X.R. Wang, P.M. Eimon, and R.M. Harland. 1998. The *Xenopus* dorsalizing factor gremlin identifies a novel family of secreted proteins that antagonize BMP activities. *Molecular Cell*. 1:673-683.
- Hu, M.C., T.D. Piscione, and N.D. Rosenblum. 2003. Elevated SMAD1/beta-catenin molecular complexes and renal medullary cystic dysplasia in ALK3 transgenic mice. *Development*. 130:2753-2766.
- Hu, M.C., D. Wasserman, S. Hartwig, and N.D. Rosenblum. 2004. p38MAPK Acts in the BMP7-dependent Stimulatory Pathway during Epithelial Cell Morphogenesis and Is Regulated by Smad1. *Journal of Biological Chemistry*. 279:12051-12059.

- Ikeya, M., M. Kawada, H. Kiyonari, N. Sasai, K. Nakao, Y. Furuta, and Y. Sasai. 2006. Essential pro-Bmp roles of crossveinless 2 in mouse organogenesis. *Development*. 133:4463-4473.
- Imamura, T., M. Takase, A. Nishihara, E. Oeda, J. Hanai, M. Kawabata, and K. Miyazono. 1997. Smad6 inhibits signalling by the TGF-beta superfamily. *Nature*. 389:622-626.
- Jain, S., M. Encinas, E.M. Johnson, and J. Milbrandt. 2006. Critical and distinct roles for key RET tyrosine docking sites in renal development. *Genes & Development*. 20:321-333.
- Jena, N., C. MartinSeisdedos, P. McCue, and C.M. Croce. 1997. BMP7 null mutation in mice: Developmental defects in skeleton, kidney, and eye. *Experimental Cell Research*. 230:28-37.
- Karsenty, G., G.B. Luo, C. Hofmann, and A. Bradley. 1996. BMP 7 is required for nephrogenesis, eye development, and skeletal patterning. *Molecular and Developmental Biology of Cartilage*. 785:98-107.
- Katagiri, T., S. Boorla, J.-L. Frendo, B.L.M. Hogan, and G. Karsenty. 1998. Skeletal abnormalities in doubly heterozygous *Bmp4* and *Bmp7* mice. *Developmental Genetics*. 22:340-348.
- Kim, J., K. Johnson, H.J. Chen, S. Carroll, and A. Laughon. 1997. Drosophila Mad binds to DNA and directly mediates activation of vestigial by Decapentaplegic. *Nature*. 388:304-308.
- Kingsley, D.M., A.E. Bland, J.M. Grubber, P.C. Marker, L.B. Russell, N.G. Copeland, and N.A. Jenkins. 1992. The mouse short ear skeletal morphogenesis locus is associated with defects in a bone morphogenetic member of the TGF[beta] superfamily. *Cell*. 71:399-410.

- Kobayashi, A., M.T. Valerius, J.W. Mugford, T.J. Carroll, M. Self, G. Oliver, and A.P. McMahon. 2008. Six2 defines and regulates a multipotent self-renewing nephron progenitor population throughout mammalian kidney development. *Cell Stem Cell*. 3:169-181.
- Koenig, B.B., J.S. Cook, D.H. Wolsing, J. Ting, J.P. Tiesman, P.E. Correa, C.A. Olson, A.L. Pecquet, F.S. Ventura, R.A. Grant, G.X. Chen, J.L. Wrana, J. Massague, and J.S. Rosenbaum. 1994. CHARACTERIZATION AND CLONING OF A RECEPTOR FOR BMP-2 AND BMP-4 FROM NIH 3T3 CELLS. *Molecular and Cellular Biology*. 14:5961-5974.
- Kulesa, H., and B.L.M. Hogan. 2002. Generation of a loxP flanked Bmp4(loxP-lacZ) allele marked by conditional lacZ expression. *Genesis*. 32:66-68.
- Kume, T., K.Y. Deng, and B.L.M. Hogan. 2000. Murine forkhead/winged helix genes Foxc1 (Mf1) and Foxc2 (Mfh1) are required for the early organogenesis of the kidney and urinary tract. *Development*. 127:1387-1395.
- Leung-Hagesteijn, C., M.C. Hu, A.S. Mahendra, S. Hartwig, H.J. Klamut, N.D. Rosenblum, and G.E. Hannigan. 2005. Integrin-linked kinase mediates bone morphogenetic protein 7-dependent renal epithelial cell morphogenesis. *Molecular and Cellular Biology*. 25:3648-3657.
- Lin, J.M., S.R. Patel, X. Cheng, E.A. Cho, I. Levitan, M. Ullenbruch, S.H. Phan, J.M. Park, and G.R. Dressler. 2005. Kielin/chordin-like protein, a novel enhancer of BMP signaling, attenuates renal fibrotic disease. *Nature Medicine*. 11:387-393.
- Lin, J.M., S.R. Patel, M. Wang, and G.R. Dressler. 2006. The cysteine-rich domain protein KCP is a suppressor of transforming growth factor

- beta/activin signaling in renal epithelia. *Molecular and Cellular Biology*. 26:4577-4585.
- Lin, Y.F., S.B. Zhang, M. Rehn, P. Itaranta, J. Tuukkanen, R. Heljasvaara, H. Peltoketo, T. Pihlajaniemi, and S. Vainio. 2001. Induced repatterning of type XVIII collagen expression in ureter bud from kidney to lung type: association with sonic hedgehog and ectopic surfactant protein C. *Development*. 128:1573-1585.
- Little, S.C., and M.C. Mullins. 2009. Bone morphogenetic protein heterodimers assemble heteromeric type I receptor complexes to pattern the dorsoventral axis. *Nat Cell Biol*. 11:637-643.
- Liu, Y., H. Jiang, H.C. Crawford, and B.L.M. Hogan. 2003. Role for ETS domain transcription factors Pea3/Erm in mouse lung development. *Developmental Biology*. 261:10-24.
- Lu, B.C., C. Cebrian, X. Chi, S. Kuure, R. Kuo, C.M. Bates, S. Arber, J. Hassell, L. MacNeil, M. Hoshi, S. Jain, N. Asai, M. Takahashi, K.M. Schmidt-Ott, J. Barasch, V. D'Agati, and F. Costantini. 2009. Etv4 and Etv5 are required downstream of GDNF and Ret for kidney branching morphogenesis. *Nat Genet*. 41:1295-1302.
- Luo, G., C. Hofmann, A. Bronckers, M. Sohocki, A. Bradley, and G. Karsenty. 1995. BMP-7 IS AN INDUCER OF NEPHROGENESIS, AND IS ALSO REQUIRED FOR EYE DEVELOPMENT AND SKELETAL PATTERNING. *Genes & Development*. 9:2808-2820.
- Lyons, K.M., B.L.M. Hogan, and E.J. Robertson. 1995. COLOCALIZATION OF BMP-7 AND BMP-2 RNAS SUGGESTS THAT THESE FACTORS

- COOPERATIVELY MEDIATE TISSUE INTERACTIONS DURING MURINE DEVELOPMENT. *Mechanisms of Development*. 50:71-83.
- Majumdar, A., S. Vainio, A. Kispert, J. McMahon, and A.P. McMahon. 2003. Wnt11 and Ret/Gdnf pathways cooperate in regulating ureteric branching during metanephric kidney development. *Development*. 130:3175-3185.
- Martinez, G., Y. Mishina, and J.F. Bertram. 2002. BMPs and BMP receptors in mouse metanephric development: in vivo and in vitro studies. *International Journal of Developmental Biology*. 46:525-533.
- Massagué, J. 1998. TGF- β SIGNAL TRANSDUCTION. *Annual Review of Biochemistry*. 67:753-791.
- Massagué, J., J. Seoane, and D. Wotton. 2005. Smad transcription factors. *Genes & Development*. 19:2783-2810.
- McClive, P.J., and A.H. Sinclair. 2001. Rapid DNA extraction and PCR-sexing of mouse embryos. *Molecular Reproduction and Development*. 60:225-226.
- McMahon, J.A., S. Takada, L.B. Zimmerman, C.M. Fan, R.M. Harland, and A.P. McMahon. 1998. Noggin-mediated antagonism of BMP signaling is required for growth and patterning of the neural tube and somite. *Genes & Development*. 12:1438-1452.
- McMahon, R., M. Murphy, M. Clarkson, M. Taal, H.S. Mackenzie, C. Godson, F. Martin, and H.R. Brady. 2000. IHG-2, a mesangial cell gene induced by high glucose, is human gremlin - Regulation by extracellular glucose concentration, cyclic mechanical strain, and transforming growth factor-beta 1. *Journal of Biological Chemistry*. 275:9901-9904.

- Michos, O., A. Goncalves, J. Lopez-Rios, E. Tiecke, F. Naillat, K. Beier, A. Galli, S. Vainio, and R. Zeller. 2007. Reduction of BMP4 activity by gremlin 1 enables ureteric bud outgrowth and GDNF/WNT11 feedback signalling during kidney branching morphogenesis. *Development*. 134:2397-2405.
- Michos, O., L. Panman, K. Vintersten, K. Beier, R. Zeller, and A. Zuniga. 2004. Gremlin-mediated BMP antagonism induces the epithelial-mesenchymal feedback signaling controlling metanephric kidney and limb organogenesis. *Development*. 131:3401-3410.
- Mishina, Y., R. Crombie, A. Bradley, and R.R. Behringer. 1999. Multiple Roles for Activin-Like Kinase-2 Signaling during Mouse Embryogenesis. *Developmental Biology*. 213:314-326.
- Mishina, Y., A. Suzuki, N. Ueno, and R.R. Behringer. 1995. Bmpr encodes a type I bone morphogenetic protein receptor that is essential for gastrulation during mouse embryogenesis. *Genes & Development*. 9:3027-3037.
- Miyazaki, Y., K. Oshima, A. Fogo, B.L.M. Hogan, and I. Ichikawa. 2000. Bone morphogenetic protein 4 regulates the budding site and elongation of the mouse ureter. *Journal of Clinical Investigation*. 105:863-873.
- Miyazaki, Y., H. Ueda, T. Yokoo, Y. Utsunomiya, T. Kawamura, T. Matsusaka, I. Ichikawa, and T. Hosoya. 2006. Inhibition of endogenous BMP in the glomerulus leads to mesangial matrix expansion. *Biochemical and Biophysical Research Communications*. 340:681-688.
- Miyazono, K., Y. Kamiya, and M. Morikawa. 2010. Bone morphogenetic protein receptors and signal transduction. *J Biochem*. 147:35-51.

- Miyazono, K., S. Maeda, and T. Imamura. 2005. BMP receptor signaling: Transcriptional targets, regulation of signals, and signaling cross-talk. *Cytokine & Growth Factor Reviews*. 16:251-263.
- Moore, M.W., R.D. Klein, I. Farinas, H. Sauer, M. Armanini, H. Phillips, L.F. Reichardt, A.M. Ryan, K. CarverMoore, and A. Rosenthal. 1996. Renal and neuronal abnormalities in mice lacking GDNF. *Nature*. 382:76-79.
- Moustakas, A., and C.-H. Heldin. 2009. The regulation of TGF β ² signal transduction. *Development*. 136:3699-3714.
- Nakao, A., M. Afrakhte, A. Moren, T. Nakayama, J.L. Christian, R. Heuchel, S. Itoh, N. Kawabata, N.E. Heldin, C.H. Heldin, and P. tenDijke. 1997. Identification of Smad7, a TGF beta-inducible antagonist of TGF-beta signalling. *Nature*. 389:631-635.
- Nickel, J., W. Sebald, J.C. Groppe, and T.D. Mueller. 2009. Intricacies of BMP receptor assembly. *Cytokine & Growth Factor Reviews*. In Press, Corrected Proof.
- Nishimatsu, S.-i., and G.H. Thomsen. 1998. Ventral mesoderm induction and patterning by bone morphogenetic protein heterodimers in *Xenopus* embryos. *Mechanisms of Development*. 74:75-88.
- Niwa, H., K. Yamamura, and J. Miyazaki. 1991. EFFICIENT SELECTION FOR HIGH-EXPRESSION TRANSFECTANTS WITH A NOVEL EUKARYOTIC VECTOR. *Gene*. 108:193-199.
- Nohno, T., T. Ishikawa, T. Saito, K. Hosokawa, S. Noji, D.H. Wolsing, and J.S. Rosenbaum. 1995. Identification of a Human Type II Receptor for Bone Morphogenetic Protein-4 That Forms Differential Heteromeric Complexes

- with Bone Morphogenetic Protein Type I Receptors. *Journal of Biological Chemistry*. 270:22522-22526.
- Obara-Ishihara, T., J. Kuhlman, L. Niswander, and D. Herzlinger. 1999. The surface ectoderm is essential for nephric duct formation in intermediate mesoderm. *Development*. 126:1103-1108.
- Ohno, S. 1995. Why ontogeny recapitulates phylogeny. *Electrophoresis*. 16:1782-1786.
- Oxburgh, L., A.T. Dudley, R.E. Godin, C.H. Koonce, A. Islam, D.C. Anderson, E.K. Bikoff, and E.J. Robertson. 2005. BMP4 substitutes for loss of BMP7 during kidney development. *Developmental Biology*. 286:637-646.
- Panman, L., A. Galli, N. Lagarde, O. Michos, G. Soete, A. Zuniga, and R. Zeller. 2006. Differential regulation of gene expression in the digit forming area of the mouse limb bud by SHH and gremlin 1/FGF-mediated epithelial-mesenchymal signalling. *Development*. 133:3419-3428.
- Pearce, J.J.H., G. Penny, and J. Rossant. 1999. A mouse cerberus/Dan-related gene family. *Developmental Biology*. 209:98-110.
- Pichel, J.G., L.Y. Shen, H.Z. Sheng, A.C. Granholm, J. Drago, A. Grinberg, E.J. Lee, S.P. Huang, M. Saarma, B.J. Hoffer, H. Sariola, and H. Westphal. 1996. Defects in enteric innervation and kidney development in mice lacking GDNF. *Nature*. 382:73-76.
- Piscione, T.D., T.D. Yager, I.R. Gupta, B. Grinfeld, Y. Pei, L. Attisano, J.L. Wrana, and N.D. Rosenblum. 1997. BMP-2 and OP-1 exert direct and opposite effects on renal branching morphogenesis. *American Journal of Physiology-Renal Physiology*. 273:F961-F975.

- Pope, J.C., J.W. Brock, M.C. Adams, F.D. Stephens, and I. Ichikawa. 1999. How they begin and how they end: Classic and new theories for the development and deterioration of congenital anomalies of the kidney and urinary tract, CAKUT. *Journal of the American Society of Nephrology*. 10:2018-2028.
- Pregizer, S., and D.P. Mortlock. 2009. Control of BMP gene expression by long-range regulatory elements. *Cytokine & Growth Factor Reviews*. 20:509-515.
- Raatikainen-Ahokas, A., M. Hytonen, A. Tenhunen, K. Sainio, and H. Sariola. 2000. BMP-4 affects the differentiation of metanephric mesenchyme and reveals an early anterior-posterior axis of the embryonic kidney. *Developmental Dynamics*. 217:146-158.
- Rossini, A.A., A.A. Like, W.L. Chick, M.C. Appel, and G.F. Cahill. 1977. Studies of streptozotocin-induced insulinitis and diabetes. *Proceedings of the National Academy of Sciences of the United States of America*. 74:2485-2489.
- Sainio, K., and A. Raatikainen-Ahokas. 1999. Mesonephric kidney - a stem cell factory? *International Journal of Developmental Biology*. 43:435-439.
- Saxen, L. 1987. Organogenesis of the Kidney.
- Schedl, A. 2007. Renal abnormalities and their developmental origin. *Nature Reviews Genetics*. 8:791-802.
- Schmidt-Ott, K.M., X. Chen, N. Paragas, R.S. Levinson, C.L. Mendelsohn, and J. Barasch. 2006. c-kit delineates a distinct domain of progenitors in the developing kidney. *Developmental Biology*. 299:238-249.

- Schuchardt, A., V. Dagati, V. Pachnis, and F. Costantini. 1996. Renal agenesis and hypodysplasia in *ret-k(-)* mutant mice result from defects in ureteric bud development. *Development*. 122:1919-1929.
- Schwenk, F., U. Baron, and K. Rajewsky. 1995. A cre-transgenic mouse strain for the ubiquitous deletion of loxP-flanked gene segments including deletion in germ cells. *Nucleic Acids Research*. 23:5080-5081.
- Self, M., O.V. Lagutin, B. Bowling, J. Hendrix, Y. Cai, G.R. Dressler, and G. Oliver. 2006. Six2 is required for suppression of nephrogenesis and progenitor renewal in the developing kidney. *Embo Journal*. 25:5214-5228.
- Shakya, R., T. Watanabe, and F. Costantini. 2005. The role of GDNF/Ret signaling in ureteric bud cell fate and branching morphogenesis. *Developmental Cell*. 8:65-74.
- Sieber, C., J. Kopf, C. Hiepen, and P. Knaus. 2009. Recent advances in BMP receptor signaling. *Cytokine & Growth Factor Reviews*. 20:343-355.
- Smith, W.C., and R.M. Harland. 1992. Expression cloning of noggin, a new dorsalizing factor localized to the Spemann organizer in *Xenopus* embryos. *Cell*. 70:829-840.
- Smith, W.C., A.K. Knecht, M. Wu, and R.M. Harland. 1993. SECRETED NOGGIN PROTEIN MIMICS THE SPEMANN ORGANIZER IN DORSALIZING XENOPUS MESODERM. *Nature*. 361:547-549.
- Solloway, M.J., A.T. Dudley, E.K. Bikoff, K.M. Lyons, B.L.M. Hogan, and E.J. Robertson. 1998. Mice lacking *Bmp6* function. *Developmental Genetics*. 22:321-339.

- Srinivas, S., M.R. Goldberg, T. Watanabe, V. D'Agati, Q. Al-Awqati, and F. Costantini. 1999. Expression of green fluorescent protein in the ureteric bud of transgenic mice: A new tool for the analysis of ureteric bud morphogenesis. *Developmental Genetics*. 24:241-251.
- Stark, K., S. Vainio, G. Vassileva, and A.P. McMahon. 1994. EPITHELIAL TRANSFORMATION OF METANEPHRIC MESENCHYME IN THE DEVELOPING KIDNEY REGULATED BY WNT-4. *Nature*. 372:679-683.
- Suzuki, A., E. Kaneko, J. Maeda, and N. Ueno. 1997. Mesoderm Induction by BMP-4 and -7 Heterodimers. *Biochemical and Biophysical Research Communications*. 232:153-156.
- Takahara, K., R. Brevard, G.G. Hoffman, N. Suzuki, and D.S. Greenspan. 1996. Characterization of a Novel Gene Product (Mammalian Tolloid-like) with High Sequence Similarity to Mammalian Tolloid/Bone Morphogenetic Protein-1. *Genomics*. 34:157-165.
- te Welscher, P., A. Zuniga, S. Kuisper, T. Drenth, H.J. Goedemans, F. Meijlink, and R. Zeller. 2002. Progression of Vertebrate Limb Development Through SHH-Mediated Counteraction of GLI3. *Science*. 298:827-830.
- ten Dijke, P., H. Yamashita, T.K. Sampath, A.H. Reddi, M. Estevez, D.L. Riddle, H. Ichijo, C.H. Heldin, and K. Miyazono. 1994. Identification of type I receptors for osteogenic protein-1 and bone morphogenetic protein-4. *Journal of Biological Chemistry*. 269:16985-16988.
- Torres, M., E. Gomez-Pardo, G.R. Dressler, and P. Gruss. 1995. Pax-2 controls multiple steps of urogenital development. *Development*. 121:4057-4065.
- Towers, P.R., A.S. Woolf, and P. Hardman. 1998. Glial cell line-derived neurotrophic factor stimulates ureteric bud outgrowth and enhances

- survival of ureteric bud cells in vitro. *Experimental Nephrology*. 6:337-351.
- Urist, M.R. 1965. Bone: Formation by Autoinduction. *Science*. 150:893-899.
- Vainio, S., and Y.F. Lin. 2002. Coordinating early kidney development: Lessons from gene targeting. *Nature Reviews Genetics*. 3:533-543.
- Villanueva, S., C. Cespedes, and C.P. Vio. 2006. Ischemic acute renal failure induces the expression of a wide range of nephrogenic proteins. *Am J Physiol Regul Integr Comp Physiol*. 290:R861-870.
- von Bubnoff, A., and K.W.Y. Cho. 2001. Intracellular BMP Signaling Regulation in Vertebrates: Pathway or Network? *Developmental Biology*. 239:1-14.
- Wallis, M.C., P.D. Waters, and J.A.M. Graves. 2008. Sex determination in mammals - Before and after the evolution of SRY. *Cellular and Molecular Life Sciences*. 65:3182-3195.
- Walsh, D.W., S.A. Roxburgh, P. McGettigan, C.C. Berthier, D.G. Higgins, M. Kretzler, C.D. Cohen, S. Mezzano, D.P. Brazil, and F. Martin. 2008. Co-regulation of Gremlin and Notch signalling in diabetic nephropathy. *Biochimica Et Biophysica Acta-Molecular Basis of Disease*. 1782:10-21.
- Wardle, E.N. 1975. MESANGIAL CELL DYSFUNCTION DETECTED BY ACCUMULATION OF AGGREGATED PROTEIN IN RATS WITH STREPTOZOTOCIN INDUCED DIABETES. *Biomedicine Express*. 23:299-302.
- Wilkinson, D.G. 1992. The use of in situ hybridisation to study the molecular genetics of mouse development. *Russo, V. E. A., S. Brody, D. Cove and S. Ottolenghi. Development: The molecular genetic approach*.

xxxv+605p. Springer-Verlag: Berlin, Germany; New York, New York, USA. *Illus.* ISBN 3-540-54730-4; ISBN 0-387-54730-4:409-419.

- Winnier, G., M. Blessing, P.A. Labosky, and B.L.M. Hogan. 1995. BONE MORPHOGENETIC PROTEIN-4 IS REQUIRED FOR MESODERM FORMATION AND PATTERNING IN THE MOUSE. *Genes & Development*. 9:2105-2116.
- Wrana, J.L., L. Attisano, R. Wieser, F. Ventura, and J. Massague. 1994. MECHANISM OF ACTIVATION OF THE TGF-BETA RECEPTOR. *Nature*. 370:341-347.
- Yu, J., A.P. McMahon, and M.T. Valerius. 2004. Recent genetic studies of mouse kidney development. *Current Opinion in Genetics & Development*. 14:550-557.
- Yu, L., M.C. Hebert, and Y.E. Zhang. 2002. TGF-beta receptor-activated p38 MAP kinase mediates smad-independent TGF-beta responses. *Embo Journal*. 21:3749-3759.
- Yue, J.B., R.S. Frey, and K.M. Mulder. 1999. Cross-talk between the Smad1 and Ras/MEK signaling pathways for TGF beta. *Oncogene*. 18:2033-2037.
- Zhang, H., and A. Bradley. 1996. Mice deficient for BMP2 are nonviable and have defects in amnion/chorion and cardiac development. *Development*. 122:2977-2986.
- Zhu, W., J. Kim, C. Cheng, B.A. Rawlins, O. Boachie-Adjei, R.G. Crystal, and C. Hidaka. 2006. Noggin regulation of bone morphogenetic protein (BMP) 2/7 heterodimer activity in vitro. *Bone*. 39:61-71.

Zuniga, A., A.P.G. Haramis, A.P. McMahon, and R. Zeller. 1999. Signal relay by BMP antagonism controls the SHH/FGF4 feedback loop in vertebrate limb buds. *Nature*. 401:598-602.

Zuniga, A.E., O. Michos, F. Spitz, A.P.G. Haramis, L. Panman, A. Galli, K. Vintersten, C. Klasen, W. Mansfield, S. Kuc, D. Duboule, R. Dono, and R. Zeller. 2004. Mouse limb deformity mutations disrupt a global control region within the large regulatory landscape required for Gremlin expression. *Genes & Development*. 18:1553-1564.

XII. CURRICULUM VITAE AND PUBLICATION LIST

PERSONAL DETAILS

Name: Alexandre Gonçalves

Date of birth: 30.08.1977

Nationality: Portuguese

Address: Developmental Genetics,
Department of Biomedicine, Mattenstrasse 28,
4058 Basel, Switzerland

E-mail: alexandre.goncalves@unibas.ch

Tel.: +41 61 695 30 38

EDUCATION

Apr. 2005 – Present: Ph.D. student in the laboratory of Prof. Dr. Rolf Zeller, Developmental Genetics Group, Department of Biomedicine, University of Basel Medical Faculty, Switzerland.

Oct. 1996 – Feb. 2003 Licenciante degree in the scientific field of Biology at the Faculty of Sciences of the University of Lisbon, Portugal.

Sep.1992 – Jul. 1996 High School graduation in Health Sciences at Escola Secundária da Amadora (Lisbon, Portugal)

RESEARCH ACTIVITIES

Apr. 2005 – Present: Ph.D. student in the laboratory of Prof. Dr. Rolf Zeller, Developmental Genetics group, Department of Biomedicine, University of Basel Medical Faculty, Switzerland.

Thesis title: Epithelial-Mesenchymal Feedback Signalling during Vertebrate Organogenesis:Genetic Analysis of BMP-Gremlin Antagonistic Interactions

Apr. 2003 – Feb. 2005 Research assistant in the laboratory of Prof. Dr. Maria Leonor Saúde, Segmentation Group, Instituto Gulbenkian de Ciência, Oeiras, Portugal.

Project title: Molecular and cellular characterization of segmentation in the chick embryo

Oct. 2002 – Feb. 2003 Research trainee / graduation thesis under the supervision of Dr. Joaquín Rodríguez-León and Professor Dr. Juan Carlos Belmonte, Organogenesis group, Instituto Gulbenkian de Ciência, Oeiras, Portugal.

Project title: Searching for genes involved in the early differentiation of organs by screening a 5 to 10 HH stage chicken embryos cDNA library.

Aug. 2001 – Sep. 2002 Research trainee under the supervision of Dr. Joaquín Rodríguez-León, Organogenesis group, Instituto Gulbenkian de Ciência, Oeiras, Portugal.

Project title: cDNA chicken embryo library screening. Search and characterization of organogenesis related genes.

FELLOWSHIPS

Feb. 2006 – Jan. 2010 Ph.D. student fellowship.

FCT; SFRH/BD/24301/2005

Apr. 2005 – Jan. 2006 SNF Ph.D. student fellowship

Apr. 2003 – Mar. 2005 Research fellowship.

POCTI/45914/2002 (FCT/POCTI/FEDER)

TECHNICAL SKILLS

Chicken embryo: Embryo collection, *in vitro* culture, bead implantation, microsurgery, mRNA *in situ* hybridization and histology sectioning.

Zebrafish embryo: Embryo collection and mRNA *in situ* hybridization.

Mouse embryo: Colony management, genetic loss-of-function assays (Cre-LoxP system and tamoxifen injection), genotyping, embryo collection, kidney collection, *in situ* hybridization, kidney culture and video time lapse assays.

Molecular biology: Cloning, genomic DNA and RNA extraction, *in vitro* transcription, PCR, DNA sequencing and sequence analysis.

Histology techniques: Fixing and embedding embryos and tissues in paraffin and gelatine. Cryostat, microtome and vibratome sectioning.

Microscopy: General use of bright field, fluorescence and confocal microscopes.

Software: Microsoft and Apple operating systems. Microsoft Office. Adobe Photoshop. Adobe Dreamweaver. Macvector and Endnote.

LANGUAGES

Portuguese	Mother tongue
English	Written and spoken
Spanish	Basic knowledge
French	Basic knowledge
Italian	Basic knowledge

POSTER PRESENTATIONS

- BioValley Life Sciences Week 2009. Basel, Switzerland, 2009.
- Cells into Organs Symposium 2009. Lisbon. Portugal, 2009.
- 10th International Workshop on Developmental Nephrology. Pécs, Hungary, 2007.
- USGEB / [BC]2 conference. Basel, Switzerland, 2007.
- Société Française de Biologie du Développement. Obernai, France, 2005.
- ELSO Congress 2003. Desden, Germany, 2003.

ORAL PRESENTATIONS

- 10th International Workshop on Developmental Nephrology. Pécs, Hungary, 2007.

PUBLICATIONS

Jean-Denis Bénazet, Mirko Bischofberger, Eva Tieke, **Alexandre Gonçalves**, James F. Martin, Aimée Zuniga, Felix Naef and Rolf Zeller. **A self-regulatory system of interlinked signalling feedback loops controls mouse limb patterning**. Science 323(5917):1050-3 (2009).

Odyssé Michos⁺, **Alexandre Gonçalves**⁺, Javier Lopez-Rios, Eva Tiecke, Florence Naillat, Konstantin Beier, Antonella Galli, Seppo Vainio and Rolf Zeller (2007) **“Reduction of BMP4 activity by Gremlin1 enables ureteric bud outgrowth and GDNF/Wnt11 feedback signalling during kidney branching morphogenesis”**. Development 134, 2397-2405. ⁺These authors contributed equally to this study.

Leonor Saúde, Raquel Lourenço, **Alexandre Gonçalves** and Isabel Palmeirim (2005) **“*terra* is a left-right asymmetry gene required for left-right synchronization of the segmentation clock”**. Nature Cell Biology. 7, (9) 918 – 920.

AWARDS

BioValley - Poster Award.

“Kidney Morphogenesis: A Genetic Analysis of the BMP-Gremlin1 Antagonistic Interactions.” **A. Gonçalves**, K. Beier, and R. Zeller. Basel, Switzerland, 2009.

10th International Workshop on Developmental Nephrology - Poster Award.

“Reduction of BMP4 activity by Gremlin1 enables ureteric bud outgrowth and GDNF/Wnt11 feedback signalling during kidney branching morphogenesis”

A. Gonçalves, O. Michos, E. Tiecke, F. Naillat, J. Lopez-Rios, K. Beier, A. Galli, S. Vainio and R. Zeller. Pécs, Hungary, 2007.

Pfizer Award 2005. Pfizer Award for Basic Research.

“Terra é um gene que promove a assimetria esquerda-direita ao mesmo tempo que é necessário para a sincronização esquerda-direita do relógio da segmentação”. Leonor Saúde, Raquel Lourenço, **Alexandre Gonçalves** and Isabel Palmeirim. Lisbon, Portugal, 2005.

REFEREES

Professor Dr. Rolf Zeller

Developmental Genetics - Centre for Biomedicine

University of Basel Medical School, Switzerland

E-mail: Rolf.Zeller@unibas.ch

Phone Number: +41 61 695 30 31 (Sec. 13:30-17:30) Fax +41 61 695 30 32

Professor Dr. Markus Affolter

Biozentrum der Uni Basel

Abt. Zellbiologie

E-mail: Markus.Affolter@unibas.ch

Phone Number: +41 61 267 20 72 Fax +41 61 267 20 78

Dr. Joaquín León

Instituto Gulbenkian de Ciência

E-mail: jleon@igc.gulbenkian.pt

Phone Number: + 351 21 446 4664